Uncertainty Through the Lenses of A Mixed-Frequency Bayesian Panel Markov Switching Model*

Roberto Casarin† Claudia Foroni‡
Massimiliano Marcellino¶ Francesco Ravazzolo§

†University Ca' Foscari of Venice
‡European Central Bank and Norges Bank
§Free University of Bozen/Bolzano and BI Norwegian Business School
¶Bocconi University, IGIER, and C.E.P.R.

December 1, 2016

Abstract

We propose a Bayesian panel model for mixed frequency data whose parameters can change over time according to a Markov process. Our model allows for both structural instability and random effects. We develop a proper Markov Chain Monte Carlo algorithm for sampling from the joint posterior distribution of the model parameters and test its properties in simulation experiments. We use the model to study the effects of macroeconomic uncertainty and financial uncertainty on a set of variables in a multi-country context including the US, several European countries and Japan. We find that for most of the variables financial uncertainty dominates macroeconomic uncertainty. Furthermore, we show that uncertainty coefficients differ if the economy is in a contraction regime or in an expansion regime.

JEL codes: C13, C14, C51, C53.

Keywords: dynamic panel model, mixed-frequency, Markov switching, Bayesian inference, MCMC.

*We thank Sylvia Kaufmann, Dimitris Korobilis, Haroon Mumtaz, Christian Schumacher, Michael Smiths, the participants at the Bayesian Analysis and Modeling Summer Workshop 2015 in Melbourne, at the 9th International Conference on Computational and Financial Econometrics, the CAMP Workshop on Commodities, business cycles and monetary policy, the 10th Annual RCEA Bayesian Econometric Workshop, the Bank of England and Essex Business School Workshop on "Time Variation and Non-Linear Models in Econometrics and Macroeconomics", the 3rd Padova Macro Talks, the 22nd Computing in Economics and Finance conference, the Bundesbank seminar, the University of Padova seminar, the 7th European Seminar On Bayesian Econometric annual meeting for their useful comments. This research used the SCSCF multiprocessor cluster system at University Ca' Foscari of Venice. This paper is part of the research activities at the Centre for Applied Macro and Petroleum economics (CAMP) at the BI Norwegian Business School. The views expressed are those of the authors and do not necessarily reflect those of European Central Bank nor of Norges Bank.

1 Introduction

The role of uncertainty as a driver of macroeconomic fluctuations has been at the center of attention especially since the beginning of the Great Recession in 2007. Most of the literature has so far focused on measuring uncertainty and its effects in the U.S. economy. Hence, there is a clear need to study whether the results for the U.S. also hold for other countries, which differ for the structure of their goods, labour and financial markets, degree of openness, conduct of fiscal and monetary policy, and other institutional characteristics.

Therefore, in this paper we take a multi-country perspective and assess the effects of uncertainty on different macroeconomic variables in various countries: U.S., Canada, Japan, Euro area as a whole and its main member States, U.K., Switzerland, Norway, Sweden.[1] To properly address this question, we take a panel approach, as an unrestricted model for many variables and countries would be too large. We also want to allow for different effects of uncertainty over time, and in particular in expansionary and recessionary times. Finally, we want to exploit the presence of mixed frequency data to improve estimation efficiency and reduce identification problems, see e.g. Foroni and Marcellino (2014).[2]

Our main contribution is therefore methodological. We develop a multi-country panel Markov-Switching unrestricted mixed-data sampling regression (panel MS-UMIDAS from now on). This framework allows us to model a large panel of countries and several variables for each country. At the same time, it allows us to use an endogenous time-varying transition mechanism and include nonlinearity in the model. Finally, it makes possible to consider variables at mixed frequencies.

The model is at the crossing of different strands of literature. Markov-switching dynamic panel models have been introduced by Kaufmann (2010) and extended first by Kaufmann (2015) with the introduction of endogenous transition, and second by Billio et al. (2016b) to a VAR context allowing for multiple series per unit. Our model builds on Kaufmann (2010) and Kaufmann (2015) and extends her model in two directions. First, we introduce unit-specific and variable-specific random effects which allow us to obtain heteroskedastic effects with time-variation in the error variance (that is, we do not need to include a Markov-switching mechanism in the variance once it is present in the random effects). Second, we allow the Markov-switching panel model to use data at different frequencies.

There is an increasing literature on mixed frequency data. Here, we focus on one of the main strands of the literature, mixed-data sampling (MIDAS) models. MIDAS regressions in their original specification, as introduced by Ghysels et al. (2005), are tightly parameterized reduced form equations, which use distributed lag polynomials to parsimoniously incorporate high frequency information into models for low-frequency variables. While initially applied to financial data, Clements and Galvao (2008) show that MIDAS regressions can lead to forecasting

[1] We chose to focus on the countries for which we have many macroeconomic series available and for which we can construct a measure of uncertainty based on the Consensus Economic Forecasts.

[2] A multi-country study on uncertainty has been recently proposed by Baker et al. (2015). However, the main focus of their work is to develop a new index of economic policy uncertainty (EPU) and the focus on a panel of countries is limited.

gains also for macroeconomic variables. Foroni et al. (2015a) show that an unrestricted variant of MIDAS which does not resort to functional distributed lag polynomials and preserves linearity of the model (UMIDAS) is particularly suited when the frequency mismatch is not too big, as in the case of macroeconomic data that are typically available either at monthly or quarterly frequencies. As we are interested in modelling macroeconomic variables and due to the simplicity of the UMIDAS approach, we adopt it in our panel MS context.[3]

Our paper relates also to other contributions in the mixed-frequency literature. In particular, Guérin and Marcellino (2013) introduce Markov-switching MIDAS and apply this model to the prediction of the U.S. economic activity. Further, Khalaf et al. (2013) have extended the MIDAS approach to the panel regression models suitable for analysis with GMM methods. As we already stated, we extend both these papers because we introduce here a Markov-switching panel MIDAS.

The estimation of our model is conducted in a Bayesian framework, in order to deal with the large number of parameters, which nevertheless makes our approach very flexible. In order to avoid overparameterization issues and overfitting problems we follow a hierarchical strategy in the specification of the prior as suggested in the Bayesian dynamic panel modeling literature (e.g., Canova and Ciccarelli (2004), Canova and Ciccarelli (2009), Kaufmann (2010), and Bassetti et al. (2014)). The hierarchical prior can be used to incorporate cross-equation interdependencies and various degrees of information pooling across units (e.g., see Chib and Greenberg (1995) and Min and Zellner (1993)). Also, the hierarchical prior as a part of the model allows us to naturally introduce random effects into the panel model. It is worth noticing that, although the MIDAS models have been typically used in a classical estimation context, recently the literature has expanded into the Bayesian estimation of this class of models (see e.g. Pettenuzzo et al. (2014), Rodriguez and Puggioni (2010) and Foroni et al. (2015b)).

In simulation studies, we show that our proposed MCMC method for the posterior approximation is efficient and reaches convergence to the true parameters. In particular, both time instability via Markov switching regimes, and the random effects are precisely estimated.

Next we apply our model to study the effects of uncertainty shocks on different sectors and variables across a panel of countries. We aim at shedding light on the effects of uncertainty in a panel framework, including data at different frequencies and at the same time allowing for different regimes.

In our analysis, we consider different measures of uncertainty available in the literature: a measure of forecast disagreement (as in Dovern et al. (2012)) and the VIX, as proposed by Bloom (2009) in his seminal paper. We use the former as proxy for macroeconomic uncertainty, and the latter as proxy of financial uncertainty.[4] We assume that monthly uncertainty is exogenous

[3]We highlight that the use of different MIDAS parameterizations, such as the Almon lag polynomials (e.g., see Pettenuzzo et al. (2014)), the exponential Almon lag (e.g., see Ghysels et al. (2005)), the normalized beta function (e.g., see Ghysels et al. (2007)), or the stepwise weights (e.g., see Ghysels et al. (2007)), is allowed within our framework and does not pose any additional conceptual difficulty. It would imply though an enlargement of the parameter space and the addition of a step in the estimation algorithm. The choice of a different polynomial requires a Metropolis Hastings step in the Gibbs sampler and the choice of a good proposal distribution.

[4]In the Appendix, we repeat the exercise using the Financial Uncertainty Index developed in Ludvigson et al. (2015) for the US economy. Moreover, in the spirit of Gourio (2012) and in order to analyse the effects of large

to quarterly macroeconomic variables. The identification scheme relies on the release time of the uncertainty-related and macroeconomic variables, with the former generally released earlier and in higher frequency and the latter released with some delay and in low frequency. Mumtaz and Theodoridis (2016) find substantial changes over time in the transmission of uncertainty shocks in the US; Caggiano et al. (2014) show that the relevance of uncertainty shocks is larger in recession regimes; and Alessandri and Mumtaz (2014) document that uncertainty shocks have radically different implications depending on the state financial markets are in when they occur. Our Markov switching specification can capture this type of parameter time variation. It also partially protects from omitted variable bias, as potential unmodelled variables which affect both macroeconomic variables and uncertainty are captured by the regime switching mechanism.

Our empirical results can be summarized as follows. There are large differences in the effects of the uncertainty shocks in the contraction regime and the expansion regime. The use of mixed frequency data rather than quarterly uncertainty variables amplifies the relevance of the asymmetry.

Moreover, financial uncertainty shocks play a more important role than macroeconomic uncertainty shocks. Their effects are stronger in the contraction regime than in the expansion regime, in particular this is more evident for real variables. The effects of financial uncertainty shocks are also more homogeneous across variables and countries than those of macroeconomic uncertainty.

Finally, when financial uncertainty is removed, the role of macroeconomic uncertainty increases, capturing part of the financial uncertainty shock and highlighting the need of jointly considering both types of uncertainty to avoid biased results, in line with the results in Jurado et al. (2015) and Carriero et al. (2016).

The remainder of the paper is organized as follows. Section 2 presents our Bayesian panel Markov-switching MIDAS model. Section 3 discusses the Bayesian inference framework. Section 4 presents our simulation results to confirm efficiency and convergence of our estimation method. Section 5 presents empirical results on the effects of financial and macroeconomic uncertainty on macroeconomic variables. Finally, Section 6 concludes. Proofs of the results and additional details are presented in a set of appendices.

2 A panel Markov-switching MIDAS model

We assume the sampling frequency for the ith variable of the g-th unit of the panel, y_{igt}, is $t = m, 2m, \ldots, mT_q$, with m integer and larger than or equal to one, for $i = 1, \ldots, n_g$, $g = 1, \ldots, G$, and that for the covariates x_{igjt}, $j = 1, \ldots, N$, is $t = 1, 2, 3, \ldots, mT_q$. The following model is evaluated at $t = m, 2m, 3m, \ldots, mT_q$

$$c_{ig}(L^m, s_{gt})y_{igt} = \mu_{ig}(s_{gt}) + \sum_{j=1}^{N} \delta_{igj}(L, s_{gt})x_{igjt} + \varepsilon_{igt} \tag{1}$$

financial shocks, we also consider a financial uncertainty measure based on systemic risk and proposed in Billio et al. (2016a) for the EU financial market.

$\forall i, g$, where $\varepsilon_{igt} \sim \mathcal{N}(0, \sigma^2_{ig})$ i.i.d. for all t, and

$$c_{ig}(L^m, s_{gt}) = 1 - \sum_{l=1}^{c} L^{ml} c_{igl}(s_{gt}) \tag{2}$$

$$\delta_{igj}(L, s_{gt}) = \sum_{l=0}^{v} \delta_{igjl}(s_{gt}) L^l \tag{3}$$

with L^m the lag operator defined as $L^m y_{igt} = y_{igt-m}$, and s_{gt}, $t = m, \ldots, mT_q$ is a unit-specific Markov chain process with transition probability $P(s_{gt} = k | s_{gt-m} = l) = p_{glk}$, $l, k = 1, \ldots, K$.

The model presented above is quite general since it assumes the dependent variables are observed at the same ($m = 1$) or lower ($m > 1$) frequency then the independent variables. In bridge models, the independent variables are temporally aggregated and a dynamic model is then specified for the aggregated variables. We take here a more flexible modelling approach, as the independent variables can be aggregated with estimated rather than fixed weights.

The modelling framework is quite general, since in principle it allows, through the specification of country- and variable-specific covariates, x_{igjt}, for dynamic interaction effects between the variables of each country and also between variables of different countries. Unfortunately, the interaction effects would lead to a larger number of parameters to estimate and to a potential overfitting problem. Therefore, we leave the modelling of these effects for further research.

The switching coefficients of the model are defined as

$$\mu_{ig}(s_{gt}) = \sum_{k=1}^{K} \xi_{gkt} \mu_{igk}, \tag{4}$$

$$c_{igl}(s_{gt}) = \sum_{k=1}^{K} \xi_{gkt} c_{iglk}, \tag{5}$$

$$\delta_{ijlg}(s_{gt}) = \sum_{k=1}^{K} \xi_{gkt} \delta_{ijlgk}, \tag{6}$$

for $i = 1, \ldots, n_g$, where $\xi_{gkt} = \mathbb{I}_{\{k\}}(s_{it})$.

We assume a hierarchical prior on the switching coefficients, designed in a way that the regime-specific coefficients of the different time series are shrinked toward unit-specific and regime-specific common means, that is

$$\mu_{igk} = \mu_k + \zeta_{\mu,gk} + \eta_{\mu,igk}, \qquad \zeta_{\mu,gk} \sim \mathcal{N}(0, r_{\mu,k}), \;\; \eta_{\mu,igk} \sim \mathcal{N}(0, q_{\mu,gk}) \tag{7}$$

$$c_{iglk} = c_{lk} + \zeta_{c,glk} + \eta_{c,iglk}, \qquad \zeta_{c,glk} \sim \mathcal{N}(0, r_{c,k}), \;\; \eta_{c,iglk} \sim \mathcal{N}(0, q_{c,gk}) \tag{8}$$

$$\delta_{igjlk} = \delta_{jlk} + \zeta_{\delta,gjlk} + \eta_{\delta,igjlk}, \; \zeta_{\delta,gjlk} \sim \mathcal{N}(0, r_{\delta,k}), \; \eta_{\delta,igjlk} \sim \mathcal{N}(0, q_{\delta,gk}) \tag{9}$$

with $Cov(\eta_{\mu,igk}, \eta_{c,i'g'lk'}) = 0$, $Cov(\eta_{\mu,igk}, \eta_{\delta,i'g'jlk'}) = 0$, and $Cov(\eta_{c,iglk}, \eta_{\delta,i'g'jlk'}) = 0$, for all i, i', g, g', j, l, k, k'. The unit- and regime-specific random effects are $\zeta_{\mu,gk}$, $\zeta_{c,glk}$ and $\zeta_{\delta,gjlk}$.[5]

[5] An alternative modelling strategy is to shrink the coefficients towards a variable-specific mean, $\zeta_{\mu,ik}$, instead of a unit-specific mean, $\zeta_{\mu,gk}$. This can be obtained by setting $\mu_{igk} = \mu_k + \zeta_{\mu,ik} + \eta_{\mu,igk}$, $\eta_{\mu,igk} \sim \mathcal{N}(0, q_{\mu,gk})$, $\zeta_{\mu,ik} \sim \mathcal{N}(0, r_{\mu,k})$. A similar model can be used for c_{iglk} and δ_{igjlk}. The choice of the hierarchical prior distribution depends mainly on the application. In our empirical exercise we believe the impact of uncertainty shocks might

The hierarchical prior specification is particularly suited in this context where the number of parameters to estimate is large also due to the Markov switching mechanism. While the estimation of all the model parameters can lead to overfitting problems, the use of restrictions, such as parameter pooling, can be a strong assumption leading to misleading results and bad forecasting performance. The hierarchical specification allows instead for different degrees of information pooling across units and series, by assuming conditional independence across units and series and by introducing panel- and country-specific common factors (e.g., see Canova and Ciccarelli (2004, 2009), Bassetti et al. (2014), Billio et al. (2016b)). Also, this motivates the use of panel models with random effects instead of using pooling or equation-by-equation estimation.

In order to complete the elicitation of the hierarchical prior distribution, we assume a truncated normal prior distribution for the common intercepts $\boldsymbol{\mu} = (\mu_1, \ldots, \mu_K)'$

$$\boldsymbol{\mu} \sim \mathcal{N}_K(\mathbf{0}_K, s_0^2 I_K)\mathbb{I}_{\mathcal{A}_\mu}(\boldsymbol{\mu}) \tag{10}$$

where $\mathbf{0}_k$ is the k-dimensional null vector, I_k the k-dimensional identity matrix, and $\mathcal{A}_\mu$ is the set of all possible values of $\boldsymbol{\mu}$ which satisfy some identification constrains, such as $\mu_1 < \ldots < \mu_K$. See Frühwirth-Schnatter (2006), ch. 3-4 for an introduction to the problems of regime identification and label switching and Billio et al. (2016b) and Billio et al. (2012) for the use of such constrains in business cycle analysis. We shall notice that alternative identification constrains can be used. E.g., if one expects the durations of the states are different, then constraints on the transition matrix can be employed to effectively identify the regimes.

We assume cross-regime independent normal prior distributions for common coefficients $\mathbf{c}_k = (c_{1k}, \ldots, c_{ck})'$ and $\boldsymbol{\delta}_k = (\delta_{10k}, \ldots, \delta_{1pk}, \ldots, \delta_{\nu 0k}, \ldots, \delta_{\nu pk})'$

$$\mathbf{c}_k \sim \mathcal{N}_c(\mathbf{0}_c, r_0^2 I_c) \tag{11}$$

$$\boldsymbol{\delta}_k \sim \mathcal{N}_{N(\nu+1)}(\mathbf{0}_{N(\nu+1)}, r_0^2 I_{N(\nu+1)}) \tag{12}$$

i.i.d. over $k = 1, \ldots, K$. We assume cross-regime independent inverse gamma prior distributions for the two sets of scale hyper-parameters $q_{\mu,gk}$, $q_{c,gk}$, $q_{\delta,gk}$ and $r_{\mu,k}$, $r_{c,k}$, $r_{\delta,k}$ of the panel coefficients

$$q_{\mu,gk}, q_{c,gk}, q_{\delta,gk} \overset{i.i.d.}{\sim} \mathcal{IG}(n_0, s_0) \tag{13}$$

$$r_{\mu,k}, r_{c,k}, r_{\delta,k} \overset{i.i.d.}{\sim} \mathcal{IG}(n_0, s_0) \tag{14}$$

i.i.d. over $k = 1, \ldots, K$, $g = 1, \ldots, G$, where $\mathcal{IG}(n, s)$ denotes the inverse gamma distribution with shape parameters n and s and density function given in Appendix B.6.

As regards the scale parameter of the error term in Eq. 1, we apply the same strategy

substantial differ across countries (units), but variables in the same country will respond similarly with a larger negative effect in the contraction regime than in the expansion regime. This motives our choice for unit- and regime-specific random effects.

followed in the specification of the coefficients prior, that is

$$\sigma_{ig}^2 = \sigma^2 \lambda_{ig}^{-1} \chi_g^{-1} \tag{15}$$

for $g = 1, \ldots, G$, $i = 1, \ldots, n_g$, where σ^2 is a common scaling factor, and χ_g is a unit-specific factor which captures the potential cross-unit variance heterogeneity, and λ_{ig} is a variable-specific scale factor.

The following inverted gamma and gamma hierarchical prior distributions are usually assumed for the scale parameters in multi country panel models (see, e.g., Bassetti et al. (2014) and references therein)

$$\begin{aligned} \sigma^2 &\sim \mathcal{IG}(a_0, b_0) && (16)\\ \lambda_{ig} &\sim \mathcal{G}a(c_{10}, d_{10}) && (17)\\ \chi_g &\sim \mathcal{G}a(c_{20}, d_{20}), && (18) \end{aligned}$$

i.i.d. over $g = 1, \ldots, G$, $i = 1, \ldots, n_g$, where $\mathcal{G}a(n, s)$ denotes the gamma distribution with shape parameters n and s and density function given in Appendix B.7.

Finally, we assume independent hierarchical Dirichlet prior distributions for the rows of the unit-specific transition probabilities. Let $\mathbf{p}_{gl} = (p_{g,l1}, \ldots, p_{g,lK})'$ and $\boldsymbol{\nu}_l = (\nu_{l1}, \ldots, \nu_{lK})'$, then our prior distribution is

$$\begin{aligned} \mathbf{p}_{gl} &\sim \mathcal{D}ir(\phi\nu_1, \ldots, \phi\nu_K) && (19)\\ \boldsymbol{\nu}_l &\sim \mathcal{D}ir(1/K, \ldots, 1/K) && (20) \end{aligned}$$

i.i.d. over $l = 1, \ldots, K$ and $g = 1, \ldots, G$, where $\phi = \sum_{k=1}^{K} \nu_K$.

Note that under the hierarchical prior assumption, the dynamic panel model can be re-interpreted as a random effect model with unit-specific and regime-specific effects for intercepts, regression coefficients and scale parameters. In fact, by replacing the coefficients in Eq. 1 with the switching representation in Eq. 4-6 and the hierarchical prior structure in Eq. 7-9, and rearranging terms one obtains the following model

$$\begin{aligned} y_{igt} = \sum_{k=1}^{K} \xi_{gkt} \Big((\mu_k + \zeta_{\mu,gk} + \eta_{\mu,igk}) + \sum_{l=1}^{c} y_{igt-ml} (c_{lk} + \zeta_{c,glk} \\ + \eta_{c,iglk}) + \sum_{j=1}^{N} \sum_{l=0}^{\nu} x_{igjt-l} (\delta_{jlk} + \zeta_{\delta,gjlk} + \eta_{\delta,igjlk}) \Big) + \varepsilon_{igt} \end{aligned} \tag{21}$$

for $t = m, 2m, \ldots, T_q m$, which can be regarded as the Markov-switching extension of a panel MIDAS model such as the one discussed in Khalaf et al. (2013).

The expanded representation of our Bayesian panel MS-UMIDAS model can be useful in order to understand how the random effects enter into the model, but it can result uneasy for presentation of the inference procedure. Nevertheless, conditionally on the allocation variables,

and combining the compact MIDAS representation (see, e.g., Pettenuzzo et al. (2014)) with a compact switching regression representation (see, e.g., Billio et al. (2016b)), the model given above can still be written in a compact form. Let us define the allocation variable vector $\boldsymbol{\xi}_{gt} = (\xi_{g1t}, \ldots, \xi_{gKt})'$, the autoregressive component vector $\mathbf{v}_{igt} = (y_{igt-m}, \ldots, y_{igt-mc})'$ and the vector $\mathbf{x}_{ig,jt} = (x_{ig,jt}, \ldots, x_{ig,jt-\nu})'$ of the j-th exogenous variable, $j = 1, \ldots, N$, contemporaneous and at different lags. Also, define the parameter vectors $\boldsymbol{\mu} = (\mu_1, \ldots, \mu_K)'$, $\mathbf{c}_l = (c_{l1}, \ldots, c_{lK})'$, $\boldsymbol{\delta}_{jl} = (\delta_{jl1}, \ldots, \delta_{jlK})'$, $\boldsymbol{\zeta}_{\mu,g} = (\zeta_{\mu,g1}, \ldots, \zeta_{\mu,gK})'$, $\boldsymbol{\zeta}_{c,gl} = (\zeta_{c,gl1}, \ldots, \zeta_{c,glK})'$, $\boldsymbol{\zeta}_{\delta,gjl} = (\zeta_{\delta,gjl1}, \ldots, \zeta_{\delta,gjlK})'$, $\boldsymbol{\eta}_{\mu,ig} = (\eta_{\mu,ig1}, \ldots, \eta_{\mu,igK})'$, $\boldsymbol{\eta}_{c,igl} = (\eta_{c,igl1}, \ldots, \eta_{c,iglK})'$, and $\boldsymbol{\eta}_{\delta,igjl} = (\eta_{\delta,igjl1}, \ldots, \eta_{\delta,igjlK})'$. Then the following result holds.

Proposition 1. *The model in Eq. 21 can be written as*

$$y_{igt} = \mathbf{z}'_{igt}(\boldsymbol{\beta} + \boldsymbol{\zeta}_g + \boldsymbol{\eta}_{ig}) + \varepsilon_{igt} \tag{22}$$

with $\boldsymbol{\beta} = (\boldsymbol{\mu}, \mathbf{c}_1, \ldots, \mathbf{c}_c, \boldsymbol{\delta}_{10}, \ldots, \boldsymbol{\delta}_{N\nu})'$ *the parameter vector,* $\mathbf{z}_{igt} = (\boldsymbol{\xi}'_{gt}, \mathbf{v}'_{igt} \otimes \boldsymbol{\xi}'_{gt}, \mathbf{x}'_{ig,1t} \otimes \boldsymbol{\xi}'_{gt}, \ldots, \mathbf{x}'_{ig,Nt} \otimes \boldsymbol{\xi}'_{gt})'$ *the covariate vector of dimension* $K(1 + c + N(\nu + 1)) \times 1$, $\boldsymbol{\eta}_{ig} = (\boldsymbol{\eta}_{\mu,ig}, \boldsymbol{\eta}_{c,ig1}, \ldots, \boldsymbol{\eta}_{c,igc}, \boldsymbol{\eta}_{\delta,ig10}, \ldots, \boldsymbol{\eta}_{\delta,igN\nu})'$, *the variable-specific random effects vector and* $\boldsymbol{\zeta}_g = (\boldsymbol{\zeta}_{\mu g}, \boldsymbol{\zeta}_{c,g1}, \ldots, \boldsymbol{\zeta}_{c,gc}, \boldsymbol{\zeta}_{\delta,g10}, \ldots, \boldsymbol{\zeta}_{\delta,gN\nu})'$ *the unit-specific random effects vector.*

Proof. See Appendix A. □

3 Posterior approximation

Let $\mathbf{y} = (\mathbf{y}'_{m(c+1)}, \ldots, \mathbf{y}'_{mT_q})'$ be the observation vector, with $\mathbf{y}_t = (\mathbf{y}'_{1t}, \ldots, \mathbf{y}'_{Gt})'$, $\mathbf{y}_{gt} = (y_{1gt}, \ldots, y_{n_ggt})'$, $\boldsymbol{\xi} = (\boldsymbol{\xi}'_1, \ldots, \boldsymbol{\xi}'_G)'$ the allocation variable vector, with $\boldsymbol{\xi}_g = (\boldsymbol{\xi}'_{g,m(c+1)}, \ldots, \boldsymbol{\xi}'_{g,mT_q})'$, $\boldsymbol{\eta}_{igk} = (\eta_{\mu,igk}, \eta_{c,igk}, \eta_{\delta,igk})'$, $\boldsymbol{\zeta} = (\boldsymbol{\zeta}'_1, \ldots, \boldsymbol{\zeta}'_G)'$, $\boldsymbol{\eta} = (\boldsymbol{\eta}'_{11}, \ldots, \boldsymbol{\eta}'_{n_GG})'$, then the complete likelihood of the model in Eq. 22 is

$$L(\mathbf{y}, \boldsymbol{\xi} | \boldsymbol{\theta}, \boldsymbol{\zeta}, \boldsymbol{\eta}) = \prod_{t \in \mathcal{T}} \prod_{g=1}^{G} \prod_{i=1}^{n_g} (2\pi\sigma^2_{ig})^{-1/2} \exp\left\{ -\frac{\varepsilon^2_{igt}}{2\sigma^2_{ig}} \right\} \prod_{l=1}^{K} \prod_{k=1}^{K} p_{glk}^{\xi_{glt-1}\xi_{gkt}} \tag{23}$$

where $\varepsilon_{igt} = y_{igt} - \mathbf{z}'_{igt}(\boldsymbol{\beta} + \boldsymbol{\zeta}_g + \boldsymbol{\eta}_{ig})$, $\mathbf{z}_{igt}$ is defined in Proposition 1, $\mathcal{T} = \{m(c+1), mc + 2m, \ldots, mT_q\}$, and $\boldsymbol{\theta} = (\boldsymbol{\beta}, \sigma^2, \boldsymbol{\lambda}, \boldsymbol{\chi}, \mathbf{q}, \mathbf{p})$ is the parameter vector, with $\boldsymbol{\lambda} = (\lambda_{11}, \ldots, \lambda_{n_GG})'$, $\boldsymbol{\chi} = (\chi_1, \ldots, \chi_G)'$, $\mathbf{q} = (\mathbf{q}'_{11}, \ldots, \mathbf{q}'_{GK})'$, $\mathbf{r} = (\mathbf{r}'_1, \ldots, \mathbf{r}'_K)'$, $\mathbf{q}_{gk} = \text{diagrv}\{Q_{gk}\}$, $\mathbf{r}_k = \text{diagrv}\{R_k\}$, and $\mathbf{p} = (\text{vec}\{P_1\}, \ldots, \text{vec}\{P_G\})$.

The joint posterior distribution is

$$\begin{aligned} \pi(\boldsymbol{\xi}, \boldsymbol{\zeta}, \boldsymbol{\eta}, \boldsymbol{\theta} | \mathbf{y}) \propto L(\mathbf{y}, \boldsymbol{\xi} | \boldsymbol{\theta}, \boldsymbol{\zeta}, \boldsymbol{\eta}) \pi(\sigma^2) \prod_{k=1}^{K} \pi(\mu_k) \pi(\mathbf{c}_k) \pi(\boldsymbol{\delta}_k) \pi(R_k) \pi(\boldsymbol{\nu}_k) \\ \prod_{g=1}^{G} \pi(\chi_g) \pi(\boldsymbol{\zeta}_{gk}) \pi(Q_{gk}) \pi(\mathbf{p}_{gk}) \prod_{i=1}^{n_g} \pi(\lambda_{ig}) \pi(\boldsymbol{\eta}_{igk}) \end{aligned} \tag{24}$$

which is not analytically tractable. Thus a Gibbs sampler is applied, which iterates over the

following steps:

i) Draw $\boldsymbol{\zeta}, \boldsymbol{\eta}, \boldsymbol{\xi}, \boldsymbol{\beta}, P_1, \ldots, P_G, \boldsymbol{\nu}$ from $p(\boldsymbol{\zeta}, \boldsymbol{\eta}, \boldsymbol{\xi}, \boldsymbol{\beta}, \mathbf{p}, \boldsymbol{\nu} | \sigma^2, \boldsymbol{\lambda}, \boldsymbol{\chi}, \mathbf{q}, \mathbf{r}, \mathbf{y})$.

ii) Draw σ^2, $\boldsymbol{\lambda}$, $\boldsymbol{\chi}$, $\mathbf{q}$, $\mathbf{r}$ from $p(\sigma^2, \boldsymbol{\lambda}, \boldsymbol{\chi}, \mathbf{q}, \mathbf{r} | \boldsymbol{\beta}, \mathbf{p}, \boldsymbol{\nu}, \boldsymbol{\zeta}, \boldsymbol{\eta}, \boldsymbol{\xi}, \mathbf{y})$.

We consider a blocked and collapsed multi-move Gibbs sampler (e.g., see Liu (1994), Roberts and Sahu (1997)). As regard the collapsed part, we apply the following result.

Proposition 2. *Marginalizing out the random effects in the right-hand side of Eq. 22 one obtains*

$$y_{igt} = \mathbf{z}'_{igt}\boldsymbol{\beta} + \tilde{\varepsilon}_{igt}, \quad \tilde{\varepsilon}_{igt} \sim \mathcal{N}(0, \sigma^2_{igt}) \tag{25}$$

$t = m(c+1), 2m, \ldots, mT_q$, *with* $\sigma^2_{igt} = \sigma^2 \lambda_{ig}^{-1} \chi_g^{-1} + \mathbf{z}'_{igt}(R + Q_g)\mathbf{z}_{igt}$.

Proof. See Appendix A. □

The model in Eq. 25 naturally exhibits heteroskedastic effects, with time-variation in the error variance driven by the Markov-switching process, and is still linear in the parameter $\boldsymbol{\beta}$, conditionally to the hidden Markov chain. This motivates the use of a collapsed Gibbs (see Kaufmann (2010)) for the Step *i)*

i.1) Draw $\boldsymbol{\beta}, P_1, \ldots, P_G, \boldsymbol{\nu}, \boldsymbol{\xi}$ from $p(\boldsymbol{\beta}, \mathbf{p}, \boldsymbol{\nu}, \boldsymbol{\xi} | \sigma^2, \boldsymbol{\lambda}, \boldsymbol{\chi}, \mathbf{q}, \mathbf{r}, \mathbf{y})$.

i.2) Draw $\boldsymbol{\zeta}, \boldsymbol{\eta}$ from $p(\boldsymbol{\zeta}, \boldsymbol{\eta} | \boldsymbol{\beta}, \mathbf{p}, \boldsymbol{\nu}, \sigma^2, \boldsymbol{\lambda}, \boldsymbol{\chi}, \mathbf{q}, \mathbf{r}, \boldsymbol{\xi}, \mathbf{y})$.

In the derivation of the full conditional distribution in the step *i.1)* we use the complete data likelihood of the model in Eq. 25. Each step of the Gibbs sampler is blocked further. The details of the derivation of the full conditional distributions and the sampling methods used are given in Appendix B.

4 Simulation Study

In this section, we study the efficiency of the proposed MCMC procedure for posterior approximation.

4.1 Setting

We consider the following model for the unit-specific exogenous variable

$$z_{gt} = 0.9 z_{gt-1} + 0.5\kappa_{gt}, \quad \kappa_{gt} \overset{i.i.d.}{\sim} \mathcal{N}(0, 1) \tag{26}$$

$g = 1, \ldots, 13$, with sampling frequency, $t = 1, 2, 3, \ldots, 1200$. For the endogenous variables, we assume

$$y_{igt} = \mu_{ig}(s_{gt}) + 0.2 y_{igt-3} + \mathbf{x}'_{igt}\boldsymbol{\delta}_{ig}(s_{gt}) + \varepsilon_{igt}, \quad \varepsilon_{igt} \overset{i.i.d.}{\sim} \mathcal{N}(0, 0.1^2) \tag{27}$$

$i = 1, \ldots, 5$, with a sampling frequency $t = 3, 6, 9, \ldots, 1200$ which is lower than the frequency of the exogenous variables. $\boldsymbol{\delta}_{ig}(s_{gt}) = (\delta_{ig1}(s_{gt}), \delta_{ig2}(s_{gt}), \delta_{ig3}(s_{gt}))'$ is the vector of exogenous

Table 1: Results on convergence and efficiency

Panel (a)					
	ACF(1)	ACF(5)	ACF(10)	MSE(20)	MSE(100)
Parameters ($\boldsymbol{\theta}$)	0.049	0.036	0.021	$8.2 \cdot 10^{-4}$	$9.4 \cdot 10^{-5}$
States (s_{gt}, $\forall g, t$)	0.833	0.252	0.048	$4.7 \cdot 10^{-3}$	$1.1 \cdot 10^{-3}$
Panel (b)					
	ACF(1)	ACF(5)	ACF(10)	MSE(20)	MSE(100)
Parameters ($\boldsymbol{\theta}$)	0.029	0.021	0.019	$1.3 \cdot 10^{-5}$	$2.0 \cdot 10^{-5}$
States (s_{gt}, $\forall g, t$)	0.311	0.012	0.031	$0.16 \cdot 10^{-5}$	$0.93 \cdot 10^{-5}$

Note: Panel (a): persistent regimes ($p_{gii} = 0.95$, $\forall i, g$). Panel (b): strongly persistent regimes ($p_{gii} = 0.99$, $\forall i, g$). In all panels: cross-parameter (first row) and cross-state (second row) maximum empirical autocorrelation at the lag k (ACF(k)) and average mean square error at the j-th iteration of the MCMC chain (MSE(j)).

coefficients and $\mathbf{x}_{igt} = (x_{ig1t}, x_{ig2t}, x_{ig3t})'$ is a vector of covariates. In the above equation, s_{gt} is a unit-specific hidden Markov chain process with values in $\{1, 2\}$. We consider two cases for the transition probabilities: persistent regimes, i.e. $p_{g11} = 0.95$, $p_{g22} = 0.95$, $\forall g$ and strongly persistent regimes, i.e. $p_{g11} = 0.99$, $p_{g22} = 0.99$, $\forall g$.

The unit-specific exogenous variable z_{gt} is common to all series of the i-th unit and is included in the model with its current value and with two lags, i.e. $x_{ig1t} = z_{gt}$, $x_{ig2t} = z_{gt-1}$ and $x_{ig3t} = z_{gt-2}$, $\forall i$, $\forall t$.

For the coefficients in the first regime, we assume

$$\delta_{ig1}(1) \overset{i.i.d.}{\sim} \mathcal{N}(1, 0.1^2),\ \delta_{ig2}(1) \overset{i.i.d.}{\sim} \mathcal{N}(-0.1, 0.1^2),\ \delta_{ig3}(1) \overset{i.i.d.}{\sim} \mathcal{N}(0.5, 0.1^2),$$

$i = 1, \ldots, 5$. For the second regime we set:

$$\delta_{ig1}(2) \overset{i.i.d.}{\sim} \mathcal{N}(1, 0.1^2),\ \delta_{ig2}(1) \overset{i.i.d.}{\sim} \mathcal{N}(-0.1, 0.1^2),\ \delta_{ig3}(1) \overset{i.i.d.}{\sim} \mathcal{N}(-0.5, 0.1^2)$$

An example of time series generated from the model in Eq. 27 is given in Figure C.1, Appendix C.

4.2 MCMC convergence and efficiency

We fit the model given in Eq. 1, on the simulated dataset, assuming $c = 3$ and $\nu = 1$. Figure C.2 in Appendix C shows the MCMC raw output, the MCMC progressive averages and the MCMC chain empirical autocorrelation function (ACF). From a graphical inspection of the MCMC raw output one can see that the mixing of the MCMC chain is good, resulting in a low autocorrelation level. As documented in Table 1, panel (a), in the case of persistent regimes the maximum ACF at the 10th lag is 0.021 for the parameters and 0.048 for the hidden states (see also the ACF plots in Figure C.2).

The progressive averages in Figure C.2 show that the MCMC chain is converging. The

posterior estimates for the coefficients δ_{ijgk}, obtained after removing an initial burn-in sample of 1,000 MCMC iterations, are given in Fig C.2. The mean values of the coefficients δ_{ijlk} in the two regimes is recovered.

The overall average MSE for the parameter estimates is documented in Table 1. The MSE decreases rapidly over the MCMC iterations and at the 100th iteration it is equal to $9.4 \cdot 10^{-5}$ which suggests convergence to the true parameter values (see also Figure C.4 in Appendix C).

As regards the latent variables, the good mixing of the MCMC chain and its convergence in the latent space is clear from the allocation maps in Figure 1. In each plot we report the unit-specific allocation variables $\mathbb{I}_k(s_{gt}^{(j)})$, for each unit, i.e. $g = 1, \ldots, 13$ (vertical axis), over the first 20 MCMC iterations, i.e. $j = 1, \ldots, 20$ (horizontal axis). The average MSE across the hidden Markov processes in the panel is decreasing over the MCMC iterations and at the 100th iteration it is equal to $1.1 \cdot 10^{-3}$ (see Table 1, panel (a)), which indicates convergence of the MCMC chain to the true values of the hidden states (see Figure C.4 in Appendix C). The MSE and MCMC mixing improve for both parameter and hidden state in the strong persistent case (see Table 1, panel (b)).

5 Economic Uncertainty in a Panel of Countries

In this section, we apply our model to study the effects of uncertainty shocks on different sectors and variables across a panel of countries. After a brief overview on the main contributions in the uncertainty literature, we describe the dataset and the measures of uncertainty that we consider, comment on the main empirical results, and present some robustness analysis.

5.1 Uncertainty and macroeconomic effects

The interest in uncertainty has grown enormously over the recent years. Since the seminal paper of Bloom (2009), research has focused on creating new approaches to measure uncertainty and its effects. Bloom (2009) himself defines his measure of uncertainty as the unconditional volatility of stock market returns. Baker et al. (2015) develop an index of economic policy uncertainty which reflects the frequency of uncertainty-related words in the articles of leading newspapers. Scotti (2013) proposes an uncertainty index which aims at capturing how uncertain agents are about the current real economic activity, using surprises from Bloomberg forecasts. Rossi and Sekhposyan (2015) create a macroeconomic uncertainty index based on comparing the realized forecast error of the real GDP growth with the historical forecast error distribution of the same variable. Jurado et al. (2015) and Carriero et al. (2016) provide a measure of uncertainty based on whether a large set of macroeconomic and financial variables become more or less predictable.

Despite different measures of uncertainty have been proposed, the evidence on the effects of uncertainty on the macroeconomic activity is pretty homogeneous, and different studies agree that macroeconomic uncertainty is countercyclical. Here we sketch only some of the contributions to a voluminous and expanding literature. For a more extensive review see Bloom (2014). An increase in uncertainty is typically associated with large declines in real activity.

Figure 1: Allocation maps for the simulated study

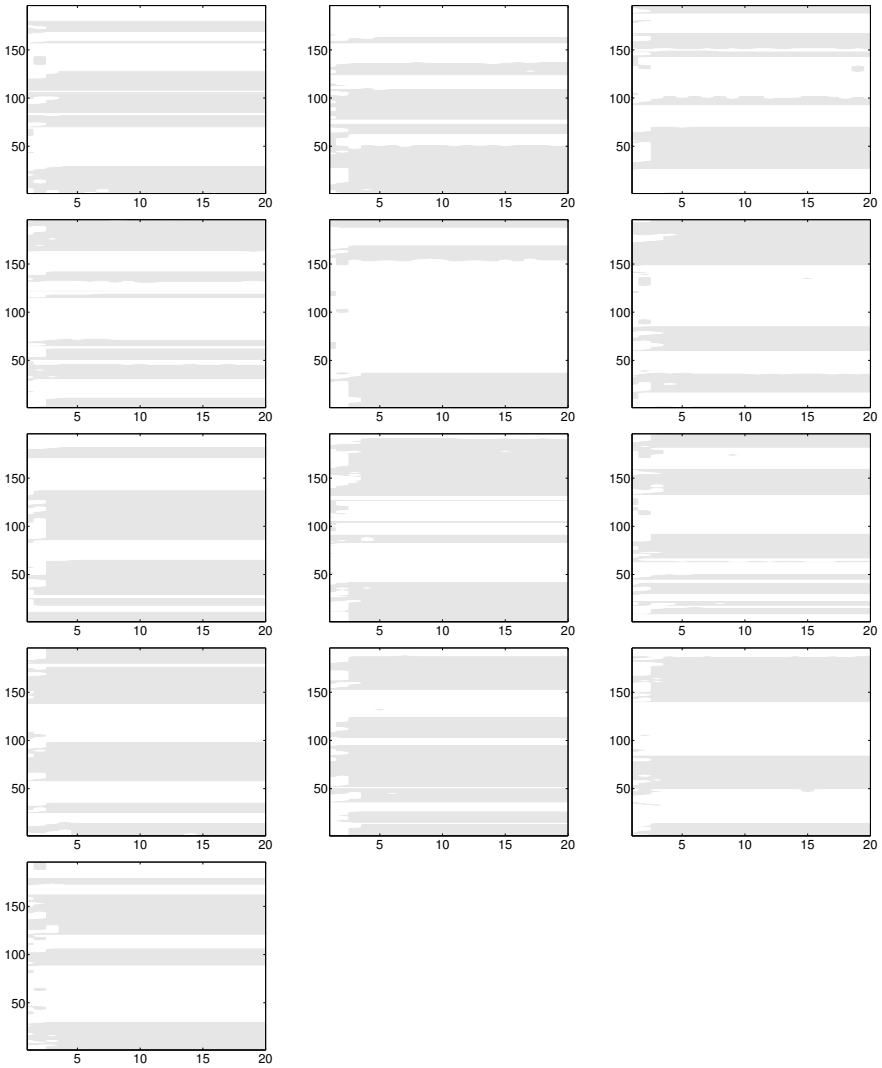

Note: the figure shows the unit-specific (one for each plot) allocation variables ($\mathbb{I}_k(s_{gt}^{(j)})$) over time (vertical axis, $t = 1, \ldots, 196$) and over the first 20 MCMC iterations (horizontal axis, $j = 1, \ldots, 20$).

Caggiano et al. (2014) show that the impact of an uncertainty shock on unemployment in the U.S. is much larger during recessions, suggesting a different behavior depending on the state of the economy. A new study by Carriero et al. (2016) proposes an econometric framework for jointly measuring uncertainty and capturing its impact on the economy. The authors find sizeable effects of uncertainty on key macroeconomic variables. Ferrara and Guerin (2015) analyze the role of uncertainty for the U.S. in a mixed-frequency set up and find that credit and labor market variables react the most to uncertainty shocks, showing a prolonged negative response. Ludvigson et al. (2015) address the question on whether uncertainty and real economic activity could affect one another contemporaneously. They find that higher uncertainty in recessions is endogenous to business cycle fluctuations.

Our empirical analysis enters as a contribution to compare the effects of two different types of uncertainty, precisely macroeconomic uncertainty and financial uncertainty, on macroeconomic variables and it does this by extending the analysis in previous literature to a panel of countries, allowing for the possibility of switching in the effects, and to data at different frequencies.

5.2 Dataset

In our analysis, we consider a panel of $G = 13$ countries, that are: United States (US), Europe (EU), Japan (JP), Germany (DE), France(FR), United Kingdom (UK), Italy (IT), Canada (CA), the Netherlands (NE), Norway (NW), Spain (SP), Sweden (SW) and Switzerland (CH). The choice of the countries is based on the availability of data from the Consensus Economics, from which we construct our measure of macroeconomic uncertainty.

Our macroeconomic uncertainty measure is based on the disagreement about the projections for the real GDP growth among the professional forecasters participating to the Consensus economic polls. In particular, we take the standard deviations of the projections as our uncertainty measure. A further clarification on how we compute the measure is needed. The respondents to the survey are asked to give their expectations on the current and next calendar year. Following Dovern et al. (2012), we construct our measure of disagreement on one-year-ahead forecasts. Ferrara and Guérin (2015) also use the same approach for US data. Therefore, as in their papers, we need first to transform fixed-event forecasts into fixed-horizon forecasts, by taking the average of the forecasts for the current and next calendar year weighted by their share in the forecasting horizon:

$$x_t^e = \frac{k}{12} x_{t+k|t} + \frac{12-k}{12} x_{t+12+k|t}, \tag{28}$$

where x_t^e is the one-year-ahead expectation, $x_{t+k|t}$ is the current-year expectation, $x_{t+12+k|t}$ is the next-year expectation and k are the months to the end of the current year at the moment the survey is made. The standard deviation is then computed on this one-year-ahead expectation.

As a measure of financial uncertainty we consider the U.S. VIX, as in Bloom (2009). We consider the U.S. measure also when looking at the uncertainty in other countries because it is the longest series available. Further, we computed the correlation of the U.S. VIX with the series of VIX available for other countries (e.g. UK, Canada, Italy) and the correlation is high.

[6] In Appendix E, we nevertheless repeat the exercise using the Financial Uncertainty Index developed in Ludvigson et al. (2015) for the US economy and a financial uncertainty measure based on systemic risk and proposed in Billio et al. (2016a) for the EU financial market.

The macroeconomic variables we consider for each country in the panel are the following: real GDP (labelled GDP in tables) and industrial production growth rates (IPI), employment growth rate (Emp), consumption growth (Con), inflation (Inf), nominal earnings growth (Ner), real earnings growth (Rer), working hours growth (Hours), nominal interest rates (IR), stock market index growth (Stock) and monetary M2 aggregate growth (M2). All variables are sampled at a quarterly frequency from 1997 to 2014. The availability of the data for each country, the sample period and the source are given in Appendix D. Figures D.1-D.2 show the dependent variables in the panel. Figure D.3 shows the exogenous variables (i.e. forecast disagreement and VIX). All the variables are standardized to have comparable scales for the coefficients.[7]

The uncertainty variables are collected at monthly frequency and the other macroeconomic variables at quarterly frequency. The model uses four lags for the quarterly variables and two lags (contemporaneous and 1-quarter lag) for the monthly variables, and two regimes. The first regime requires that the common intercepts $\boldsymbol{\mu}$ are non-positive. We define it as *contraction* regime. In the second regime, the common intercepts are equal to zero or positive. We define it as *expansion* regime.[8] As mentioned, the use of different regimes and of data at different frequencies attenuates possible endogeneity problems of uncertainty.

5.3 Results

Following the notation outlined in the previous sections, we first look at the country- and series-specific impact $\delta_{ijlgk} = \delta_{jlk} + \zeta_{\delta,gjlk} + \eta_{\delta,igjlk}$ in the two regimes. Given that we consider the information in the contemporaneous and previous quarter, we end up with six months of information and correspondingly six coefficients. In Table 2 we therefore provide a summary representation of them by reporting the median of the sum of the six coefficients, monthly contemporaneous and lagged variables, that have 90% of the mass different from zero for the two regimes. This allows us to take into account the parameter uncertainty in the results, since we sum the full distributions of the coefficients and we drop those that include zero in the 90% highest posterior density (HDP). The table reports results only for the VIX because the HDP of coefficients associated to macroeconomic uncertainty includes in all cases zero, confirming the marginal role of macroeconomic uncertainty with respect to financial uncertainty [9]. In all cases the sum of coefficients is larger in absolute value in regime 1 than in regime 2, supporting

[6] In Figure D.4 in Appendix E, we report the 3-year rolling correlation of the U.S. VIX with the VIX for the other countries we have available. In Figure D.5 we show the correlation of the VIX with the macroeconomic uncertainty measures for each country. The three monthly series are kept seperately in this graph.

[7] See figures E.3-E.5 in Appendix E for the impact of uncertainty on the different variables in the original variable-specific scale.

[8] Economic theory supports that the variable M2 can both grow or decrease in contraction periods. We notice that in all the countries in our dataset M2 mostly increases during recessions, therefore we take minus its growth rate and apply the described restriction.

[9] While the sum of the effects of macroeconomic uncertainty is insignificant, as we will see some of the monthly effects are instead significant.

evidence in Caggiano et al. (2014), Alessandri and Mumtaz (2014) and Ludvigson et al. (2015). Moreover, the sum of coefficients is significant for both regimes for almost all countries for the variables GDP, Industrial production, real earnings, stock markets, M2, whereas it sometimes includes zero in the HDP for employment, consumption, inflation, nominal earnings and hours, in particular for the second regime. Also, the effect of financial uncertainty shocks on interest rate is homogeneous across 10 countries, but it differs for Japan (not significant on both regimes), Canada and Switzerland (not significant in expansion). The Abenomics for Japan, the stronger expansion of Canada in periods of high US financial uncertainty, and the Switzerland exchange rate interventions are possible explanations for this finding.

We now move to look at the disaggregated results in more detail. Figures 2-4 show the impact of uncertainty shocks on the variables of different countries (GDP and IPI growth rates, employment, consumption, Nominal ER, Real ER, Inflation, Hours, IR, Stock and M2) at different months, $j = 1, 2, 3$, lags, $l = 0, 1$ and regimes $k = 1, 2$. The left column plots the impact of the forecast disagreement and the right column plots the impact of VIX. The regimes extracted for each country are reported in Figures E.1-E.2 in section E.

In each plot, the circles represent the common impact δ_{jlk} in the two regimes, i.e. $(\delta_{jl1}, \delta_{jl2})$, for the pair shock lag l and variable j labelled with (l, j) in the plot. Thus the uncertainty coefficients at the first, second and third month of the contemporaneous quarter are labelled with $(0,1), (0,2), (0,3)$ for the forecast disagreement and with $(0,4), (0,5), (0,6)$ for the VIX. The uncertainty coefficients at the first, second and third month of the previous quarter are labelled with $(1,1), (1,2), (1,3)$ and with $(1,4), (1,5), (1,6)$ for the forecast disagreement and the VIX respectively.

The dots represent country- and series-specific impact $\delta_{ijlgk} = \delta_{jlk} + \zeta_{\delta,gjlk} + \eta_{\delta,igjlk}$ in the two regimes, i.e. $(\delta_{ijlg1}, \delta_{ijlg2})$ for all countries, $g = 1, \ldots, G$. The dots for each lag are indicated in a different color.

The first clear result is that for all variables, in all countries and both measures of uncertainty, all the estimates (mean of the posterior distributions) are not on the 45 degree line. This means that there is an asymmetric effect of the uncertainty shocks across regimes. For the macroeconomic uncertainty, measured as forecast disagreement, in the contraction regime, contemporaneous shocks in the first and third months (labelled $(0,1)$ and $(0,3)$) have negative impact on GDP, IPI and consumption, whereas at one quarter lag (labelled $(1,1)$ and $(1,3)$) have positive impact on GDP, IPI and consumption. This seems to confirm the drop, rebound and overshoot dynamics described in Bloom (2009). For the same variables, in the expansion regime the coefficients $(0,1)$, $(1,1)$ and $(1,3)$ are negative whereas $(0,2)$, and $(1,2)$ are positive. So, the effects are different in the two regimes, confirming the asymmetric evidence in Caggiano et al. (2014).

The same results apply to the VIX: in the contraction regime the first and third month effects (i.e. label $(0,4)$ and $(0,6)$ in the plots) are negative on GDP, IPI and consumption, whereas at one quarter lag the first and second months (labelled $(1,5)$ and $(1,4)$) have a positive impact on GDP, IPI and consumption. In the expansion regime, the coefficients $(0,4)$, $(1,4)$ and $(1,5)$ are negative whereas $(0,5)$, $(0,6)$ and $(1,6)$ are positive.

Table 2: Effects of financial uncertainty on macroeconomic variables

	GDP		IPI		Emp		Con		Inf		Ner		Rer		Hours		IR		Stock		M2	
Regimes	1	2	1	2	1	2	1	2	1	2	1	2	1	2	1	2	1	2	1	2	1	2
US	-1.07	-0.28	-2.53	-0.67	-0.80	-0.21	-0.84	-0.23	-0.66		-0.26		-0.76	-0.22			-0.78	-0.21	-14.09	-3.72	-1.22	-0.33
EU	-1.18	-0.30	-3.27	-0.85	-0.53		-0.65		-0.86	-0.23	-	-	-	-	-	-	-0.88	-0.23	-17.83	-4.72	-1.25	-0.33
JP	-1.83	-0.46	-7.54	-1.98	-0.27		-1.61	-0.41	-0.66	-0.18	-2.06		-0.76	-0.21	-0.61				-17.17	-4.54	-0.26	
DE	-1.50	-0.39	-4.26	-1.12	-0.51		-1.01	-0.26	-0.54		-0.52		-0.69	-	-1.31		-0.88	-0.23	-19.64	-5.19	-1.97	-0.52
FR	-0.87	-0.22	-2.95	-0.77	-0.48		-0.72		-0.62		-0.26		-0.55		-0.43		-0.85	-0.22	-17.01	-4.51	-	-
UK	-1.1	-0.28	-2.5	-0.65	-0.57		-1.23	-0.32	-0.86	-0.22	-1.01		-1.25	-0.32	-0.86		-0.86	-0.21	-11.97	-3.17	-1.23	-0.32
IT	-1.24	-0.32	-4.21	-1.10	-0.56		-0.94	-0.24	-0.67		-0.29		-0.75	-0.22	-	-	-0.87	-0.23	-18.60	-4.92	-3.87	-1.03
CA	-1.01	-0.26	-3.18	-0.83	-0.56		-0.71		-0.52		-2.27	-	-2.32	-0.62	-0.22		-0.66		-14.87	-3.93	-1.16	-0.32
NE	-1.22	-0.32	-4.47	-1.17	-	-	-	-	-0.85	-0.21	-0.32		-0.87	-0.23	-0.86	-0.22	-0.86	-0.22	-20.20	-5.35	-	-
NW	-1.77	-0.48	-6.52	-1.72	-	-	-	-	-1.32	-0.35	-1.48	-0.38	-2.15	-0.55	-	-	-0.88	-0.24	-21.25	-5.63	-3.12	-0.83
SP	-1.18	-0.3	-3.73	-0.97	-	-	-	-	-1.07	-0.26	-0.82	-0.21	-1.22	-0.33	-1.47	-0.39	-0.89	-0.22	-17.99	-4.78	-	-
SW	-1.67	-0.44	-	-	-	-	-	-			-0.82	-0.21	-0.97	-0.26	-1.03	-0.29	-0.98	-0.26	-19.92	-5.28	-2.95	-0.80
CH	-1.01		-	-	-	-	-	-	-0.46		-	-	-	-	-0.61		-0.87		-15.41	-4.06	-	-

Note: the table reports the sum of the VIX coefficients for the different variables in the 13 countries in regime 1 (recession, first column) and regime 2 (second column). Symbol "-": not available. Empty cell: not significant.

The outcome is similar for other macroeconomic variables, even if some of the coefficients are closer to zero, in particular for the effect of macroeconomic uncertainty. For example, the coefficients for forecast disagreement of the third month in the first regime $(0, 3)$ for the variables employment, nominal and real exchange rates, inflation, hours, interest rate, stock returns and M2 are basically zero for all countries. Such pattern is less evident for the VIX coefficients $(0, 6)$ where only in few occasions the coefficient is zero.

The second important finding is that the coefficients of financial uncertainty are in almost all cases larger than those of macroeconomic uncertainty. For example, a 1% increase in financial uncertainty in the first month of the quarter results in the first regime in a reduction of quarterly GDP higher than 0.2% for all countries, and in the second regime in a reduction of quarterly GDP around 0.15% for all countries. Similar evidence are found for other variables, confirming numbers in Caggiano et al. (2014) that just focus on unemployment. On the contrary, a 1% increase in macroeconomic uncertainty in the first month of the quarter results in the first regime in a reduction of GDP around 0.05%, and in the second regime in a reduction of GDP bigger than 0.05%. Similar evidence is found for the other variables. Interesting, financial uncertainty shocks cause larger drops in the contraction regime, whereas macroeconomic uncertainty shocks in the expansion regime.

The plots also show that the effects of the VIX are more homogeneous across countries, with most of the coefficients close to the common impacts; on the contrary, more heterogeneity exists for the forecast disagreement. The result can be explained by the fact that we use the same US VIX variable for all countries, as it is highly correlated to the VIX of the countries for which it is available, even if for a shorter sample. Forecast disagreement is different across countries, also suggesting that financial uncertainty shocks are rather uniform across countries in our sample whereas macroeconomic uncertainty shocks depend more on domestic economic conditions.

5.4 Robustness

We now investigate the robustness of our results to a set of different hypotheses. First, we remove the contemporaneous effect of financial and macroeconomic uncertainty and only consider the three months of the one-quarter lag. This choice shall remove any possible remaining effects of endogeneity of the uncertainty variables that the Markov-Switching mixed frequency approach cannot capture. Second, we include in our panel MIDAS model only VIX. Third, we include in our panel MIDAS model only the forecast disagreement. For both the second and third cases, we study a model with uncertainty used at higher frequency, but also as quarterly average, to provide evidence on the usefulness of mixed frequency data. Fourth, we investigate different measures of financial uncertainty, addressing the concern that VIX might not be the best measure to account for such uncertainty, see for example Jurado et al. (2015). We apply the Financial Uncertainty Index developed in Ludvigson et al. (2015) and the Financial Entropy Index proposed in Billio et al. (2016a). The former index is built on a large set of financial variables using a new methodology called iterative projection IV. The indicator is only available for the US. The latter index captures the level of systemic risk and measures the entropy of the loss cascades

Figure 2: Impact of uncertainty shocks on different macroeconomic variables

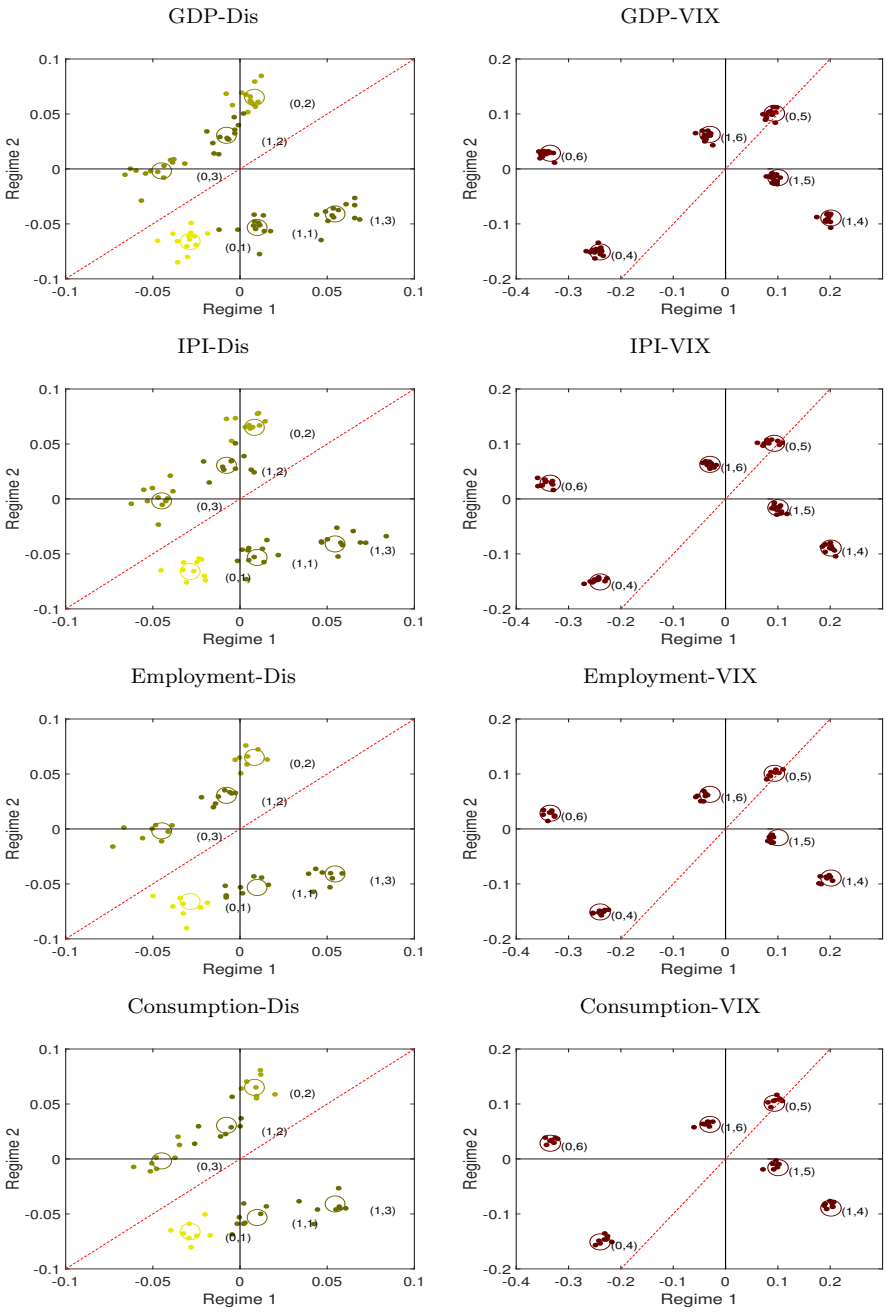

Note: the figure reports the impact of uncertainty on different variables ($i = 1, \ldots, n_g$, $g = 1, \ldots, G$), at lag $l = 0, 1$ in regime $k = 1, 2$. The circles indicate the common impact δ_{jlk} for the pair lag l and shock j, denoted with (l, j). The dots indicate country- and series- specific impact $\delta_{ijlgk} = \delta_{jlk} + \zeta_{\delta,gjlk} + \eta_{\delta,igjlk}$ in the two regimes. The dashed line indicates the 45° line. Different shades of color indicate the dots referred to a specific lag.

Figure 3: Impact of uncertainty shocks on different macroeconomic variables

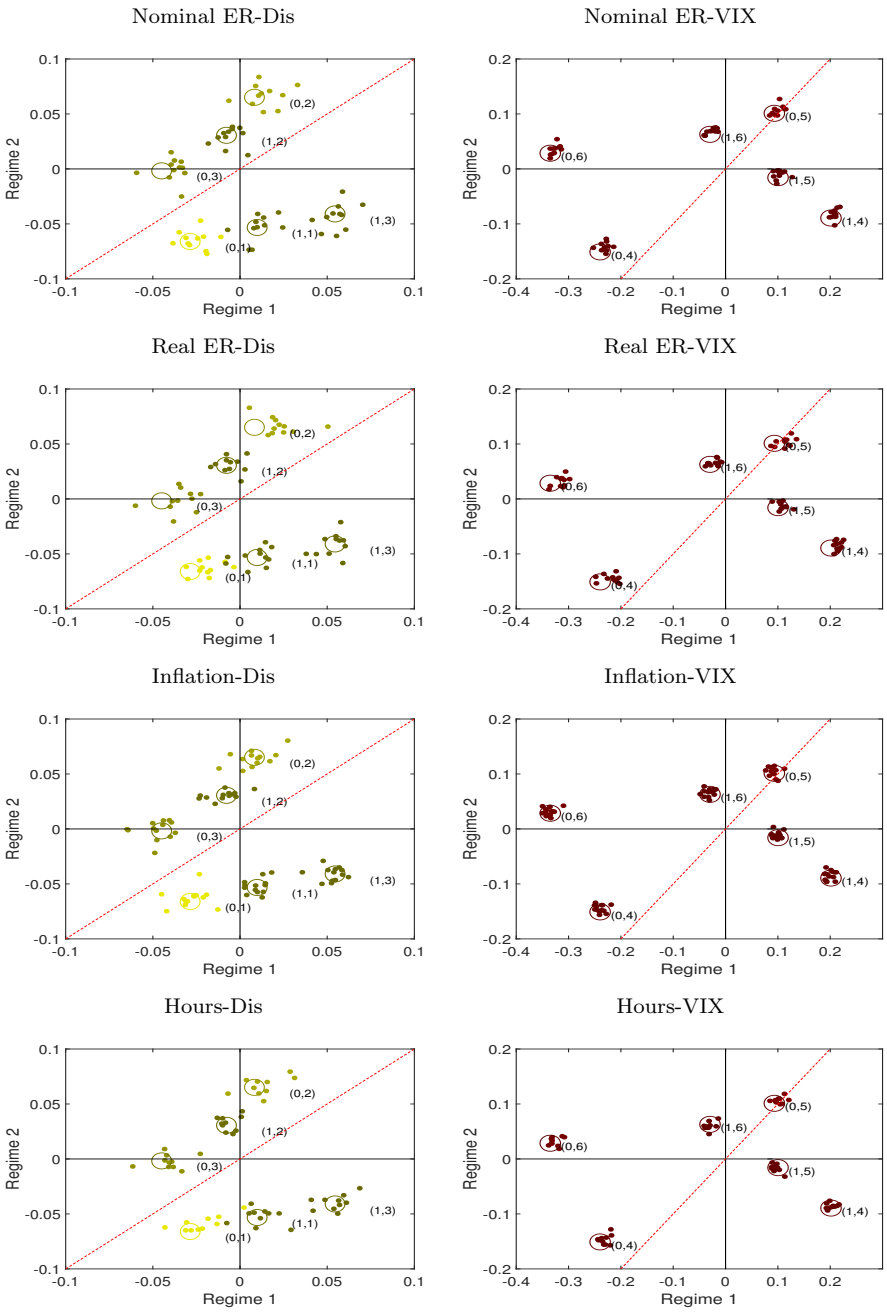

Note: the figure reports the impact of uncertainty on different variables ($i = 1, \ldots, n_g$, $g = 1, \ldots, G$), at lag $l = 0, 1$ in regime $k = 1, 2$. The circles indicate the common impact δ_{jlk} for the pair lag l and shock j, denoted with (l, j). The dots indicate country- and series- specific impact $\delta_{ijlgk} = \delta_{jlk} + \zeta_{\delta,gjlk} + \eta_{\delta,igjlk}$ in the two regimes. The dashed line indicates the 45° line. Different shades of color indicate the dots referred to a specific lag.

Figure 4: Impact of uncertainty shocks on different macroeconomic variables

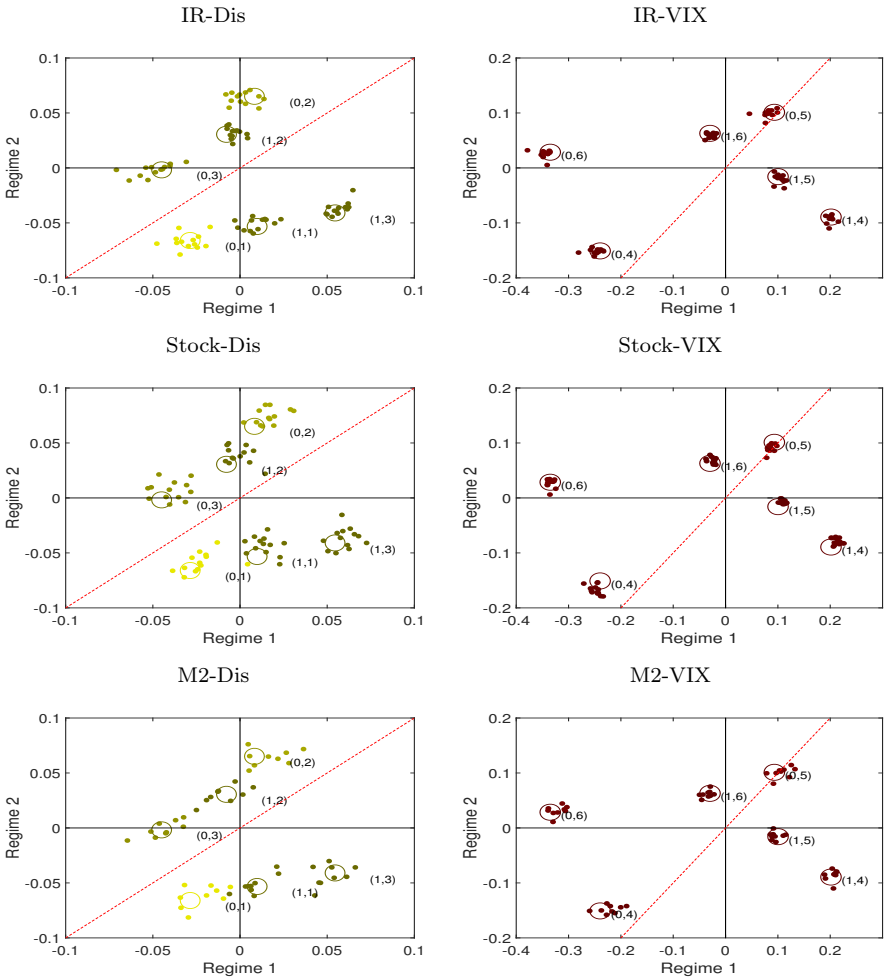

Note: the figure reports the impact of uncertainty on different variables ($i = 1, \ldots, n_g$, $g = 1, \ldots, G$), at lag $l = 0, 1$ in regime $k = 1, 2$. The circles indicate the common impact δ_{jlk} for the pair lag l and shock j, denoted with (l, j). The dots indicate country- and series- specific impact $\delta_{ijlgk} = \delta_{jlk} + \zeta_{\delta,gjlk} + \eta_{\delta,igjlk}$ in the two regimes. The dashed line indicates the 45° line. Different shades of color indicate the dots referred to a specific lag.

on the financial market. It detects loss cascades by ΔCoVaR, which represents the value at risk (VaR) of the financial system conditional on institutions being under distress. The entropy indicator for the EU is built on a dataset of daily closing price series for the European firms (active and dead) of the financial sector from January 1990 to December 2014. In both cases, we follow the same assumption applied to the VIX and use it for all countries. All the results of the robustness analysis are reported in section E and here we only briefly summarize the main findings.

First and interestingly, the evidence is qualitatively similar when the model only allows for a one-quarter lag effect of uncertainty. Financial uncertainty is still dominant on macroeconomic uncertainty and differences across regimes clearly emerge.

When dropping the VIX from the model, coefficients of forecast disagreement become larger in absolute value, probably capturing part of the effects that our model assigns to financial uncertainty. When we use quarterly uncertainty measures, the heterogeneity across countries for both VIX and forecast disagreement increases substantially, and for several variables the total effect of uncertainty is less pronounced, especially for the second regime, confirming the usefulness of mixed frequency data.

Finally, when using different measures of financial uncertainty, the main results are also confirmed. Both the Financial Uncertainty Index of Ludvigson et al. (2015) and the Financial Entropy Index of (Billio et al., 2016a) yield a negative impact (mainly) during the recession regime, thus supporting evidence of asymmetric effects of uncertainty in different phases of the economic activity.[10]

6 Conclusions

This paper develops a Bayesian multi-country panel Markov-Switching unrestricted mixed-data sampling model. This framework allows to model a large panel of countries and several variables for each country. At the same time, it allows to use an endogenous time-varying transition mechanism, to include nonlinearity in the model, and to consider variables sampled at mixed frequencies.

In order to avoid overparameterization issues and overfitting problems, we implement a hierarchical strategy in the specification of the prior. The hierarchical prior allows to naturally introduce random effects into the panel model without specifying a Markov-Switching mechanism in the variance of the errors. We develop a proper MCMC algorithm for sampling from the joint posterior distribution of the model parameters and test its properties in a simulation experiment.

We use the model to study the effects of macroeconomic uncertainty, measured as forecast disagreement, and financial uncertainty, measured as stock market volatility, on a set of variables in a multi-country context including the US, several European countries and Japan. We find

[10]We also investigate an example where US forecast disagreement is used as measure of macroeconomic uncertainty for all the countries, therefore similarly to the application of US VIX as measure of financial uncertainty for all the countries. The correlation of US forecast disagreement with other country measures is lower than the case of financial uncertainty. The role of financial uncertainty is amplified with respect to the benchmark example. Results are available upon request.

that for most of the variables financial uncertainty dominates macroeconomic uncertainty. Furthermore, we show that uncertainty coefficients differ if the economy is in a contraction regime or in an expansion regime.

References

Alessandri, P. and Mumtaz, H. (2014). Financial regimes and uncertainty shocks. Queen Mary, University of London.

Baker, S. R., Bloom, N., and Davis, S. J. (2015). Measuring economic policy uncertainty. working paper 21633, nber.

Bassetti, F., Casarin, R., and Leisen, F. (2014). Beta-product dependent Pitman-Yor processes for Bayesian inference. *Journal of Econometrics*, 140:49–72.

Billio, M., Casarin, R., Costola, M., and Pasqualini, A. (2016a). An entropy-based early warning indicator for systemic risk. *Journal of International Financial Markets, Institutions and Money, forthcoming*.

Billio, M., Casarin, R., Ravazzolo, F., and Van Dijk, H. (2016b). Interactions between eurozone and US booms and busts: A Bayesian panel Markov-switching VAR model. *Journal of Applied Econometrics, forthcoming*.

Billio, M., Casarin, R., Ravazzolo, F., and van Dijk, H. K. (2012). Combination schemes for turning point predictions. *Quarterly Review of Economics and Finance*, 52(4):402–412.

Bloom, N. (2009). The Impact of Uncertainty Shocks. *Econometrica*, 77(3):623–685.

Bloom, N. (2014). Fluctuations in Uncertainty. *Journal of Economic Perspectives*, 28(2):153–76.

Caggiano, G., Castelnuovo, E., and Groshenny, N. (2014). Uncertainty shocks and unemployment dynamics in U.S. recessions. *Journal of Monetary Economics*, 67(C):78–92.

Canova, F. and Ciccarelli, M. (2004). Forecasting and turning point predictions in a Bayesian panel VAR model. *Journal of Econometrics*, 120(2):327–359.

Canova, F. and Ciccarelli, M. (2009). Estimating multicountry VAR models. *International Economic Review*, 50(3):929–959.

Carriero, A., Clark, T. E., and Marcellino, M. (2016). Measuring uncertainty and its impact on the economy. mimeo.

Chib, S. and Greenberg, E. (1995). Hierarchical analysis of SUR models with extensions to correlated serial errors and time-varying parameter models. *Journal of Econometrics*, 68:339–360.

Clements, M. P. and Galvao, A. B. (2008). Macroeconomic forecasting with mixed-frequency data. *Journal of Business and Economic Statistics*, 26:546–554.

Dovern, J., Fritsche, U., and Slacalek, J. (2012). Disagreement among forecasters in G7 countries. *The Review of Economics and Statistics*, 94(4):1081–1096.

Ferrara, L. and Guerin, P. (2015). What are the macroeconomic effects of high-frequency uncertainty shocks? Economics Working Papers 2015-12, University of Paris West - Nanterre la Dfense, EconomiX.

Ferrara, L. and Guérin, P. (2015). What are the macroeconomic effects of high-frequency uncertainty shocks? EconomiX Working Paper No. 2015-12, University Paris West Nanterre.

Foroni, C. and Marcellino, M. (2014). Mixed-frequency structural models: Identification, estimation, and policy analysis. *Journal of Applied Econometrics*, 29(7):1118–1144.

Foroni, C., Marcellino, M., and Schumacher, C. (2015a). Unrestricted mixed data sampling (MIDAS): MIDAS regressions with unrestricted lag polynomials. *Journal of the Royal Statistical Society A*, 178(1):57–82.

Foroni, C., Ravazzolo, F., and Ribeiro, P. J. (2015b). Forecasting commodity currencies: the role of fundamentals with short-lived predictive content. Working Paper 2015/14, Norges Bank.

Frühwirth-Schnatter, S. (2006). *Mixture and Markov-swithing Models*. Springer, New York.

Ghysels, E., Santa-Clara, P., and Valkanov, R. (2005). There is a risk-return trade-off after all. *Journal of Financial Economics*, 76(3):509–548.

Ghysels, E., Sinko, A., and Valkanov, R. (2007). Midas regressions: Further results and new directions. *Econometric Reviews*, 26(1):53–90.

Gourio, F. (2012). Disasters risk and business cycles. *American Economic Review*, 102:2734–2766.

Guérin, P. and Marcellino, M. (2013). Markov-switching MIDAS models. *Journal of Business and Economic Statistics*, 31(1):45–56.

Jurado, K., Ludvigson, S. C., and Ng, S. (2015). Measuring Uncertainty. *American Economic Review*, 105(3):1177–1216.

Kaufmann, S. (2010). Dating and forecasting turning points by Bayesian clustering with dynamic structure: A suggestion with an application to Austrian data. *Journal of Applied Econometrics*, 25:309–344.

Kaufmann, S. (2015). K-state switching models with time-varying transition distributions: Does loan growth signal stronger effects of variables on inflation? *Journal of Econometrics*, 187(1):82–94.

Khalaf, L., Kichian, M., Saunders, C., and Voia, M. (2013). Dynamic panels with MIDAS covariates: Estimation and fit. Technical report.

Liu, J. (1994). The collapsed Gibbs sampler in Bayesian computations with applications to a gene regulation problem. *Journal of the American Statistical Association*, 89(427):958 – 966.

Ludvigson, S. C., Ma, S., and Ng, S. (2015). Uncertainty and business cycles: Exogenous impulse or endogenous response? NBER Working Papers 21803.

Magnus, J. R. and Neudecker , H. (1999). *Matrix Differential Calculus with Applications in Statistics and Econometrics, 2nd Edition*. John Wiley.

Min, C. and Zellner, A. (1993). Bayesian and non-Bayesian methods for combining models and forecasts with applications to forecasting international growth rates. *Journal of Econometrics*, 56:89–118.

Mumtaz, H. and Theodoridis, K. (2016). The changing transmission of uncertainty shocks in the us: An empirical analysis. *Journal of Business Economics and Statistics,forthcoming*.

Pettenuzzo, D., Timmermann, A., and Valkanov, R. (2014). A Bayesian MIDAS approach to modeling first and second moment dynamics. Technical report, CEPR Discussion Papers 10160, C.E.P.R. Discussion Papers.

Roberts, G. and Sahu, S. (1997). Updating schemes, covariance structure, blocking and parametrisation for the Gibbs sampler. *Journal of the Royal Statistical Society, Series B*, 59:291 – 318.

Rodriguez, A. and Puggioni, G. (2010). Mixed frequency models: Bayesian approaches to estimation and prediction. *International Journal of Forecasting*, 26(2):293 – 311. Special Issue: Bayesian Forecasting in Economics.

Rossi, B. and Sekhposyan, T. (2015). Macroeconomic Uncertainty Indices Based on Nowcast and Forecast Error Distributions. *American Economic Review*, 105(5):650–55.

Scotti, C. (2013). Surprise and uncertainty indexes: real-time aggregation of real-activity macro surprises. International Finance Discussion Papers 1093, Board of Governors of the Federal Reserve System (U.S.).

A Proofs of the propositions of the paper

Proof. (Proposition 1) Let us define $C = (\boldsymbol{c}_1, \ldots, \boldsymbol{c}_c)$, $Z_{c,g} = (\boldsymbol{\zeta}_{c,g1}, \ldots, \boldsymbol{\zeta}_{c,gc})$, $E_{c,ig} = (\boldsymbol{\eta}_{c,ig1}, \ldots, \boldsymbol{\eta}_{c,igc})$ three $K \times c$-matrices, and $D_j = (\boldsymbol{\delta}_{j1}, \ldots, \boldsymbol{\delta}_{j(\nu+1)})$, $Z_{d,gj} = (\boldsymbol{\zeta}_{\delta,gj1}, \ldots, \boldsymbol{\zeta}_{\delta,gj\nu+1})$, $E_{d,ig} = (\boldsymbol{\eta}_{\delta,igj1}, \ldots, \boldsymbol{\eta}_{\delta,igj\nu+1})$ three $K \times (\nu+1)$-dimensional matrices, then Eq. 21 can be re-written as

$$\begin{aligned} y_{igt} &= (\boldsymbol{\mu} + \boldsymbol{\zeta}_{\mu,g} + \boldsymbol{\eta}_{\mu,ig})'\boldsymbol{\xi}_{gt} + \mathbf{v}'_{igt}(C + Z_{c,g} + E_{c,ig})'\boldsymbol{\xi}_{gt} \\ &\quad + \sum_{j=1}^{N} \mathbf{x}'_{ig,jt}(D_j + Z_{d,gj} + E_{d,igj})'\boldsymbol{\xi}_{gt} + \varepsilon_{igt} \end{aligned} \tag{A.1}$$

with $\varepsilon_{igt} \sim \mathcal{N}(0, \sigma^2_{ig})$, where σ^2_{ig} is defined in Eq. 15.

Let us define the covariate vector $\mathbf{w}_{it} = (1, \mathbf{v}'_{igt}, \mathbf{x}'_{igt})'$, where $\mathbf{x}_{igt} = (\mathbf{x}'_{ig,1t}, \ldots, \mathbf{x}'_{ig,Nt})'$, and the $K \times (1 + c + N(\nu+1))$-matrices $B = (\boldsymbol{\mu}, C, D_1, \ldots, D_N)$, $Z_g = (\boldsymbol{\zeta}_{\mu,g}, Z_{c,g}, Z_{d,g1}, \ldots, Z_{d,gN})$ and $E_{ig} = (\boldsymbol{\eta}_{\mu,ig}, E_{c,ig}E_{d,ig1}, \ldots, E_{d,igN})$. Then Eq. A.1 becomes

$$y_{igt} = \mathbf{w}'_{it}(B + Z_g + E_{ig})'\boldsymbol{\xi}_{gt} + \varepsilon_{igt} \tag{A.2}$$

Then by applying the vec operator, its properties and the properties of the Kronecker's product, $\otimes$, (see Magnus and Neudecker (1999)) we obtain the result

$$\begin{aligned} \mathrm{vec}(y_{igt}) &= \mathrm{vec}(\boldsymbol{\xi}'_{gt}(B + Z_g + E_{ig})\mathbf{w}_{it} + \varepsilon_{igt}) \\ &= (\mathbf{w}'_{it} \otimes \boldsymbol{\xi}'_{gt})\mathrm{vec}((B + Z_g + E_{ig})) + \varepsilon_{igt} \\ &= \mathbf{z}'_{it}(\boldsymbol{\beta} + \boldsymbol{\zeta}_g + \boldsymbol{\eta}_{ig}) + \varepsilon_{igt} \end{aligned} \tag{A.3}$$

where $\mathbf{z}'_{it} = \mathbf{w}'_{it} \otimes \boldsymbol{\xi}'_{it} = (\boldsymbol{\xi}'_{it}, \mathbf{v}'_{igt} \otimes \boldsymbol{\xi}'_{it}, \mathbf{x}'_{igt} \otimes \boldsymbol{\xi}'_{it})$, $\boldsymbol{\beta} = \mathrm{vec}B$, $\boldsymbol{\zeta}_g = \mathrm{vec}(Z_g)$ and $\boldsymbol{\eta}_{ig} = \mathrm{vec}(E_{ig})$. □

Proof. (Proposition 2) From the representation given in Proposition 1 it follows that $\boldsymbol{\beta}$ has distribution $\mathcal{N}_d(\mathbf{0}_d, S)$ with $d = K(1 + c + N(\nu+1))$ and $S = \mathrm{diag}\{(s^2_0\boldsymbol{\iota}'_K, r^2_0\boldsymbol{\iota}'_{K(c+N(\nu+1))})\}$ a diagonal covariance matrix and $\boldsymbol{\iota}_q$ the q-dimensional unit vector. $\boldsymbol{\zeta}_g$ has distribution $\mathcal{N}_d(\mathbf{0}_d, R)$ with $R = \mathrm{diag}\{((r_{\mu,1}, \ldots, r_{\mu,K}),\ \boldsymbol{\iota}'_c \otimes (r_{c,1}, \ldots, r_{c,K}),\ \boldsymbol{\iota}'_{N(\nu+1)} \otimes (r_{\delta,1}, \ldots, r_{\delta,K}))'\}$, and $\boldsymbol{\eta}_{ig}$ has distribution $\mathcal{N}_d(\mathbf{0}_d, Q_g)$ where $Q_g = \mathrm{diag}\{((q_{\mu,g1}, \ldots, q_{\mu,gK}), \boldsymbol{\iota}'_c \otimes (q_{c,g1}, \ldots, q_{c,gK}), \boldsymbol{\iota}'_{N(\nu+1)} \otimes (q_{\delta,g1}, \ldots, q_{\delta,gK}))\}$.

Let $f(y_{igt}|\boldsymbol{\beta}, \boldsymbol{\zeta}_g, \boldsymbol{\eta}_{ig})$ be the pdf of the dependent variable in Eq. 21 which is the pdf of a normal with mean $\mathbf{z}'_{igt}(\boldsymbol{\beta} + \boldsymbol{\zeta}_g + \boldsymbol{\eta}_{ig})$ and variance σ^2_{ig}. We consider the marginal distribution $f(y|\boldsymbol{\beta})$ of the observable obtained by integrating out the random effects. Let us consider the

m.g.f.

$$\begin{aligned}\int \exp\{\theta y\} f(y|\boldsymbol{\beta}) dy &= \int \exp\{\theta y\} f(y|\boldsymbol{\beta}, \boldsymbol{\zeta}_g, \boldsymbol{\eta}_{ig}) f(\boldsymbol{\zeta}_g) f(\boldsymbol{\eta}_{ig}) d\boldsymbol{\zeta}_g d\boldsymbol{\eta}_{ig} dy \\ &= \int \exp\left(\theta \mathbf{z}'_{igt}(\boldsymbol{\beta} + \boldsymbol{\zeta}_g + \boldsymbol{\eta}_{ig}) + \frac{\sigma^2_{ig}}{2}\theta^2\right) f(\boldsymbol{\zeta}_g) f(\boldsymbol{\eta}_{ig}) d\boldsymbol{\zeta}_g d\boldsymbol{\eta}_{ig} \\ &= \exp\left(\theta \mathbf{z}'_{igt}\boldsymbol{\beta}\right) \exp\left(\theta^2 \mathbf{z}'_{igt} R \mathbf{z}_{igt} + \theta^2 \mathbf{z}'_{igt} Q_g \mathbf{z}_{igt} + \frac{\sigma^2_{ig}}{2}\theta^2\right) \end{aligned} \tag{A.4}$$

which is the m.g.f. of a normal with mean $\mathbf{z}'_{igt}\boldsymbol{\beta}$ and variance $\sigma^2_{ig} + \mathbf{z}'_{igt}(R + Q_g)\mathbf{z}_{igt}$ □

B Computational details

The proposed Gibbs sampler (see Section 3) iterates over the following steps

i) Draw $\boldsymbol{\zeta}, \boldsymbol{\eta}, \boldsymbol{\xi}, \boldsymbol{\beta}, P_1, \ldots, P_G, \boldsymbol{\nu}$ from $p(\boldsymbol{\zeta}, \boldsymbol{\eta}, \boldsymbol{\xi}, \boldsymbol{\beta}, \mathbf{p}, \boldsymbol{\nu} | \sigma^2, \boldsymbol{\lambda}, \boldsymbol{\chi}, \mathbf{q}, \mathbf{r}, \mathbf{y})$.

i.1) Draw $\boldsymbol{\beta}, P_1, \ldots, P_G, \boldsymbol{\nu}, \boldsymbol{\xi}$ *from* $p(\boldsymbol{\beta}, \mathbf{p}, \boldsymbol{\nu}, \boldsymbol{\xi} | \sigma^2, \boldsymbol{\lambda}, \boldsymbol{\chi}, \mathbf{q}, \mathbf{r}, \mathbf{y})$.

i.2) Draw $\boldsymbol{\zeta}, \boldsymbol{\eta}$ *from* $p(\boldsymbol{\zeta}, \boldsymbol{\eta} | \boldsymbol{\beta}, \mathbf{p}, \boldsymbol{\nu}, \sigma^2, \boldsymbol{\lambda}, \boldsymbol{\chi}, \mathbf{q}, \mathbf{r}, \boldsymbol{\xi}, \mathbf{y})$.

ii) Draw σ^2, $\boldsymbol{\lambda}$, $\boldsymbol{\chi}$, $\mathbf{q}$, $\mathbf{r}$ *from* $p(\sigma^2, \boldsymbol{\lambda}, \boldsymbol{\chi}, \mathbf{q}, \mathbf{r} | \boldsymbol{\beta}, \mathbf{p}, \boldsymbol{\nu}, \boldsymbol{\zeta}, \boldsymbol{\eta}, \boldsymbol{\xi}, \mathbf{y})$

Steps *i.1)* and *ii)* of the Gibbs sampler are blocked further. Let $\boldsymbol{\mu} = (\boldsymbol{\mu}'_1, \ldots, \boldsymbol{\mu}'_K)$, $\mathbf{c} = (\mathbf{c}'_1, \ldots, \mathbf{c}'_K)'$, $\boldsymbol{\delta} = (\boldsymbol{\delta}'_1, \ldots, \boldsymbol{\delta}'_K)$, and $\boldsymbol{\nu} = (\boldsymbol{\nu}'_1, \ldots, \boldsymbol{\nu}'_K)'$, then draws from $p(\boldsymbol{\beta}, \mathbf{p}, \boldsymbol{\xi}, \boldsymbol{\nu} | \sigma^2, \boldsymbol{\lambda}, \boldsymbol{\chi}, \mathbf{q}, \mathbf{r}, \mathbf{y})$ at step *i.1)* are obtained by iterating over the following steps

i.1.1) Draw $\boldsymbol{\mu}_k$ from $p(\boldsymbol{\mu}_k | \boldsymbol{\mu}_{-k}, \mathbf{c}, \boldsymbol{\delta}, \sigma^2, \boldsymbol{\lambda}, \mathbf{p}, \boldsymbol{\nu}, \boldsymbol{\chi}, \mathbf{q}, \mathbf{r}, \boldsymbol{\xi}, \mathbf{y})$, $k = 1, \ldots, K$.

i.1.2) Draw $\mathbf{c}_k$ from $p(\mathbf{c}_k | \boldsymbol{\mu}, \mathbf{c}_{-k}, \boldsymbol{\delta}, \sigma^2, \boldsymbol{\lambda}, \mathbf{p}, \boldsymbol{\nu}, \boldsymbol{\chi}, \mathbf{q}, \mathbf{r}, \boldsymbol{\xi}, \mathbf{y})$, $k = 1, \ldots, K$.

i.1.3) Draw $\boldsymbol{\delta}_k$ from $p(\boldsymbol{\delta}_k | \boldsymbol{\mu}, \mathbf{c}, \boldsymbol{\delta}_{-k}, \boldsymbol{\delta}, \sigma^2, \boldsymbol{\lambda}, \mathbf{p}, \boldsymbol{\nu}, \boldsymbol{\chi}, \mathbf{q}, \mathbf{r}, \boldsymbol{\xi}, \mathbf{y})$, $k = 1, \ldots, K$.

i.1.4) Draw $(\mathbf{p}_l, \boldsymbol{\nu}_l)$ from $p(\mathbf{p}_l, \boldsymbol{\nu}_l | \boldsymbol{\mu}, \mathbf{c}, \boldsymbol{\delta}, \sigma^2, \boldsymbol{\lambda}, \mathbf{p}_{-l}, \boldsymbol{\nu}_{-l}, \boldsymbol{\chi}, \mathbf{q}, \mathbf{r}, \boldsymbol{\xi}, \mathbf{y})$, $l = 1, \ldots, K$.

i.1.5) Draw $\boldsymbol{\xi}$ from $p(\boldsymbol{\xi} | \boldsymbol{\mu}, \mathbf{c}, \boldsymbol{\delta}, \sigma^2, \boldsymbol{\lambda}, \mathbf{p}, \boldsymbol{\nu}, \boldsymbol{\chi}, \mathbf{q}, \mathbf{r}, \mathbf{y})$.

In the derivation of the full conditional distributions in the step *i.1.1)* we use the complete data likelihood of the model in Eq. 25, that is

$$L(\mathbf{y}, \boldsymbol{\xi} | \boldsymbol{\theta}) = \prod_{t \in \mathcal{T}} \prod_{g=1}^{G} \prod_{i=1}^{n_g} \frac{1}{(2\pi\sigma^2_{igt})^{1/2}} \exp\left\{-\frac{\tilde{\varepsilon}^2_{igt}}{2\sigma^2_{igt}}\right\} \prod_{l=1}^{K} \prod_{k=1}^{K} p_{glk}^{\xi_{glt-1}\xi_{gkt}} \tag{B.1}$$

where $\tilde{\varepsilon}_{igt} = y_{igt} - \mathbf{z}'_{igt}\boldsymbol{\beta}$.

As regards the scaling factors in Step *ii)* the following blocks are considered:

ii.1) Draw σ^2 from $p(\sigma^2 | \boldsymbol{\beta}, \boldsymbol{\lambda}, \boldsymbol{\chi}, \mathbf{p}, \boldsymbol{\nu}, \mathbf{q}, \mathbf{r}, \boldsymbol{\zeta}, \boldsymbol{\eta}, \boldsymbol{\xi}, \mathbf{y})$.

ii.2) Draw λ_{ig} from $p(\lambda_{ig} | \boldsymbol{\beta}, \sigma^2, \boldsymbol{\lambda}_{-ig}, \boldsymbol{\chi}, \mathbf{p}, \boldsymbol{\nu}, \mathbf{r}, \mathbf{q}, \boldsymbol{\zeta}, \boldsymbol{\eta}, \boldsymbol{\xi}, \mathbf{y})$, $i = 1, \ldots, n$.

ii.3) Draw χ_g from $p(\chi_g|\boldsymbol{\beta}, \sigma^2, \boldsymbol{\lambda}, \boldsymbol{\chi}_{-q}, \mathbf{p}, \boldsymbol{\nu}, \mathbf{r}, \mathbf{q}, \boldsymbol{\zeta}, \boldsymbol{\eta}, \boldsymbol{\xi}, \mathbf{y})$, $i = 1, \ldots, n$.

ii.4) Draw $\mathbf{q}$ from $p(\mathbf{q}|\boldsymbol{\beta}, \sigma^2, \boldsymbol{\lambda}, \boldsymbol{\chi}, \mathbf{p}, \boldsymbol{\nu}, \mathbf{r}, \boldsymbol{\zeta}, \boldsymbol{\eta}, \boldsymbol{\xi}, \mathbf{y})$.

ii.5) Draw $\mathbf{r}$ from $p(\mathbf{r}|\boldsymbol{\beta}, \sigma^2, \boldsymbol{\lambda}, \boldsymbol{\chi}, \mathbf{p}, \boldsymbol{\nu}, \mathbf{q}, \boldsymbol{\zeta}, \boldsymbol{\eta}, \boldsymbol{\xi}, \mathbf{y})$.

The full conditional distributions and the sampling method are discussed in the following.

B.1 Sampling $\boldsymbol{\mu}$

Following the collapsed Gibbs sampling strategy described in Section 3, we consider the likelihood function in Eq. B.1 to find the full conditional distribution of μ_k

$$
\begin{aligned}
& p(\mu_k|\boldsymbol{\mu}_{-k}, \mathbf{c}, \boldsymbol{\delta}, \sigma^2, \boldsymbol{\lambda}, \boldsymbol{\chi}, \mathbf{p}, \boldsymbol{\nu}, \mathbf{q}, \mathbf{r}, \boldsymbol{\xi}, \mathbf{y}) \propto \\
& \propto \exp\left\{-\frac{1}{2s_0^2}\mu_k^2\right\} \prod_{g=1}^{G}\prod_{i=1}^{n_g}\prod_{t\in\mathcal{T}_{gk}} \exp\left\{-\frac{1}{2\tilde{\sigma}^2_{igkt}}(y_{igt} - \mathbf{z}'_{igkt}\boldsymbol{\beta})^2\right\} \\
& \propto \exp\left\{-\frac{1}{2}\left(\mu_k^2\left(s_0^{-2} + \sum_{g=1}^{G}\sum_{i=1}^{n_g}\sum_{t\in\mathcal{T}_{gk}}\sigma^{-2}_{igkt}\right)\right.\right. \\
& \qquad \left.\left. -2\mu_k\left(\sum_{g=1}^{G}\sum_{i=1}^{n_g}\sum_{t\in\mathcal{T}_{gk}} e_{\mu,igkt}\tilde{\sigma}^{-2}_{igkt}\right)\right)\right\} \\
& \propto \mathcal{N}\left(m_{\mu,k}, \upsilon_{\mu,k}\right)\mathbb{I}_{\mathcal{A}_\mu}(\mu_k)
\end{aligned}
\tag{B.2}
$$

that is a truncated normal distribution with parameters

$$
\upsilon_{\mu,k} = \left(\sum_{g=1}^{G}\sum_{i=1}^{n_g}\sum_{t\in\mathcal{T}_{gk}}\tilde{\sigma}^{-2}_{igkt} + s_0^{-2}\right)^{-1} \tag{B.3}
$$

$$
m_k = \upsilon_{\mu,k}\left(\sum_{g=1}^{G}\sum_{i=1}^{n_g}\sum_{t\in\mathcal{T}_{gk}} e_{\mu,igkt}\tilde{\sigma}^{-2}_{igkt}\right) \tag{B.4}
$$

with

$$
\begin{aligned}
e_{\mu,igkt} &= y_{igt} - \sum_{l=1}^{c} c_{lk} y_{igt-l} - \sum_{j=1}^{N}\sum_{l=0}^{\nu}\delta_{jlk}x_{igjt-l} \\
\tilde{\sigma}^2_{igkt} &= \sigma^2\lambda_{ig}^{-1}\chi_g^{-1} + \mathbf{z}'_{igkt}(Q_g + R)\mathbf{z}_{igkt}
\end{aligned}
$$

where Q_g and R have been defined in the proof of Proposition 1, Appendix A, $\mathbf{z}_{igkt} = (\mathbf{e}'_k,$ $\mathbf{e}'_k y_{igt-m}, \ldots, \mathbf{e}'_k y_{igt-mc}, \mathbf{e}'_k x_{ig1t}, \ldots, \mathbf{e}'_k x_{ig1t-p}, \ldots, \mathbf{e}'_k x_{igNt}, \ldots, \mathbf{e}'_k x_{igNt-p})'$, $\mathbf{e}_k$ being the k-th element of the K-dimensional standard orthonormal basis, and $\mathcal{T}_{gk} = \{t \in \mathcal{T} : \xi_{gkt} = 1\}$.

B.2 Sampling c

The full conditional distribution of $\mathbf{c}_k$ is the truncated normal distribution

$$
\begin{aligned}
& p(\mathbf{c}_k|\boldsymbol{\mu}, \mathbf{c}_{-k}, \boldsymbol{\delta}, \sigma^2, \boldsymbol{\lambda}, \boldsymbol{\chi}, \mathbf{p}, \boldsymbol{\nu}, \mathbf{q}, \mathbf{r}, \boldsymbol{\xi}, \mathbf{y}) \propto \qquad \text{(B.5)} \\
& \propto \exp\left\{-\frac{1}{2r_0^2}\boldsymbol{c}_k'\boldsymbol{c}_k\right\} \prod_{g=1}^{G}\prod_{i=1}^{n_g}\prod_{t\in\mathcal{T}_{gk}} \exp\left\{-\frac{1}{2\tilde{\sigma}_{igkt}^2}(y_{igt} - \mathbf{z}_{igkt}'\boldsymbol{\beta})^2\right\} \\
& \propto \exp\left\{-\frac{1}{2}\left(\boldsymbol{c}_k'\left(r_0^{-2}I_c + \sum_{g=1}^{G}\sum_{i=1}^{n_g}\sum_{t\in\mathcal{T}_{gk}} \mathbf{v}_{igt}\mathbf{v}_{igt}'\tilde{\sigma}_{igkt}^{-2}\right)\boldsymbol{c}_k \right.\right. \\
& \qquad \left.\left. -2\boldsymbol{c}_k'\left(\sum_{g=1}^{G}\sum_{i=1}^{n_g}\sum_{t\in\mathcal{T}_{gk}} \mathbf{v}_{igt}e_{c,igkt}\tilde{\sigma}_{igkt}^{-2}\right)\right)\right\} \\
& \propto \mathcal{N}_c\left(\mathbf{m}_{c,k}, \Upsilon_{c,k}\right)\mathbb{I}_{\mathcal{A}_c}(\mathbf{c}_k) \qquad \text{(B.6)}
\end{aligned}
$$

with

$$
\begin{aligned}
\Upsilon_{c,k} &= \left(\sum_{g=1}^{G}\sum_{i=1}^{n_g}\sum_{t\in\mathcal{T}_{gk}} \mathbf{v}_{igt}\mathbf{v}_{igt}'\tilde{\sigma}_{igkt}^{-2} + r_0^{-2}I_c\right)^{-1} \qquad \text{(B.7)} \\
\mathbf{m}_{c,k} &= \Upsilon_{c,k}\left(\sum_{g=1}^{G}\sum_{i=1}^{n_G}\sum_{t\in\mathcal{T}_{gk}} \mathbf{v}_{igt}\tilde{\sigma}_{igkt}^{-2}e_{c,igkt}\right) \qquad \text{(B.8)}
\end{aligned}
$$

where $\mathbf{v}_{igt} = (y_{igt-m}, \ldots, y_{igt-mc})'$,

$$
e_{c,igkt} = y_{igt} - \mu_k - \sum_{j=1}^{N}\sum_{l=1}^{\nu}\delta_{jlk}x_{igjt-l},
$$

and $\tilde{\sigma}_{igkt}^2$ defined in B.1, and $\mathcal{T}_{gk} = \{t \in \mathcal{T} : \xi_{gkt} = 1\}$.

B.3 Sampling $\boldsymbol{\delta}$

The full conditional distribution of $\boldsymbol{\delta}_k$ is the normal distribution

$$
\begin{aligned}
& p(\boldsymbol{\delta}_k|\boldsymbol{\mu}, \mathbf{c}, \boldsymbol{\delta}_{-k}, \boldsymbol{\delta}, \sigma^2, \boldsymbol{\lambda}, \boldsymbol{\chi}, \mathbf{p}, \boldsymbol{\nu}, \mathbf{q}, \mathbf{r}, \boldsymbol{\xi}, \mathbf{y}) \propto \qquad \text{(B.9)} \\
& \propto \exp\left\{-\frac{1}{2r_0^2}\boldsymbol{\delta}_k'\boldsymbol{\delta}_k\right\} \prod_{g=1}^{G}\prod_{i=1}^{n_g}\prod_{t\in\mathcal{T}_{gk}} \exp\left\{-\frac{1}{2\tilde{\sigma}_{igkt}^2}(y_{igt} - \mathbf{z}_{igkt}'\boldsymbol{\beta})^2\right\} \\
& \propto \exp\left\{-\frac{1}{2}\left(\boldsymbol{\delta}_k'\left(r_0^{-2}I_{N(p+1)} + \sum_{g=1}^{G}\sum_{i=1}^{n_g}\sum_{t\in\mathcal{T}_{gk}} \mathbf{x}_{igt}\mathbf{x}_{igt}'\tilde{\sigma}_{igkt}^{-2}\right)\boldsymbol{\delta}_k \right.\right. \\
& \qquad \left.\left. -2\boldsymbol{c}_k'\left(\sum_{g=1}^{G}\sum_{i=1}^{n_g}\sum_{t\in\mathcal{T}_{gk}} \mathbf{x}_{igt}e_{\delta,igkt}\tilde{\sigma}_{igkt}^{-2}\right)\right)\right\} \\
& \propto \mathcal{N}_{N(p+1)}\left(\mathbf{m}_{\delta,k}, \Upsilon_{\delta,k}\right)
\end{aligned}
$$

where

$$\Upsilon_{\delta,k} = \left(\sum_{g=1}^{G} \sum_{i=1}^{n_g} \sum_{t \in \mathcal{T}_{gk}} \mathbf{x}_{igk} \mathbf{x}_{igk}^{'} \tilde{\sigma}_{igk}^{-2} + r_0^{-2} I_{N(p+1)} \right)^{-1} \tag{B.10}$$

$$\mathbf{m}_{\delta,k} = \Upsilon_{\delta,k} \left(\sum_{g=1}^{G} \sum_{i=1}^{n_g} \sum_{t \in \mathcal{T}_{gk}} \mathbf{x}_{igk} \tilde{\sigma}_{igk}^{-2} \mathbf{e}_{\delta,igk} \right) \tag{B.11}$$

with $\mathbf{x}_{igt} = (\mathbf{x}'_{ig,1t}, \ldots, \mathbf{x}'_{ig,Nt})'$,

$$e_{\delta,igkt} = y_{igt} - \mu_k - \sum_{l=1}^{c} c_{lk} y_{igt-l}$$

and $\tilde{\sigma}^2_{igkt}$ defined in B.1, and $\mathcal{T}_{gk} = \{t \in \mathcal{T} : \xi_{gkt} = 1\}$.

B.4 Sampling $\mathbf{p}_l, \boldsymbol{\nu}_l$

We apply a collapsed Gibbs step and sample first $\boldsymbol{\nu}_l$ from the marginal distribution $p(\boldsymbol{\nu}_l|\boldsymbol{\mu}, \mathbf{c}, \boldsymbol{\delta}, \sigma^2, \boldsymbol{\lambda}, \mathbf{p}, \boldsymbol{\nu}_{-l}, \boldsymbol{\zeta}, \boldsymbol{\eta}, \mathbf{q}, \mathbf{r}, \boldsymbol{\xi}, \mathbf{y})$ and then from the conditional $\mathbf{p}_l$ from $p(\mathbf{p}_l|\boldsymbol{\mu}, \mathbf{c}, \boldsymbol{\delta}, \sigma^2, \boldsymbol{\lambda}, \boldsymbol{\chi}, \mathbf{p}_{-l}, \boldsymbol{\nu}, \boldsymbol{\zeta}, \boldsymbol{\eta}, \mathbf{q}, \mathbf{r}, \boldsymbol{\xi}, \mathbf{y})$.

The marginal distribution writes as

$$\begin{aligned}
&p(\boldsymbol{\nu}_l|\boldsymbol{\mu}, \mathbf{c}, \boldsymbol{\delta}, \sigma^2, \boldsymbol{\lambda}, \boldsymbol{\chi}, \mathbf{p}, \boldsymbol{\nu}_{-l}, \boldsymbol{\zeta}, \boldsymbol{\eta}, \mathbf{q}, \mathbf{r}, \boldsymbol{\xi}, \mathbf{y}) \propto p(\boldsymbol{\nu}_l|\mathbf{p}, \boldsymbol{\xi}) \\
&\propto \int_{\Delta^m_{[0,1]^K}} \prod_{g=1}^{G} \prod_{t \in \mathcal{T}} \prod_{k=1}^{K} p_{g,lk}^{\xi_{glt-1}\xi_{gkt}} p_{g,lk}^{\phi\nu_{lk}-1} \frac{\Gamma(\phi)}{\Gamma(\phi\nu_{lk})} dp_{1,l1} \cdots dp_{G,lK} \pi(\boldsymbol{\nu}_l) \\
&\propto \int_{\Delta^G_{[0,1]^K}} \prod_{g=1}^{G} \prod_{k=1}^{K} p_{g,lk}^{n_{g,lk}+\phi\nu_{lk}-1} \frac{\Gamma(\phi)}{\Gamma(\phi\nu_{lk})} dp_{1,l1} \cdots dp_{G,lK} \pi(\boldsymbol{\nu}_l) \\
&\propto \left(\prod_{k=1}^{K} \nu_{lk}^{1/K-1} \right) \prod_{g=1}^{G} \prod_{k=1}^{K} \frac{\Gamma(\phi)}{\Gamma(\phi\nu_{lk})} \frac{\Gamma(\phi\nu_{lk} + n_{g,lk})}{\Gamma(\phi + n_{g,l})}
\end{aligned} \tag{B.12}$$

where

$$n_{g,lk} = \sum_{t \in \mathcal{T}} \xi_{gl,t-1} \xi_{gkt}$$

By using the properties of the gamma function it is possible to write

$$\Gamma(\phi\nu_{lk} + n_{g,lk}) = \prod_{r=1}^{n_{g,lk}} (\phi\nu_{lk} + r - 1)\Gamma(\phi\nu_{lk})$$

$$\Gamma(\phi + n_{g,l}) = \prod_{r=1}^{n_{g,l}} (\phi + r - 1)\Gamma(\phi)$$

thus it follows

$$p(\boldsymbol{\nu}_l|\boldsymbol{\xi}) \propto \prod_{k=1}^{K} \nu_{lk}^{1/K+m_{lk}-1} g(\boldsymbol{\nu}_l) \tag{B.13}$$
$$\propto \mathcal{D}ir(1/K+m_{l1},\ldots,1/K+m_{lK})g(\boldsymbol{\nu}_l)$$

where

$$g(\boldsymbol{\nu}_l) = \left(\prod_{r=1}^{n_{gl}}(\phi+r-1)\right)^{-1} \prod_{k=1}^{K}\prod_{g=1}^{G}\prod_{r=2}^{n_{g,lk}}(\phi\nu_{lk}+r-1)$$

and $m_{lk} = \text{Card}(\mathcal{M}_{lk})$, with $\mathcal{M}_{lk} = \{g = 1,\ldots,G|n_{g,lk} > 0\}$. We generate draws from this distribution by a Metropolis-Hastings step with independent proposal distribution $\mathcal{D}ir(1/K+m_{l1},\ldots,1/K+m_{lK})$, which allows us to obtain the following acceptance probability

$$\varrho(\boldsymbol{\nu}_l^*, \boldsymbol{\nu}_l^{(j-1)}) = \min\left\{1, \frac{g(\boldsymbol{\nu}_l^*)}{g(\boldsymbol{\nu}_l^{(j-1)})}\right\} \tag{B.14}$$

where $\boldsymbol{\nu}_l^*$ is the candidate value and $\boldsymbol{\nu}_l^{(j-1)}$ is the previous iteration value of the M.-H. chain.

It is easy to show that the conditional distribution of $\mathbf{p}_l$ is a product of conditionally independent Dirichlet distributions, that is

$$p(\mathbf{p}_l|\boldsymbol{\mu},\mathbf{c},\boldsymbol{\delta},\sigma^2,\boldsymbol{\lambda},\boldsymbol{\chi},\mathbf{p}_{-l},\boldsymbol{\nu},\boldsymbol{\zeta},\boldsymbol{\eta},\mathbf{q},\mathbf{r},\boldsymbol{\xi},\mathbf{y}) \propto p(\mathbf{p}_l|\boldsymbol{\nu}_l,\boldsymbol{\xi}) \tag{B.15}$$
$$\propto \prod_{g=1}^{G} \mathcal{D}ir(\phi\nu_{l1}+n_{g,l1},\ldots,\phi\nu_{lK}+n_{g,lK}).$$

See Frühwirth-Schnatter (2006), ch. 11.

B.5 Sampling $\boldsymbol{\xi}$

As regards to the draws from $p(\boldsymbol{\xi}|\boldsymbol{\beta},\sigma^2,\boldsymbol{\lambda},\boldsymbol{\chi},\mathbf{p},\boldsymbol{\nu},\mathbf{q},\mathbf{r},\mathbf{y})$, we follow a blocking strategy and draws in one block $\boldsymbol{\xi}_g$ from $p(\boldsymbol{\xi}_g|\boldsymbol{\beta},\sigma^2,\boldsymbol{\lambda},\mathbf{p},\boldsymbol{\nu},\mathbf{q},\mathbf{y})$, where $\boldsymbol{\xi}_g = (\boldsymbol{\xi}_{g1}',\ldots,\boldsymbol{\xi}_{gT}')'$. We apply a standard forward filtering backward sampling strategy (FFBS, see Frühwirth-Schnatter (2006), ch. 11-13, for further details), with predictive and filtered probabilities

$$p(\boldsymbol{\xi}_{gt} = \boldsymbol{e}_k|\mathbf{y}_{g,m:t-m}) = \sum_{l=1}^{K} p_{glk}\, p(\boldsymbol{\xi}_{g,t-m} = \boldsymbol{\iota}_l|\mathbf{y}_{g,m:t-m}) \tag{B.16}$$

$$p(\boldsymbol{\xi}_{g,t} = \boldsymbol{e}_k|\mathbf{y}_{g,m:t}) \propto p(\boldsymbol{\xi}_{g,t} = \boldsymbol{e}_k|\mathbf{y}_{g,m:t-m})\, p(\mathbf{y}_{gt}|\mathbf{y}_{g,t-m-cm:t-m},\boldsymbol{e}_k) \tag{B.17}$$

t, $t = m,\ldots,mT_q$, and smoothed probabilities

$$p(\boldsymbol{\xi}_{gt} = \boldsymbol{e}_k|\mathbf{y}_{g,1:T}) \propto \sum_{l=1}^{m} p(\boldsymbol{\xi}_{g,t} = \boldsymbol{e}_k|\boldsymbol{\xi}_{g,t+1} = \boldsymbol{e}_l, \mathbf{y}_{g,1:t})\, p(\boldsymbol{\xi}_{g,t+1} = \boldsymbol{e}_l|\mathbf{y}_{g,1:T}), \tag{B.18}$$

$t = mT_q, mT_q - m, \ldots, m$, where $\mathbf{y}_{gt} = (y_{1gt}, \ldots, y_{n_g gt})'$ is the observation vector for the g-th unit and $p(\mathbf{y}_{gt}|\mathbf{y}_{g,t-mc-m:t-m}, \boldsymbol{\xi}_{gt})$ is its distribution which is a normal with mean vector $Z'_{it}\boldsymbol{\beta}$, where $Z_{gt} = (\mathbf{z}_{1gt}, \ldots, \mathbf{z}_{n_g gt})$ and covariance matrix $\text{diag}\{(\sigma^2_{1gt}, \ldots, \sigma^2_{n_g gt})\}$.

B.6 Sampling σ^2

The prior distribution for σ^2 is an $\mathcal{IG}(a_0, b_0)$ with density function

$$p(\sigma^2) = \frac{1}{\Gamma(a_0/2)}(b_0/2)^{a_0/2} \exp\left\{-b_0 \frac{1}{2\sigma^2}\right\} (\sigma^2)^{-a_0/2-1} \tag{B.19}$$

$\sigma^2 > 0$, which is conditionally conjugate. Thus, the full conditional distribution of σ^2 is the inverse gamma

$$\begin{aligned} &p(\sigma^2|\boldsymbol{\mu}, \mathbf{c}, \boldsymbol{\delta}, \boldsymbol{\lambda}, \boldsymbol{\chi}, \mathbf{p}, \boldsymbol{\nu}, \boldsymbol{\zeta}, \boldsymbol{\eta}, \mathbf{q}, \mathbf{r}, \boldsymbol{\xi}, \mathbf{y}) \propto \\ &\propto (\sigma^2)^{-a_0/2-1} \exp\{-b_0 \frac{1}{2\sigma^2}\} \prod_{t\in\mathcal{T}} \prod_{g=1}^{G} \prod_{i=1}^{n_g} (\sigma^2)^{-1/2} \exp\left\{-\frac{\lambda_{ig}\chi_g}{2\sigma^2} e^2_{igt}\right\} \\ &\propto \mathcal{IG}(a_1, b_1) \end{aligned} \tag{B.20}$$

with

$$a_1 = a_0 + nT_q \tag{B.21}$$

$$b_1 = b_0 + \sum_{t\in\mathcal{T}} \sum_{g=1}^{G} \sum_{i=1}^{n_g} \lambda_{ig}\chi_g e^2_{igt} \tag{B.22}$$

where $n = \sum_{g=1}^{G} n_g$ and $e_{igt} = y_{igt} - \mathbf{z}_{igt}{}'(\boldsymbol{\beta} + \boldsymbol{\zeta}_g + \boldsymbol{\eta}_{ig})$.

B.7 Sampling λ

The prior distribution for λ_{ig} is a $\mathcal{G}a(c_{10}, d_{10})$ with density function

$$p(\lambda_{ig}) = \frac{1}{\Gamma(c_{10}/2)}(d_{10}/2)^{c_{10}/2} \lambda_{ig}^{c_{10}/2-1} \exp\left\{-\frac{d_{10}}{2}\lambda_{ig}\right\} \tag{B.23}$$

$\lambda_{ig} > 0$, which is conditionally conjugate. Thus, the full conditional distribution of λ_{ig} is the gamma distribution

$$\begin{aligned} &p(\lambda_{ig}|\boldsymbol{\mu}, \mathbf{c}, \boldsymbol{\delta}, \sigma^2, \boldsymbol{\lambda}_{-ig}, \boldsymbol{\chi}, \mathbf{p}, \boldsymbol{\nu}, \boldsymbol{\zeta}, \boldsymbol{\eta}, \mathbf{q}, \mathbf{r}, \boldsymbol{\xi}, \mathbf{y}) \propto \\ &\propto \lambda_{ig}^{c_{10}/2-1} \exp\left\{-\frac{d_{10}}{2}\lambda_{ig}\right\} \prod_{t\in\mathcal{T}} \lambda_{ig}^{1/2} \exp\left\{-\lambda_{ig}\frac{\chi_g}{2\sigma^2} e^2_{igt}\right\} \\ &\propto \mathcal{G}a(c_{1ig}, d_{1ig}) \end{aligned} \tag{B.24}$$

with

$$c_{1ig} = c_{10} + T_q \tag{B.25}$$
$$d_{1ig} = d_{10} + \frac{\chi_g}{\sigma^2} \sum_{t \in \mathcal{T}} e_{igt}^2 \tag{B.26}$$

and $e_{igt} = y_{igt} - \mathbf{z}_{igt}{}'(\boldsymbol{\beta} + \boldsymbol{\zeta}_g + \boldsymbol{\eta}_{ig})$.

B.8 Sampling χ

The prior distribution for χ_g is a $\mathcal{G}a(c_{20}, d_{20})$ with density function

$$p(\chi_g) = \frac{1}{\Gamma(c_{20}/2)} (d_{20}/2)^{c_{20}/2} \chi_g^{c_{20}/2-1} \exp\left\{-\frac{d_{20}}{2}\chi_g\right\} \tag{B.27}$$

$\chi_g > 0$, which is conditionally conjugate. Thus, the full conditional distribution of χ_g is the gamma distribution

$$\begin{aligned} &p(\chi_g|\boldsymbol{\mu}, \mathbf{c}, \boldsymbol{\delta}, \sigma^2, \boldsymbol{\lambda}, \boldsymbol{\chi}_{-g}, \mathbf{p}, \boldsymbol{\nu}, \boldsymbol{\zeta}, \boldsymbol{\eta}, \mathbf{q}, \mathbf{r}, \boldsymbol{\xi}, \mathbf{y}) \propto \\ &\propto \chi_g^{c_{20}/2-1} \exp\left\{-\frac{d_{20}}{2}\chi_g\right\} \prod_{t \in \mathcal{T}} \prod_{i=1}^{n_g} \chi_g^{1/2} \exp\left\{-\chi_g \frac{\lambda_{ig}}{2\sigma^2} e_{igt}^2\right\} \\ &\propto \mathcal{G}a(c_{2g}, d_{2g}) \end{aligned} \tag{B.28}$$

with

$$c_{2g} = c_{20} + T_q n_g \tag{B.29}$$
$$d_{2g} = d_{20} + \sum_{t \in \mathcal{T}} \sum_{i=1}^{n_g} \frac{\lambda_{ig}}{\sigma^2} e_{igt}^2 \tag{B.30}$$

and $e_{igt} = y_{igt} - \mathbf{z}_{igt}{}'(\boldsymbol{\beta} + \boldsymbol{\zeta}_g + \boldsymbol{\eta}_{ig})$.

B.9 Sampling $\mathbf{q}_{gk}$

The full conditional distribution of $\mathbf{q}_{gk} = (q_{\mu,gk}, q_{c,gk}, q_{\delta,gk})$ is

$$\begin{aligned} &p(\mathbf{q}_{gk}|\boldsymbol{\mu}, \mathbf{c}, \boldsymbol{\delta}, \sigma^2, \boldsymbol{\lambda}, \boldsymbol{\chi}, \mathbf{p}, \boldsymbol{\nu}, \boldsymbol{\zeta}, \boldsymbol{\eta}, \mathbf{q}_{-gk}, \mathbf{r}, \boldsymbol{\xi}, \mathbf{y}) \propto \\ &\propto p(q_{\mu,gk}|\boldsymbol{\eta}_{\mu,gk}) p(q_{c,gk}|\boldsymbol{\eta}_{c,gk}) p(q_{\delta,gk}|\boldsymbol{\eta}_{\delta,gk}) \end{aligned} \tag{B.31}$$

where $\boldsymbol{\eta}_{\mu,gk} = (\eta_{\mu,1gk}, \ldots, \eta_{\mu,n_g gk})'$, $\boldsymbol{\eta}_{c,gk} = (\eta_{c,1g1k}, \ldots, \eta_{c,n_g gck})'$, $\boldsymbol{\eta}_{\delta,gk} = (\eta_{\delta,1g11k}, \ldots, \eta_{\delta,n_g gN\nu+1k})'$, and

$$p(q_{\mu,gk}|\boldsymbol{\eta}_{\mu,gk}) \propto \mathcal{IG}(n_{\mu,gk}, s_{\mu,gk}) \tag{B.32}$$
$$p(q_{c,gk}|\boldsymbol{\eta}_{c,gk}) \propto \mathcal{IG}(n_{c,gk}, s_{c,gk}) \tag{B.33}$$
$$p(q_{\delta,gk}|\boldsymbol{\eta}_{\delta,gk}) \propto \mathcal{IG}(n_{\delta,gk}, s_{\delta,gk}) \tag{B.34}$$

independent for $g = 1, \ldots, G$ and $k = 1, \ldots, K$ with

$$
\begin{aligned}
n_{\mu,gk} &= n_0 + n_g, & s_{\mu,gk} &= s_0 + \sum_{i=1}^{n_g} \eta_{\mu,igk}^2, \\
n_{c,gk} &= n_0 + n_g c, & s_{c,gk} &= s_0 + \sum_{i=1}^{n_g} \sum_{l=1}^{c} \eta_{c,iglk}^2, \\
n_{\delta,gk} &= n_0 + n_g N(\nu+1), & s_{\delta,gk} &= s_0 + \sum_{i=1}^{n_g} \sum_{j=1}^{N} \sum_{l=0}^{\nu} \eta_{\delta,igjlk}^2.
\end{aligned}
$$

B.10 Sampling $\mathbf{r}_k$

The full conditional distribution of $\mathbf{r}_k = (r_{\mu,k}, r_{c,k}, r_{\delta,k})$ is

$$
\begin{aligned}
&p(\mathbf{r}_k|\boldsymbol{\mu}, \mathbf{c}, \boldsymbol{\delta}, \sigma^2, \boldsymbol{\lambda}, \boldsymbol{\chi}, \mathbf{p}, \boldsymbol{\nu}, \boldsymbol{\zeta}, \boldsymbol{\eta}, \mathbf{q}, \mathbf{r}_{-k}, \boldsymbol{\xi}, \mathbf{y}) \propto \\
&\propto p(r_{\mu,k}|\boldsymbol{\zeta}_{\mu,k}) p(r_{c,k}|\boldsymbol{\zeta}_{c,k}) p(r_{\delta,k}|\boldsymbol{\zeta}_{\delta,k})
\end{aligned} \tag{B.35}
$$

where $\boldsymbol{\zeta}_{\mu,k} = (\zeta_{\mu,1k}, \ldots, \zeta_{\mu,Ggk})'$, $\boldsymbol{\zeta}_{c,k} = (\zeta_{c,11k}, \ldots, \zeta_{c,Gck})'$, $\boldsymbol{\zeta}_{\delta,gk} = (\zeta_{\delta,111k}, \ldots, \zeta_{\delta,GN\nu+1k})'$, and

$$
p(r_{\mu,k}|\boldsymbol{\zeta}_{\mu,k}) \propto \mathcal{IG}(n_{\mu,k}, s_{\mu,k}) \tag{B.36}
$$

$$
p(r_{c,k}|\boldsymbol{\zeta}_{c,k}) \propto \mathcal{IG}(n_{c,k}, s_{c,k}) \tag{B.37}
$$

$$
p(r_{\delta,k}|\boldsymbol{\zeta}_{\delta,k}) \propto \mathcal{IG}(n_{\delta,k}, s_{\delta,k}) \tag{B.38}
$$

independent for $k = 1, \ldots, K$ with

$$
\begin{aligned}
n_{\mu,k} &= n_0 + G, & s_{\mu,k} &= s_0 + \sum_{g=1}^{G} \zeta_{\mu,gk}^2, \\
n_{c,k} &= n_0 + Gc, & s_{c,k} &= s_0 + \sum_{g=1}^{G} \sum_{l=1}^{c} \zeta_{c,glk}^2, \\
n_{\delta,k} &= n_0 + GN(\nu+1), & s_{\delta,k} &= s_0 + \sum_{g=1}^{G} \sum_{j=1}^{N} \sum_{l=0}^{\nu} \zeta_{\delta,gjlk}^2.
\end{aligned}
$$

B.11 Sampling $\boldsymbol{\zeta}$

The full conditional distribution of $\boldsymbol{\zeta}_{gk}$ is

$$
\begin{aligned}
&p(\boldsymbol{\zeta}_{gk}|\boldsymbol{\beta}, \sigma^2, \boldsymbol{\lambda}, \boldsymbol{\chi}, \mathbf{p}, \boldsymbol{\nu}, \boldsymbol{\zeta}_{-gk}, \boldsymbol{\eta}, \mathbf{q}, \mathbf{r}, \boldsymbol{\xi}, \mathbf{y}) \propto \\
&\propto \exp\Big\{ -\frac{1}{2} \boldsymbol{\zeta}_{gk}^{'} R_k^{-1} \boldsymbol{\zeta}_{gk} - \frac{1}{2\sigma_{ig}^2} \sum_{t \in \mathcal{T}_{gk}} \sum_{i=1}^{n_g} (\boldsymbol{\zeta}_{gk}^{'} \mathbf{z}_{igkt} \mathbf{z}_{igkt}^{'} \boldsymbol{\zeta}_{gk} \\
&\quad -2\mathbf{z}_{igkt}^{'} \boldsymbol{\zeta}_{gk} (y_{igt} - \mathbf{z}_{igkt}^{'} (\boldsymbol{\beta} + \boldsymbol{\eta}_{ig})) \Big\}
\end{aligned} \tag{B.39}
$$

$$
\propto \mathcal{N}_m \left(\mathbf{m}_{\zeta,gk}, \Upsilon_{\zeta,gk} \right) \tag{B.40}
$$

where $m = c + N(\nu + 1) + 1$ and

$$\Upsilon_{\zeta,gk} = \left(R_k^{-1} + \sum_{i=1}^{n_g} \sigma_{ig}^{-2} Z_{igk}^{'} Z_{igk} \right)^{-1} \tag{B.41}$$

$$\mathbf{m}_{\zeta,gk} = \Upsilon_{\zeta,gk} \sum_{i=1}^{n_g} \sigma_{ig}^{-2} Z_{igk}^{'} \mathbf{e}_{igk} \tag{B.42}$$

and $\mathbf{e}_{igk} = (e_{igk1}, \ldots, e_{igkT_{gk}})'$ with $e_{igkt} = y_{igt} - \mathbf{z}_{igkt}^{'}(\boldsymbol{\beta} + \boldsymbol{\eta}_{ig})$. We recall that $\mathbf{z}_{igkt}' = (1, \mathbf{v}_{igt}', \mathbf{x}_{ig,1t}', \ldots, \mathbf{x}_{ig,Nt}') \otimes \mathbf{e}_k'$ is a vector of dimension $K(1 + c + N(\nu + 1)) \times 1$, and σ_{ig}^2 is defined in Eq. 15.

B.12 Sampling $\boldsymbol{\eta}$

The full conditional distribution of $\boldsymbol{\eta}_{igk}$ is

$$\begin{aligned}
&p(\boldsymbol{\eta}_{igk} | \boldsymbol{\beta}, \sigma^2, \boldsymbol{\lambda}, \boldsymbol{\chi}, \mathbf{p}, \boldsymbol{\nu}, \boldsymbol{\zeta}, \boldsymbol{\eta}_{-igk}, \mathbf{q}, \mathbf{r}, \boldsymbol{\xi}, \mathbf{y}) \propto \\
&\propto \exp\Big\{ -\frac{1}{2} \boldsymbol{\eta}_{igk}^{'} Q_{gk}^{-1} \boldsymbol{\eta}_{igk} - \frac{1}{2\sigma_{ig}^2} \sum_{t \in \mathcal{T}_{gk}} (\boldsymbol{\eta}_{igk}^{'} \mathbf{z}_{igkt} \mathbf{z}_{igkt}^{'} \boldsymbol{\eta}_{igk} - \\
&\quad 2\mathbf{z}_{igkt}^{'} \boldsymbol{\eta}_{igk} (y_{igt} - \mathbf{z}_{igkt}^{'} (\boldsymbol{\beta} + \boldsymbol{\zeta}_g))) \Big\} \\
&\propto \mathcal{N}_m \left(\mathbf{m}_{\eta,igk}, \Upsilon_{\eta,igk} \right)
\end{aligned} \tag{B.43}$$

where $m = c + N(\nu + 1) + 1$ and

$$\Upsilon_{\eta,igk} = \left(Q_{gk}^{-1} + \sigma_{ig}^{-2} Z_{igk}^{'} Z_{igk} \right)^{-1} \tag{B.44}$$

$$\mathbf{m}_{\eta,igk} = \Upsilon_{\eta,igk} \sigma_{ig}^{-2} \left(Z_{igk}^{'} \mathbf{e}_{igk} \right) \tag{B.45}$$

and $\mathbf{e}_{igk} = (e_{igk1}, \ldots, e_{igkT_{gk}})'$ with $e_{igkt} = y_{igt} - \mathbf{z}_{igkt}^{'}(\boldsymbol{\beta} + \boldsymbol{\zeta}_g)$.

Supplementary materials

The supplementary materials contains additional results. In particular, Appendix C presents the results of a simulation-based efficiency analysis of the MCMC algorithm proposed in this paper. Appendices D and E detail the results of the empirical analysis.

C Further simulation results

This section provides further results on the efficiency and convergence analysis of the MCMC procedure used in this paper. Figure C.1 shows an example of simulated panel of time series. Figures C.2 presents the MCMC raw values, progressive averages and autocorrelation function. Figure C.3 the coefficient posterior mean. Figure C.4 shows the means square error for the parameters and hidden states over the MCMC iterations.

Figure C.1: Example of a simulated panel

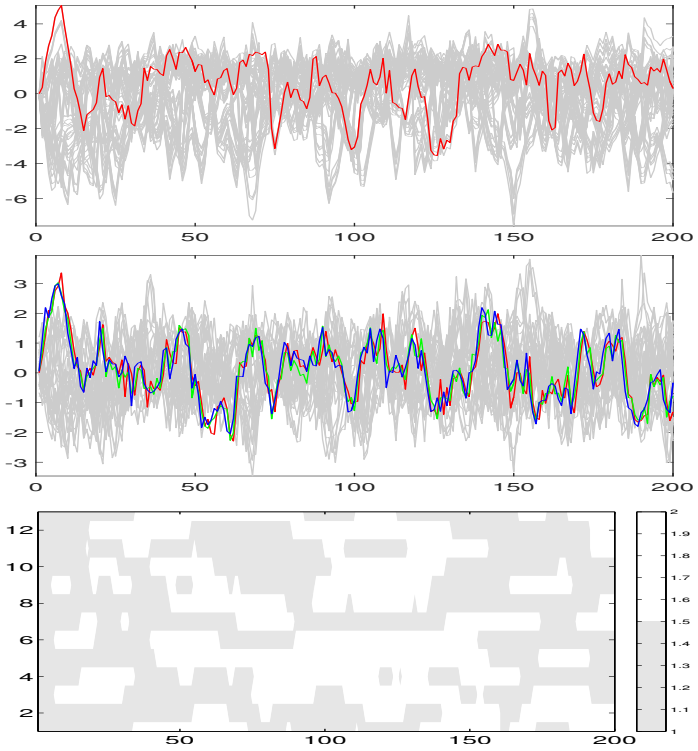

Note: Top panel: simulated panel of time series (gray lines) and a series of the first country in the panel (red line). Middle panel: simulated exogenous time series (gray lines) and three exogenous for the the first country of the panel (red line). Bottom panel: regime switching process (horizontal axis) for the different units (vertical axes).

Figure C.2: Further results on convergence and efficiency

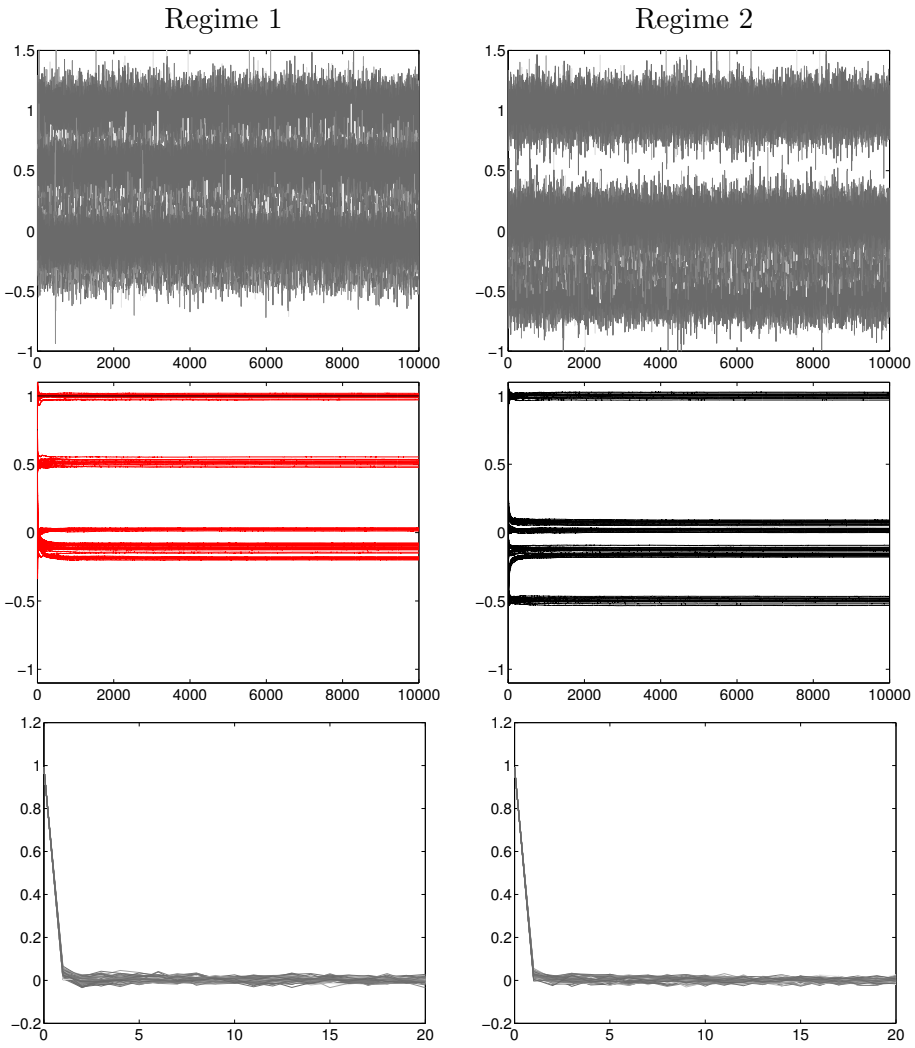

Note: MCMC raw output (first row), progressive averages (second row) and ACF (third row), based on 10,000 MCMC iterations, for the coefficients δ_{igjk}, $\forall i$, $\forall g$, $\forall j$, and for $k = 1, 2$.

Figure C.3: Further results on convergence and efficiency

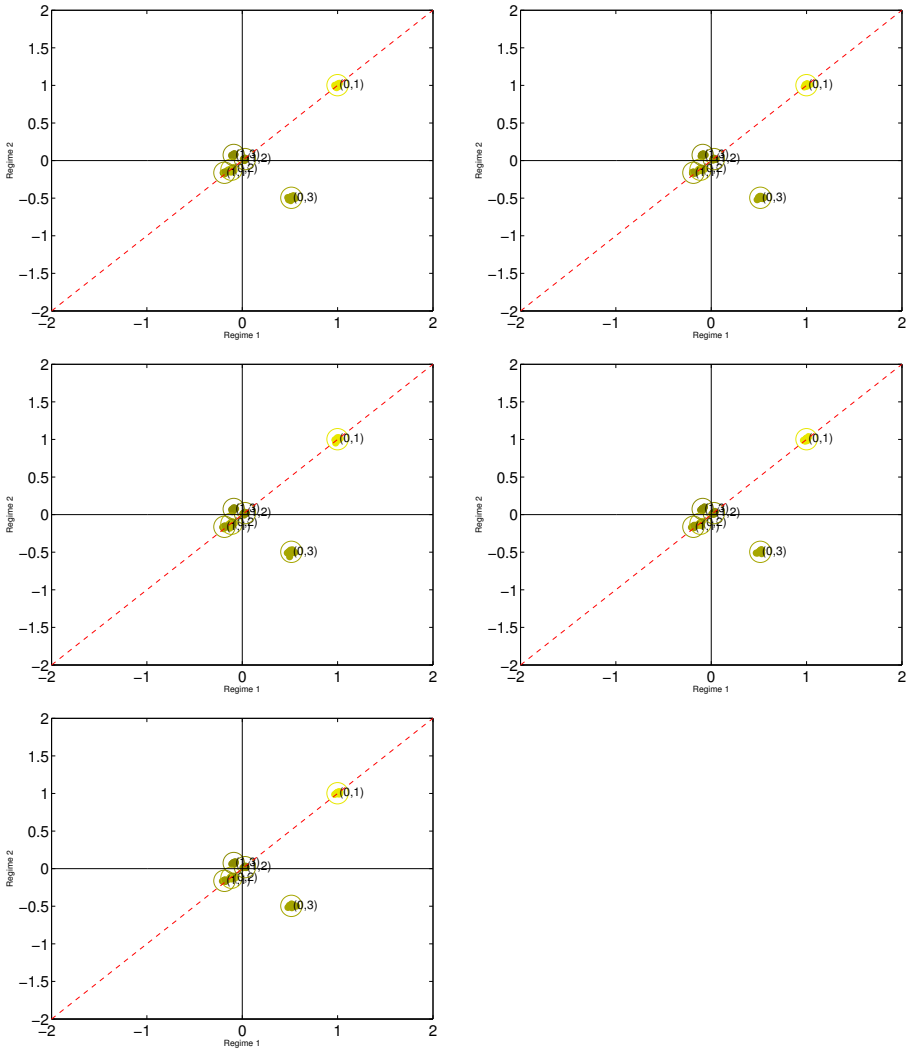

Note: Posterior mean of the coefficients δ_{igjk}. In each plot, the pairs $(\delta_{igj1}, \delta_{igj2})$ (dots), $\forall g$, $\forall j$. Different plots correspond to different timeseries index $i = 1, \ldots, 5$.

Figure C.4: Further results on convergence and efficiency

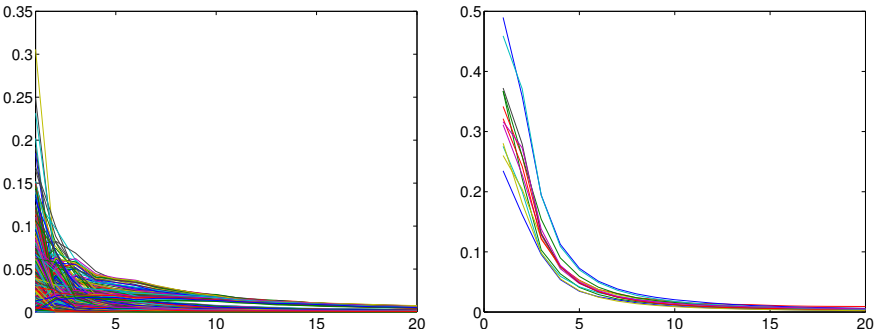

Note: Parameters (left) and hidden states (right) mean square error (MSE) over the first 20 MCMC iterations.

D Data description

We considered the following dependent variables:

1. Gross Domestic Product (GDP)
2. Industrial Productin Index (IPI) growth rates
3. Employment (Emp)
4. Consumption (Con)
5. Nominal Earnings (Ner)
6. Real Earnings (Rer)
7. Inflation (Inf): changes in the PCE deflator
8. Hours (Hou)
9. Interest Rates (IR)
10. Stock Market (Sto)
11. Money (M2)

sampled at a quarterly frequency. The availability of the time series for each country is given in Tab. D.1. In the same table the mean value of the variable is given. The sources of the complete list of variable is given in Table D.2. Figures D.1-D.2 show all series after standardization.

As measures of uncertainty we consider

1. forecast disagreement
2. VIX

Table D.1: Summary statistics

	US	EU	JP	DE	FR	UK	IT	CA	NE	NW	SP	SW	CH
GDP	0.49	0.36	0.18	0.32	0.33	0.48	0.061	0.59	0.36	0.45	0.42	0.56	0.49
IP	0.28	0.15	0.034	0.47	-0.12	-0.16	-0.29	0.21	0.3	-0.22	-0.3		
Emp	0.17	0.15	-0.03	0.17	0.16	0.21	0.08	0.36					
Con	0.65	0.25	0.19	0.22	0.39	0.56	0.072	0.74					
Inf	0.48	0.51	-0.17	0.31	0.33	0.51	0.52	0.39	0.46	0.48	0.61	0.35	0.12
Ner	0.58		0.061	0.52	0.68	0.79	0.64	0.5	0.57	1.1	0.81	0.71	
Rer	0.12		0.12	0.21	0.35	0.28	0.12	0.11	0.11	0.57	0.2	0.36	
Hou	-0.043		-0.09	-0.13	-0.1	-0.03		-0.047	-0.04		-0.04	-0.05	-0.1
IR	-0.07	0.00	-0.00	0.00	0.00	-0.09	0.00	-0.064	0.00	-0.1	0.00	0	-0.01
Sto	0.90	0.19	0.38	0.54	0.49	0.22	-0.46	1.2	-0.35	2.6	0.32	1.2	0.36
M2	1.50	1.40	0.60	1.00		1.72	1.31	1.73		1.87		1.69	
n_g	11	8	11	11	10	11	10	11	8	8	8	8	5

Mean of the available variables per country. Empty cell indicates the variables is not available for the conuntry in the column. The last row indicates the number of variables, n_g, per country.

Table D.2: Data Sources

Variable	Source
GDP	
United States	OECD Economic Outlook
Euro area	OECD Economic Outlook
Japan	OECD Economic Outlook
Germany	OECD Economic Outlook
France	OECD Economic Outlook
United Kingdom	OECD Economic Outlook
Italy	OECD Economic Outlook
Canada	OECD Economic Outlook
Netherlands	OECD Economic Outlook
Norway	OECD Economic Outlook
Spain	OECD Economic Outlook
Sweden	OECD Economic Outlook
Switzerland	OECD Economic Outlook
Industrial production	
United States	OECD Monthly Economic Indicators
Euro area	OECD Monthly Economic Indicators
Japan	OECD Monthly Economic Indicators
Germany	OECD Monthly Economic Indicators
France	OECD Monthly Economic Indicators
United Kingdom	OECD Monthly Economic Indicators
Italy	OECD Monthly Economic Indicators
Canada	OECD Monthly Economic Indicators
Netherlands	IMF
Norway	IMF
Spain	IMF
Employment	
United States	OECD Economic Outlook
Euro area	OECD Economic Outlook
Japan	OECD Economic Outlook
Germany	OECD Economic Outlook
France	OECD Economic Outlook
United Kingdom	OECD Economic Outlook
Italy	OECD Economic Outlook
Canada	OECD Economic Outlook
Consumption	
United States	OECD Economic Outlook
Euro area	OECD Economic Outlook
Japan	OECD Economic Outlook
Germany	OECD Economic Outlook
France	OECD Economic Outlook
United Kingdom	OECD Economic Outlook
Italy	OECD Economic Outlook
Canada	OECD Economic Outlook

Table D.2: Data Sources (Continued)

Variable	Source
Inflation	
United States	OECD Economic Outlook
Euro area	OECD Economic Outlook
Japan	OECD Economic Outlook
Germany	OECD Economic Outlook
France	OECD Economic Outlook
United Kingdom	OECD Economic Outlook
Italy	OECD Economic Outlook
Canada	OECD Economic Outlook
Netherlands	OECD Economic Outlook
Norway	OECD Economic Outlook
Spain	OECD Economic Outlook
Sweden	OECD Economic Outlook
Switzerland	OECD Economic Outlook
Nominal earnings	
United States	OECD Monthly Economic Indicators
Japan	OECD Monthly Economic Indicators
Germany	OECD Monthly Economic Indicators
France	OECD Monthly Economic Indicators
United Kingdom	OECD Monthly Economic Indicators
Italy	OECD Monthly Economic Indicators
Canada	OECD Monthly Economic Indicators
Netherlands	OECD Monthly Economic Indicators
Norway	OECD Monthly Economic Indicators
Spain	OECD Monthly Economic Indicators
Sweden	OECD Monthly Economic Indicators
Real earnings	
United States	Nominal earnings deflated by inflation
Japan	Nominal earnings deflated by inflation
Germany	Nominal earnings deflated by inflation
France	Nominal earnings deflated by inflation
United Kingdom	Nominal earnings deflated by inflation
Italy	Nominal earnings deflated by inflation
Canada	Nominal earnings deflated by inflation
Netherlands	Nominal earnings deflated by inflation
Norway	Nominal earnings deflated by inflation
Spain	Nominal earnings deflated by inflation
Sweden	Nominal earnings deflated by inflation
Hours worked	
United States	OECD Economic Outlook
Japan	OECD Economic Outlook
Germany	OECD Economic Outlook
France	OECD Economic Outlook
United Kingdom	OECD Economic Outlook
Canada	OECD Economic Outlook
Netherlands	OECD Economic Outlook
Spain	OECD Economic Outlook
Sweden	OECD Economic Outlook
Switzerland	OECD Economic Outlook

Table D.2: Data Sources (Continued)

Variable	Source
Interest rate/bank rate	
United States	Datastream
Euro area	Datastream
Japan	Datastream
Germany	Datastream
France	Datastream
United Kingdom	Datastream
Italy	Datastream
Canada	Datastream
Netherlands	Datastream
Norway	Norges Bank
Spain	Datastream
Sweden	IMF
Switzerland	IMF
Stock returns	
United States	OECD Monthly Economic Indicators
Euro area	OECD Monthly Economic Indicators
Japan	OECD Monthly Economic Indicators
Germany	OECD Monthly Economic Indicators
France	OECD Monthly Economic Indicators
United Kingdom	OECD Monthly Economic Indicators
Italy	OECD Monthly Economic Indicators
Canada	OECD Monthly Economic Indicators
Netherlands	OECD Monthly Economic Indicators
Norway	OECD Monthly Economic Indicators
Spain	OECD Monthly Economic Indicators
Sweden	OECD Monthly Economic Indicators
Switzerland	OECD Monthly Economic Indicators
M2	
United States	Datastream
Euro area	Datastream
Japan	Datastream
Germany	Datastream
United Kingdom	Datastream
Italy	Datastream
Canada	Datastream
Norway	Statistics Norway
Sweden	IMF

Figure D.1: Dependent variable series in the panel by type.

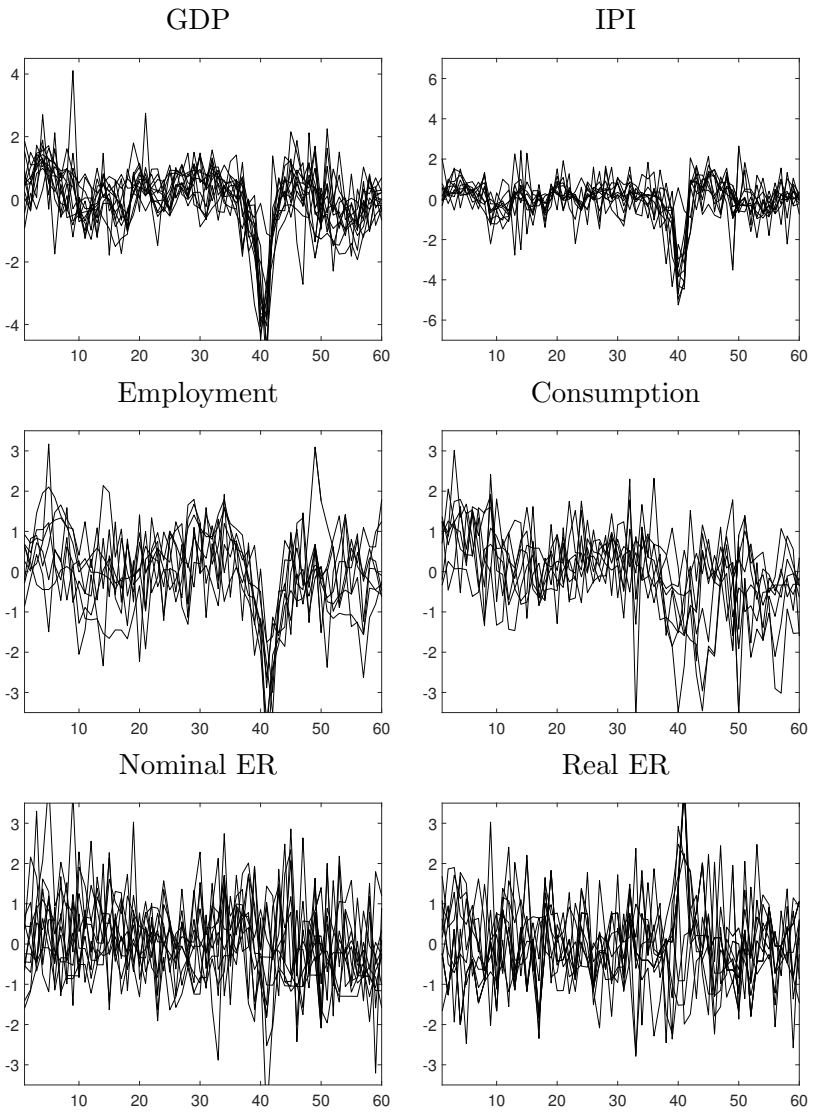

Figure D.2: Dependent variable series in the panel by type.

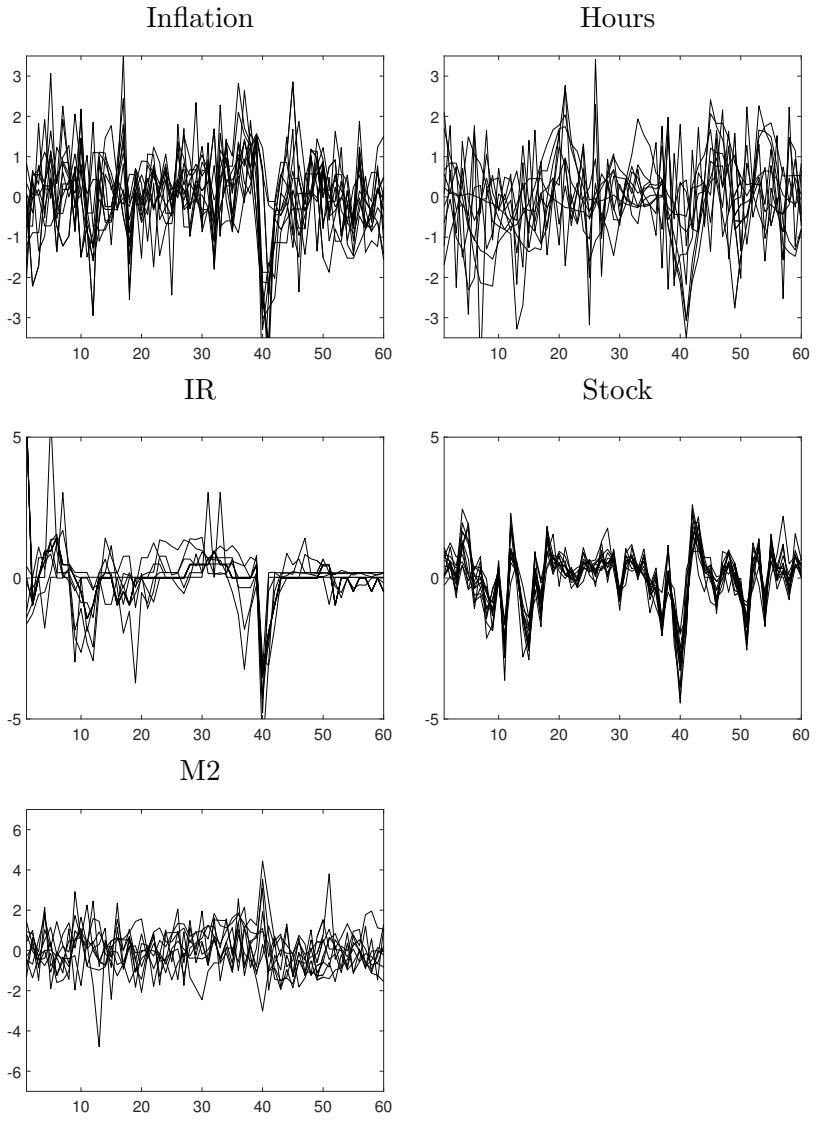

Figure D.3: Independent variable series by type.

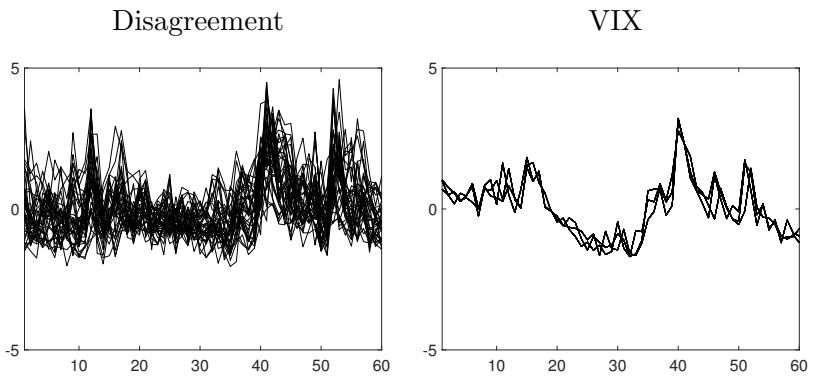

Figure D.4: Rolling (3 years) correlation across VIX of different countries.

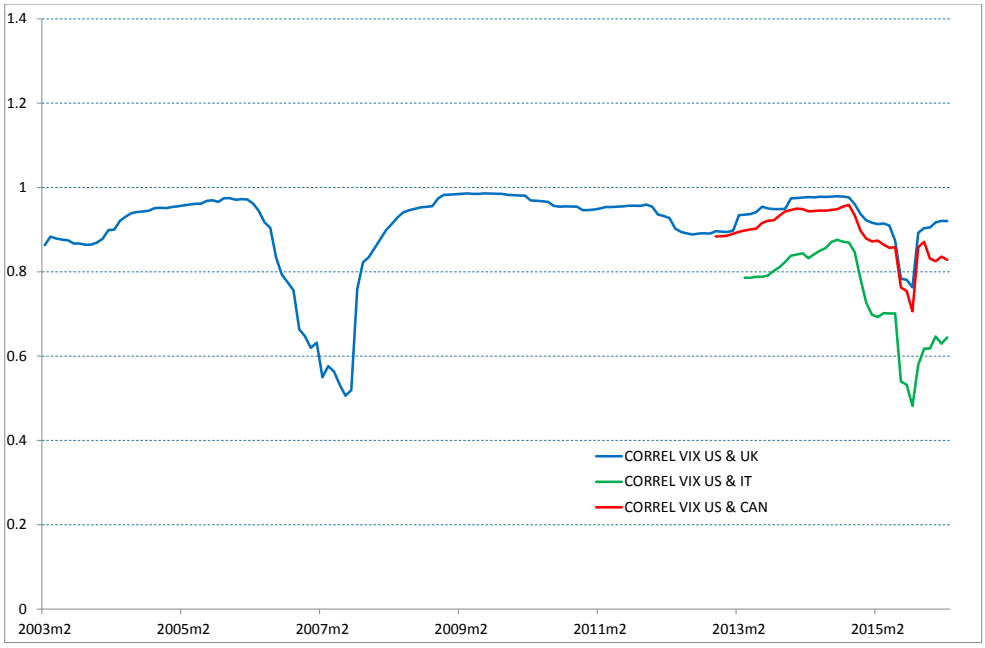

Figure D.5: Correlations between different measures of uncertainty

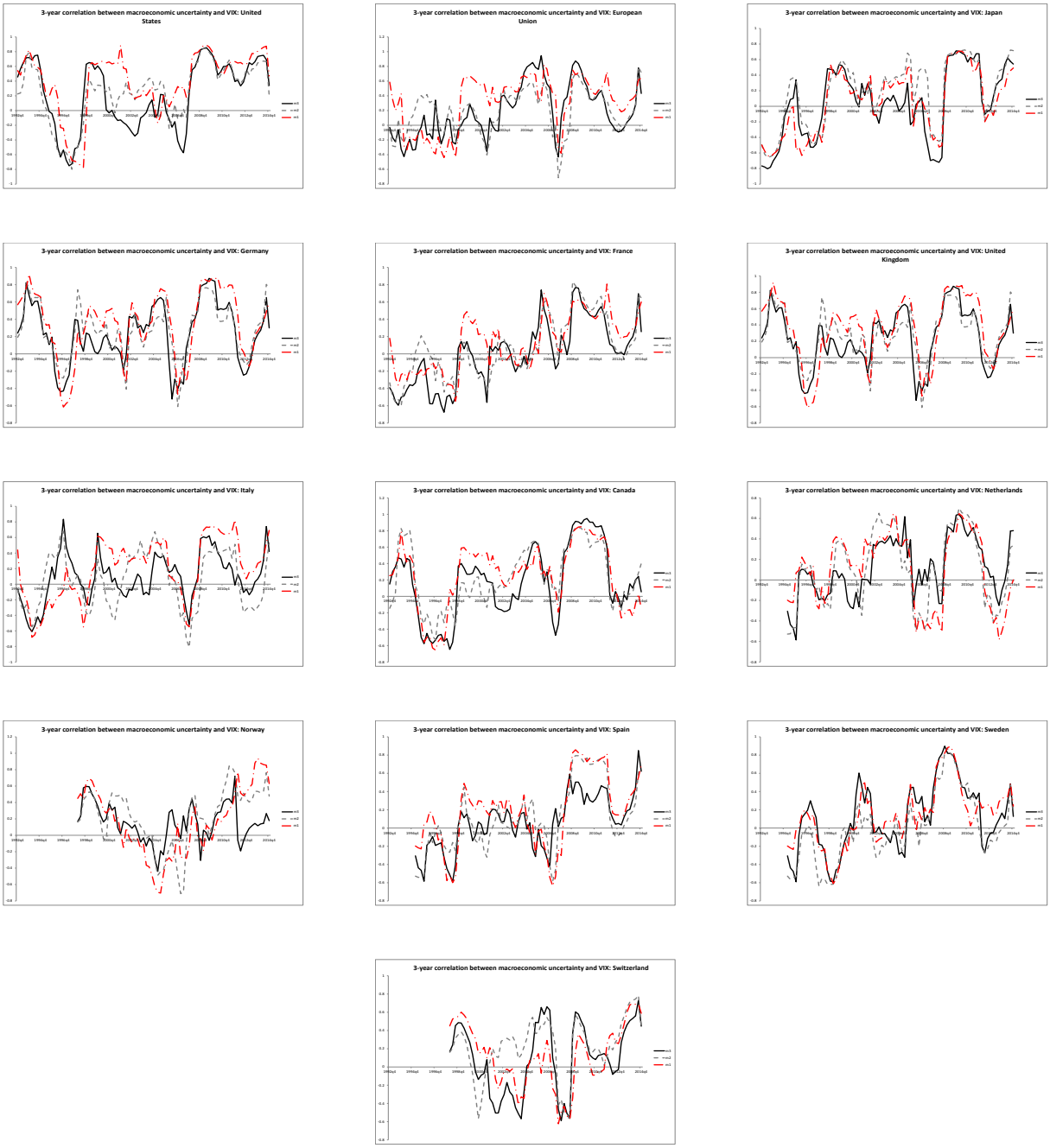

E Further empirical results

Figures E.1-E.2 report the MAP estimates of the hidden states (blue stepwise line) and the posterior probability of the second regime (solid red line) for the different units (countries) in the panel.

Figures E.3-E.5 show the effects of uncertainty shocks (Forecast Disagreement and VIX) on the original variables scale for different variables, $i = 1, \ldots, n_g$, $g = 1, \ldots, G$, different lags, $l = 0, 1$ and regimes $k = 1, 2$.

The following figures and tables report results of several robustness analysis. First, Figures E.6-E.8 exhibit the lagged effects of the uncertainty in a restricted version of our model, where contemporaneous disagreement and VIX uncertainty measures are excluded to avoid the problem of potential endogeneity of the contemporaneous uncertainty shocks. In this model only the first lag of the uncertainty shocks is considered, i.e. $l = 1$. The main results are confirmed.

Next, we report the results of our panel MIDAS model when only VIX is included:

1. Effects of the monthly uncertainty, contemporaneous and one lag (Fig. E.9-E.10)

2. Effects of the average quarterly uncertainty, contemporaneous and one lag (Fig. E.11-E.12)

Finally, we report the results of our panel MIDAS model when only forecast disagreement is included:

1. Effects of the monthly uncertainty, contemporaneous and one lag (Fig. E.13-E.14)

2. Effects of the average quarterly uncertainty, contemporaneous and one lag (Fig. E.15-E.16)

Table E.1 and Table E.2 report the median of the sum of the six coefficients, monthly contemporaneous and lagged variables, that have 90% of the mass different from zero for the two regimes for the Financial Uncertainty Index and the macroeconomic disagreement. The effect of financial uncertainty are substantially larger relative to the benchmark VIX case.

Results are confirmed when the Financial Entropy Index is used, see Tables E.3 and E.4.

Figure E.1: Country-specific posterior probability of being in regime 2 and hidden state estimates.

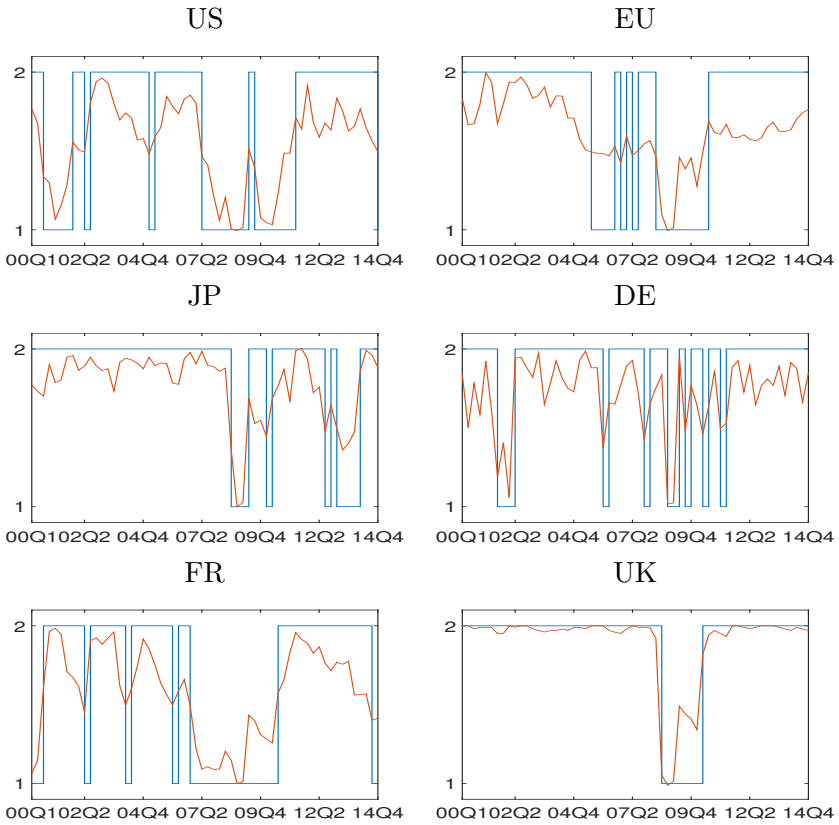

Note: the red line represents the posterior probability of being in regime 2 and the blue line the hidden state estimates.

Figure E.2: Country-specific posterior probability of being in regime 2 and hidden state estimates.

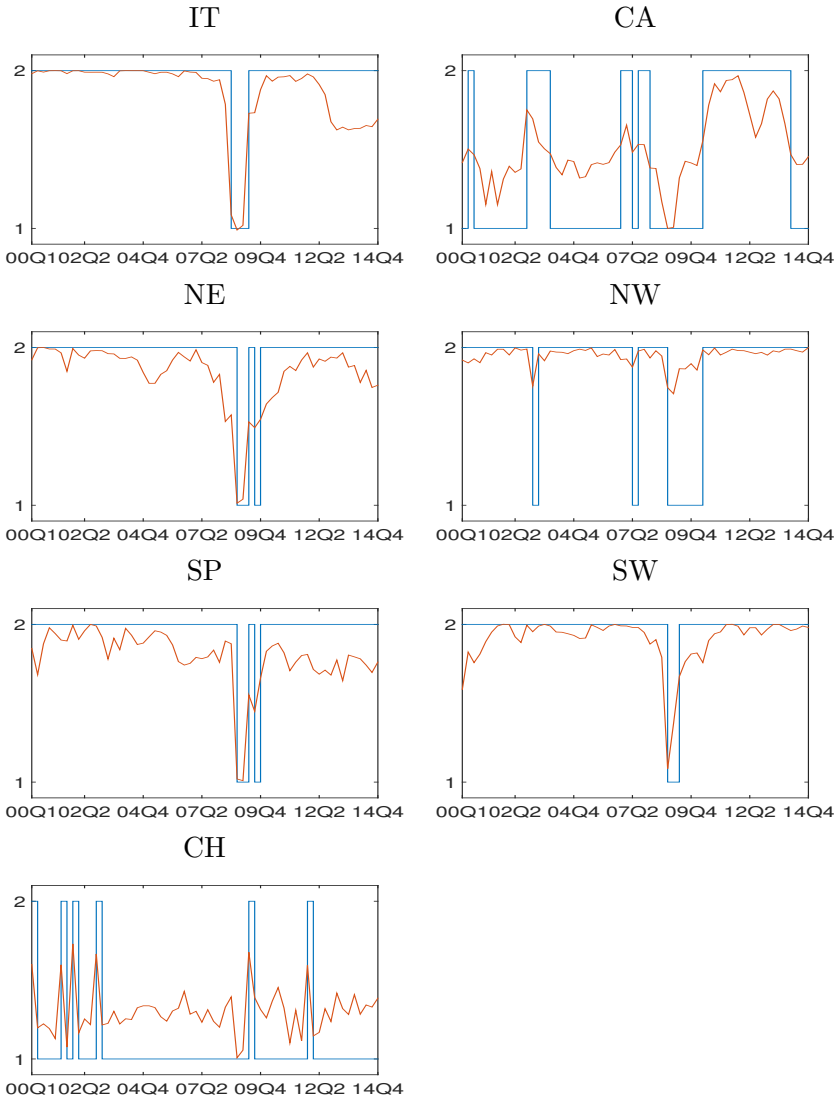

Note: the red line represents the posterior probability of being in regime 2 and the blue line the hidden state estimates.

Figure E.3: Effects of uncertainty shock on macroeconomic variables.

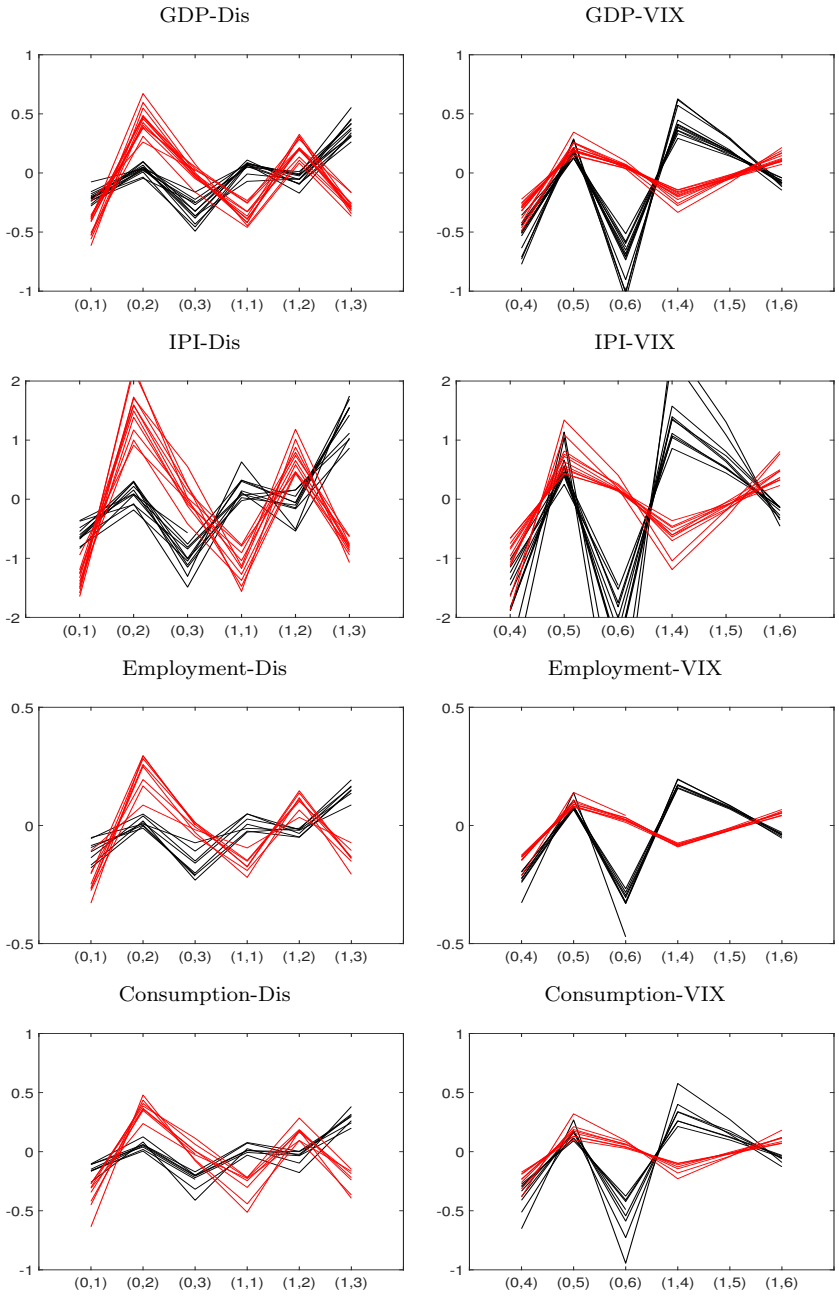

Note: Impact coefficient $\delta_{ijlgk} = \delta_{jlk} + \zeta_{\delta,gjlk} + \eta_{\delta,igjlk}$ of uncertainty shocks on different variables, $i = 1, \ldots, n_g$, $g = 1, \ldots, G$, reported on the original variables scale at different lags, $l = 0, 1$ and regimes $k = 1, 2$. The black color refers to the first regime; the red color to the second regime.

Figure E.4: Effects of uncertainty shock on macroeconomic variables.

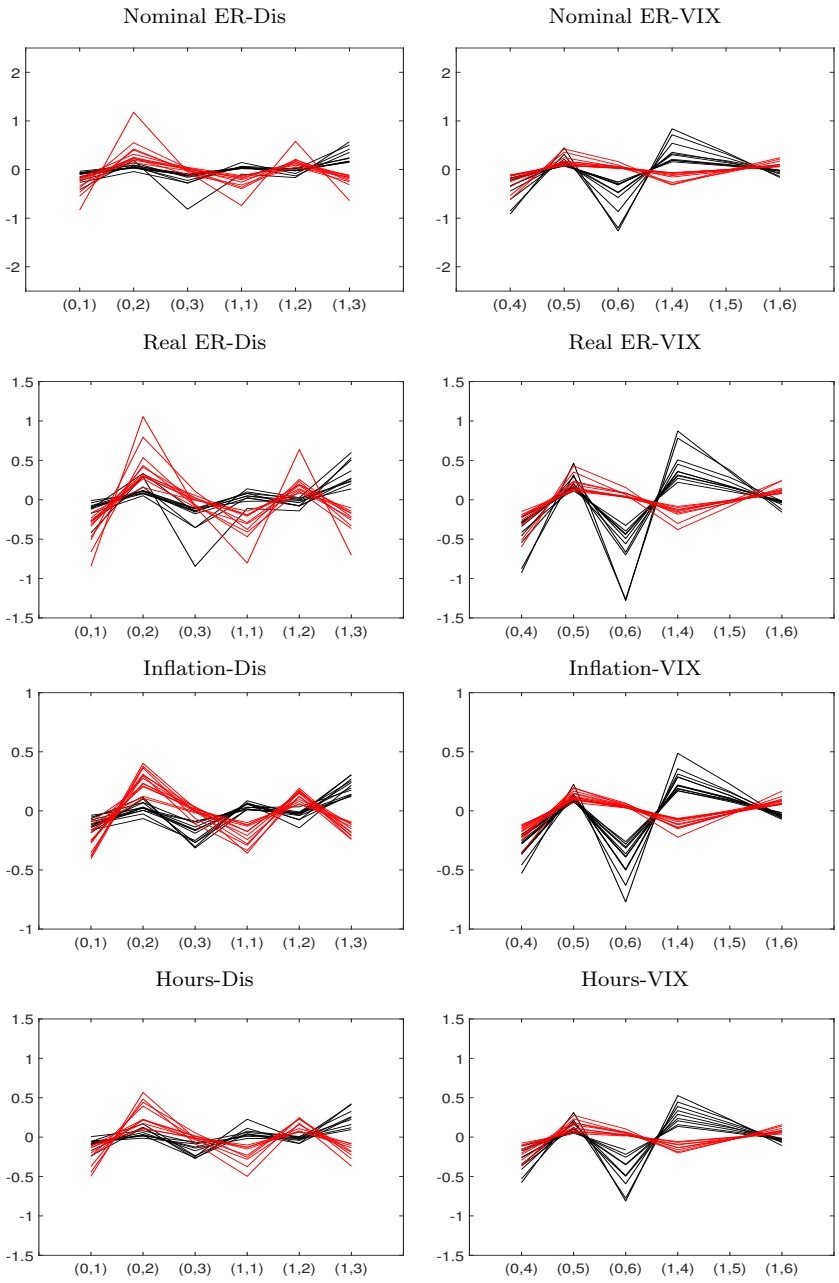

Note: Impact coefficient $\delta_{ijlgk} = \delta_{jlk} + \zeta_{\delta,gjlk} + \eta_{\delta,igjlk}$ of uncertainty shocks on different variables, $i = 1, \ldots, n_g$, $g = 1, \ldots, G$, reported on the original variables scale at different lags, $l = 0, 1$ and regimes $k = 1, 2$. The black color refers to the first regime; the red color to the second regime.

Figure E.5: Effects of uncertainty shock on macroeconomic variables.

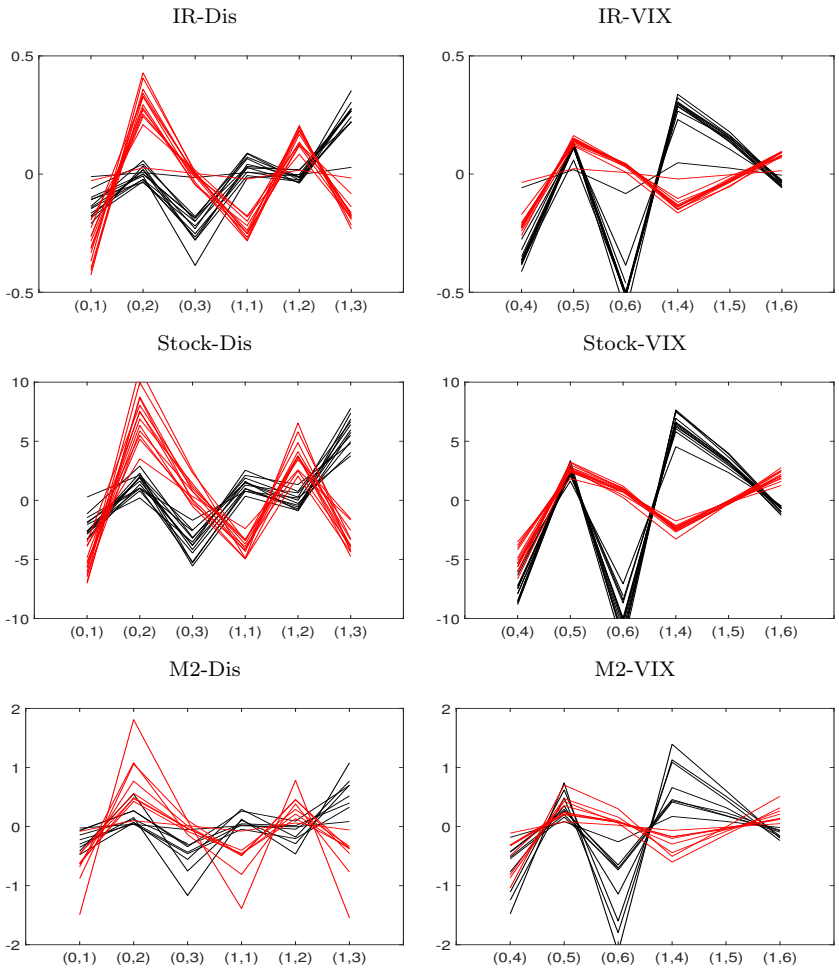

Note: Impact coefficient $\delta_{ijlgk} = \delta_{jlk} + \zeta_{\delta,gjlk} + \eta_{\delta,igjlk}$ of uncertainty shocks on different variables, $i = 1, \ldots, n_g$, $g = 1, \ldots, G$, reported on the original variables scale at different lags, $l = 0, 1$ and regimes $k = 1, 2$. The black color refers to the first regime; the red color to the second regime.

Figure E.6: Effects of monthly uncertainty, when only one lag (i.e. $l = 1$) for both macroeconomic and financial uncertainty is considered.

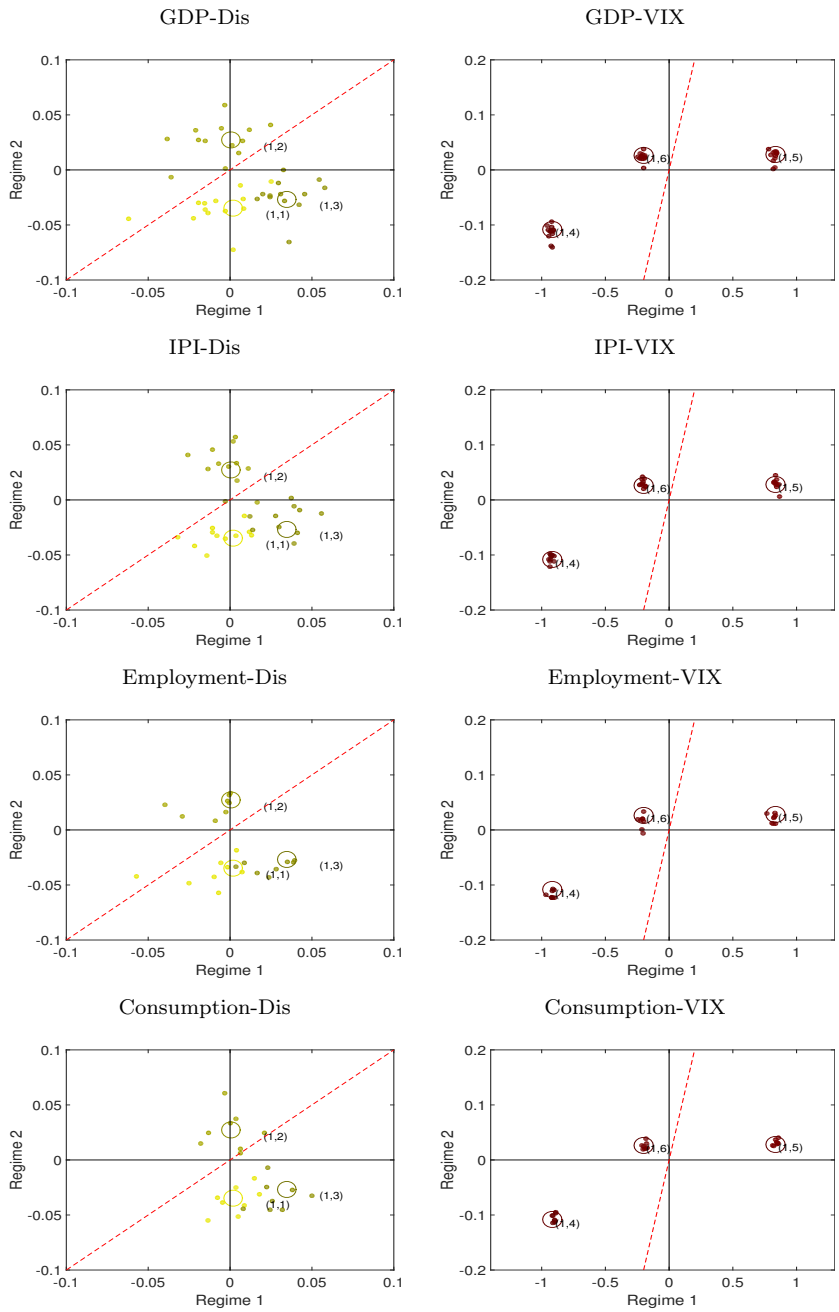

Note: the figure reports the impact of uncertainty on different variables ($i = 1, \ldots, n_g$, $g = 1, \ldots, G$), at lag $l = 0, 1$ in regime $k = 1, 2$. The circles indicate the common impact δ_{jlk} for the pair lag l and shock j, denoted with (l, j). The dots indicate country- and series- specific impact $\delta_{ijlgk} = \delta_{jlk} + \zeta_{\delta,gjlk} + \eta_{\delta,igjlk}$ in the two regimes. The dashed line indicates the 45° line. Different shades of color indicate the dots referred to a specific lag.

Figure E.7: Effects of monthly uncertainty, when only one lag (i.e. $l = 1$) for both macroeconomic and financial uncertainty is considered

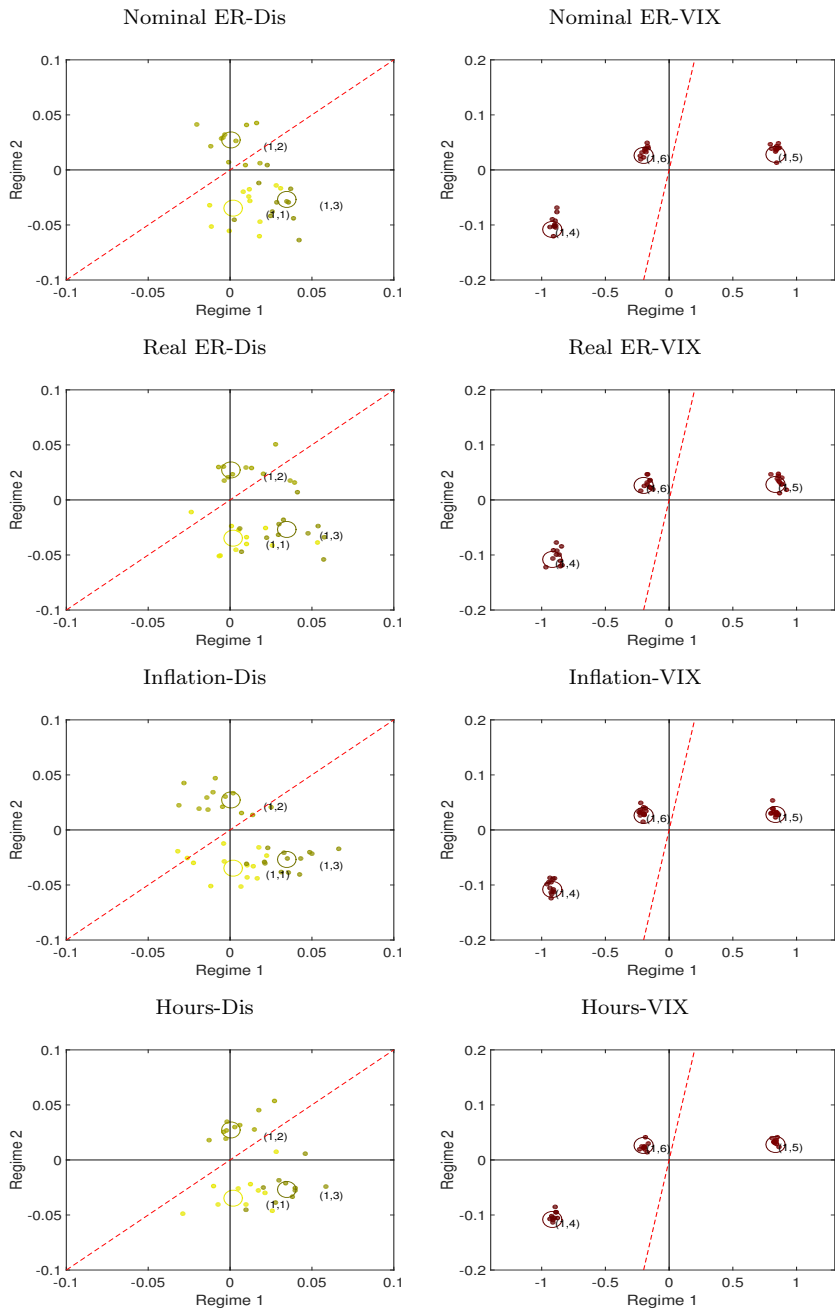

Note: the figure reports the impact of uncertainty on different variables ($i = 1, \ldots, n_g$, $g = 1, \ldots, G$), at lag $l = 0, 1$ in regime $k = 1, 2$. The circles indicate the common impact δ_{jlk} for the pair lag l and shock j, denoted with (l, j). The dots indicate country- and series- specific impact $\delta_{ijlgk} = \delta_{jlk} + \zeta_{\delta,gjlk} + \eta_{\delta,igjlk}$ in the two regimes. The dashed line indicates the 45° line. Different shades of color indicate the dots referred to a specific lag.

Figure E.8: Effects of monthly uncertainty, when only one lag (i.e. $l = 1$) for both macroeconomic and financial uncertainty is considered

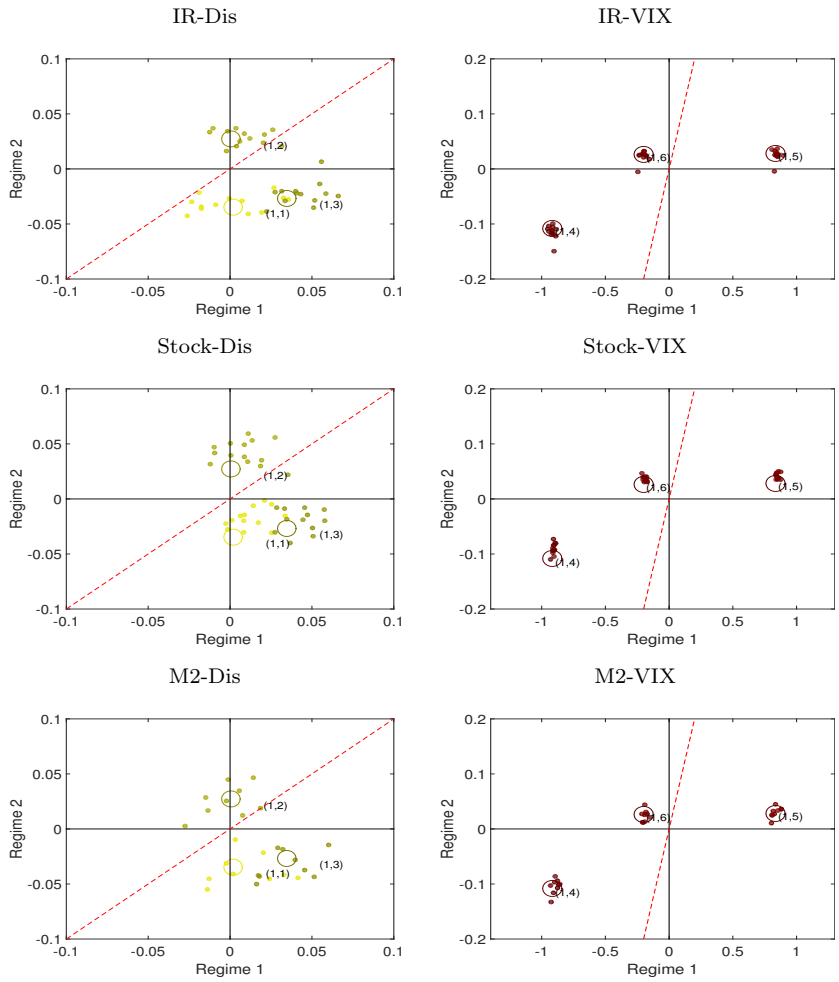

Note: the figure reports the impact of uncertainty on different variables ($i = 1, \ldots, n_g$, $g = 1, \ldots, G$), at lag $l = 0, 1$ in regime $k = 1, 2$. The circles indicate the common impact δ_{jlk} for the pair lag l and shock j, denoted with (l, j). The dots indicate country- and series- specific impact $\delta_{ijlgk} = \delta_{jlk} + \zeta_{\delta,gjlk} + \eta_{\delta,igjlk}$ in the two regimes. The dashed line indicates the 45° line. Different shades of color indicate the dots referred to a specific lag.

Figure E.9: Effects of monthly uncertainty, when only financial uncertainty is considered

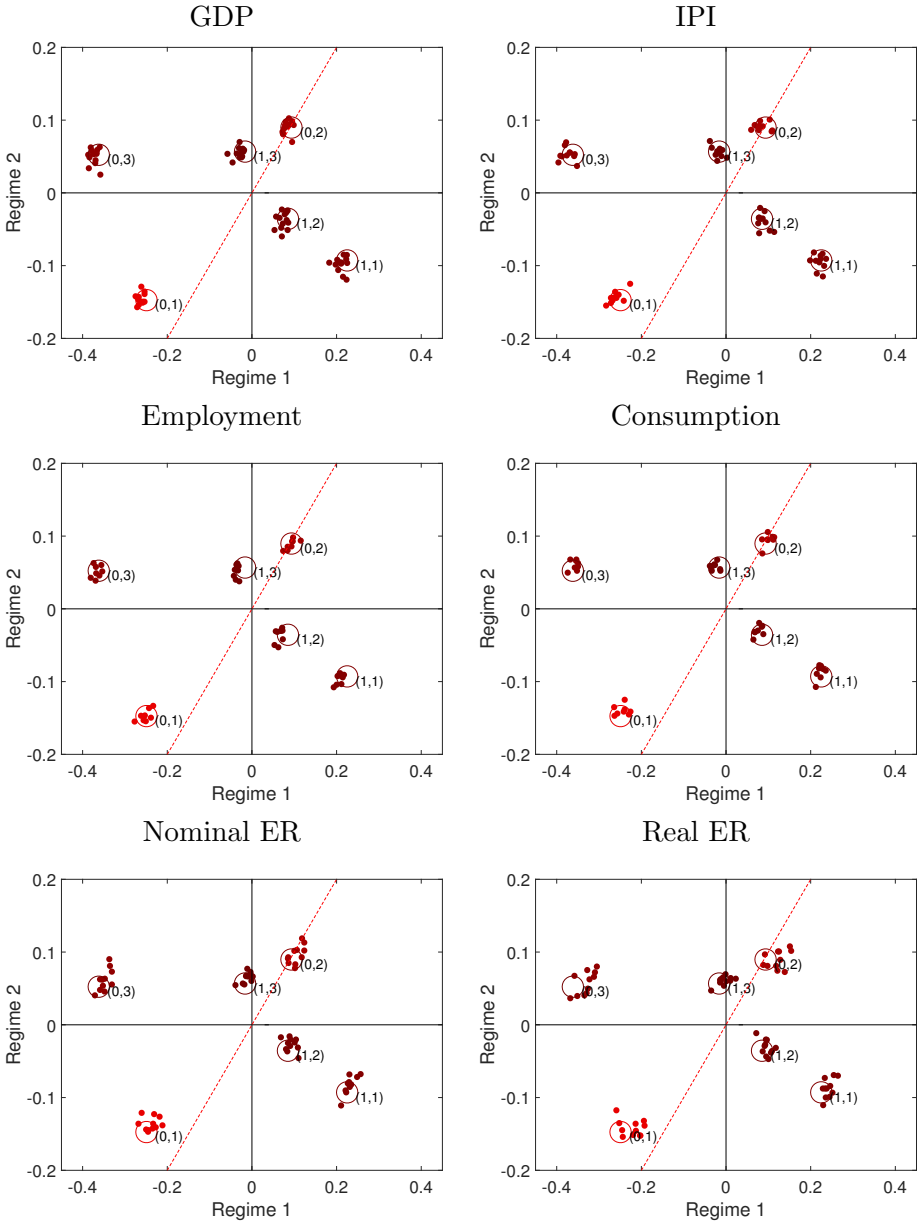

Note: Impact of uncertainty shocks on the different variables ($i = 1, \ldots, n_g$, $g = 1, \ldots, G$), at different months, $j = 1, 2, 3$, lags, $l = 0, 1$ and regimes $k = 1, 2$. Circles: common impact δ_{jlk} in the two regimes, i.e. $(\delta_{jl1}, \delta_{jl2})$, for the pair lag and shock (l, j). Dots: country- and series- specific impact $\delta_{ijlgk} = \delta_{jlk} + \zeta_{\delta,gjlk} + \eta_{\delta,igjlk}$ in the two regimes, i.e. $(\delta_{ijlg1}, \delta_{ijlg2})$ for all countries, $g = 1, \ldots, G$. Dashed line: 45° line.

Figure E.10: Effects of monthly uncertainty, when only financial uncertainty is considered

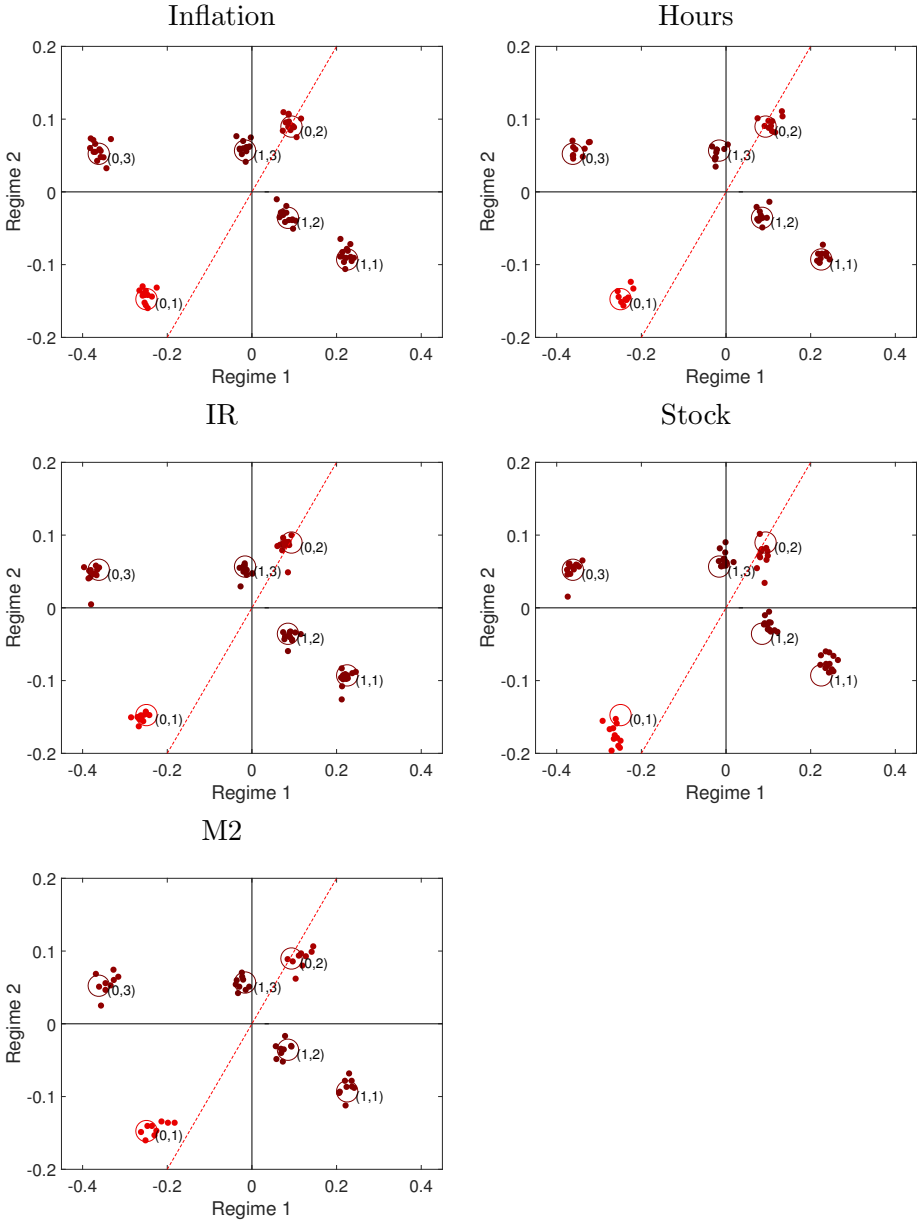

Note: Impact of uncertainty shocks on the different variables ($i = 1, \ldots, n_g$, $g = 1, \ldots, G$), at different months, $j = 1, 2, 3$, lags, $l = 0, 1$ and regimes $k = 1, 2$. Circles: common impact δ_{jlk} in the two regimes, i.e. $(\delta_{jl1}, \delta_{jl2})$, for the pair lag and shock (l, j). Dots: country- and series- specific impact $\delta_{ijlgk} = \delta_{jlk} + \zeta_{\delta,gjlk} + \eta_{\delta,igjlk}$ in the two regimes, i.e. $(\delta_{ijlg1}, \delta_{ijlg2})$ for all countries, $g = 1, \ldots, G$. Dashed line: 45° line.

Figure E.11: Effects of quarterly averaged uncertainty, when only financial uncertainty is considered

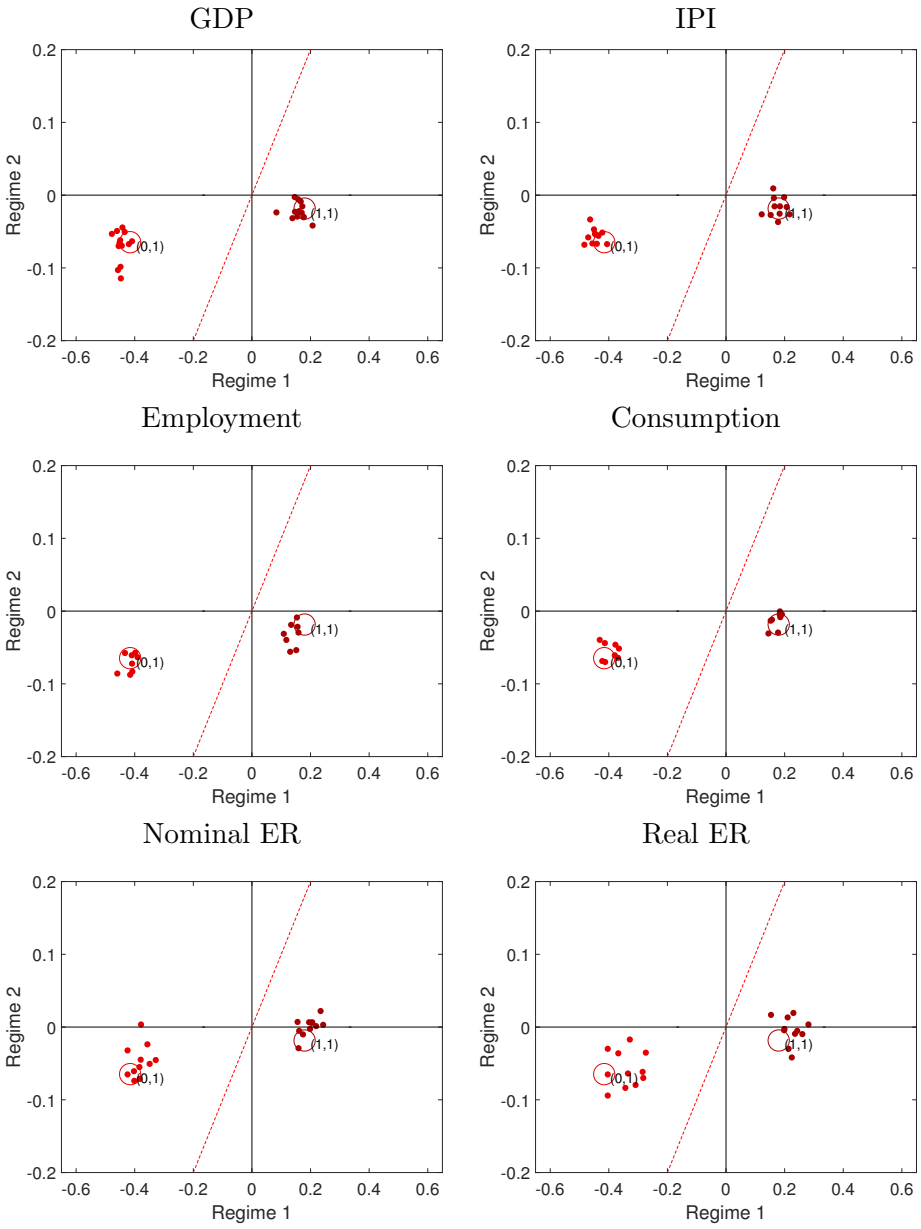

Note: Impact of the average uncertainty shocks ($j = 1$) on the different variables ($i = 1, \ldots, n_g$, $g = 1, \ldots, G$), at different lags, $l = 0, 1$ and regimes $k = 1, 2$. Circles: common impact δ_{jlk} in the two regimes, i.e. $(\delta_{jl1}, \delta_{jl2})$, for the pair lag and shock (l, j). Dots: country- and series- specific impact $\delta_{ijlgk} = \delta_{jlk} + \zeta_{\delta,gjlk} + \eta_{\delta,igjlk}$ in the two regimes, i.e. $(\delta_{ijlg1}, \delta_{ijlg2})$ for all countries, $g = 1, \ldots, G$. Dashed line: 45° line.

Figure E.12: Effects of quarterly averaged uncertainty, when only financial uncertainty is considered

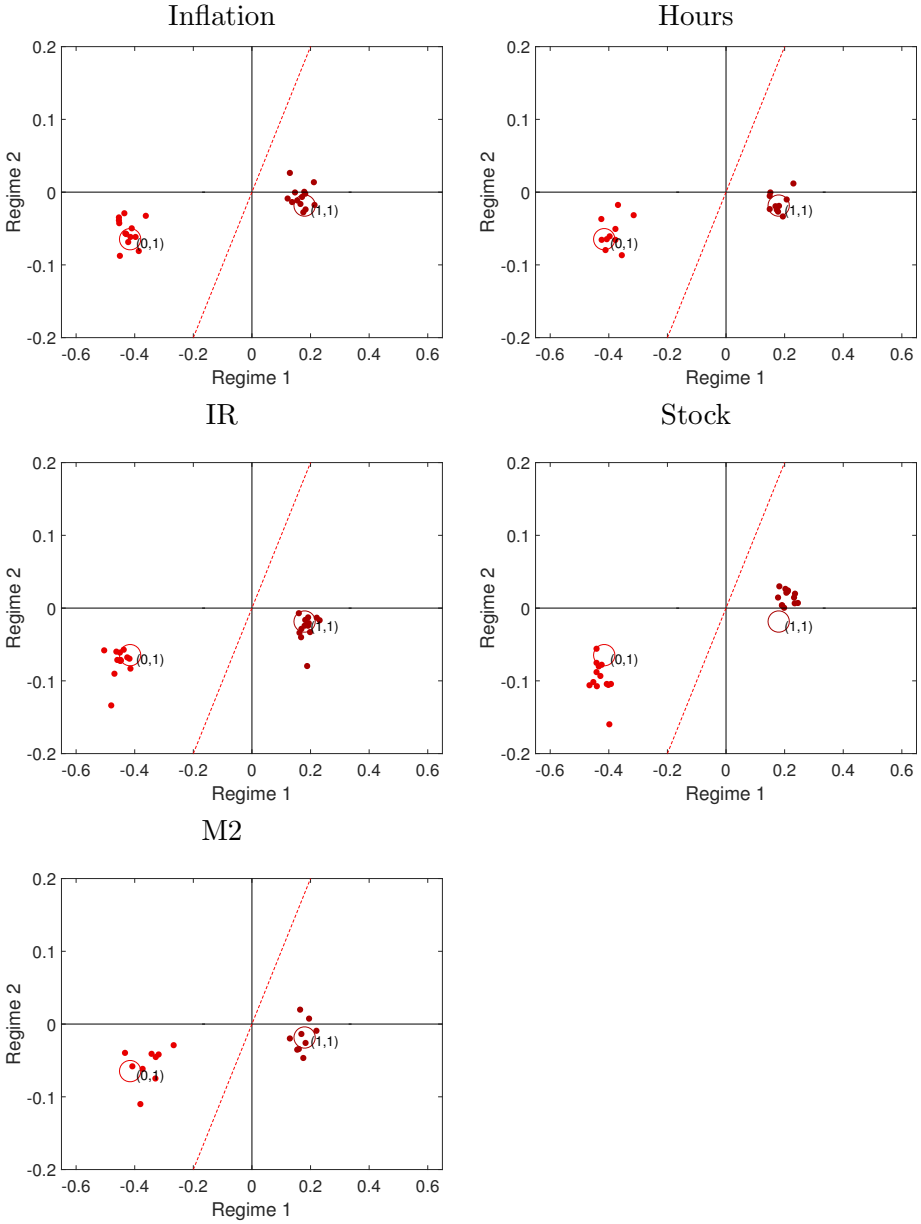

Note: Impact of the average uncertainty shocks ($j = 1$) on the different variables ($i = 1, \ldots, n_g$, $g = 1, \ldots, G$), at different lags, $l = 0, 1$ and regimes $k = 1, 2$. Circles: common impact δ_{jlk} in the two regimes, i.e. $(\delta_{jl1}, \delta_{jl2})$, for the pair lag and shock (l, j). Dots: country- and series- specific impact $\delta_{ijlgk} = \delta_{jlk} + \zeta_{\delta,gjlk} + \eta_{\delta,igjlk}$ in the two regimes, i.e. $(\delta_{ijlg1}, \delta_{ijlg2})$ for all countries, $g = 1, \ldots, G$. Dashed line: 45° line.

Figure E.13: Effects of monthly uncertainty, when only macroeconomic uncertainty is considered.

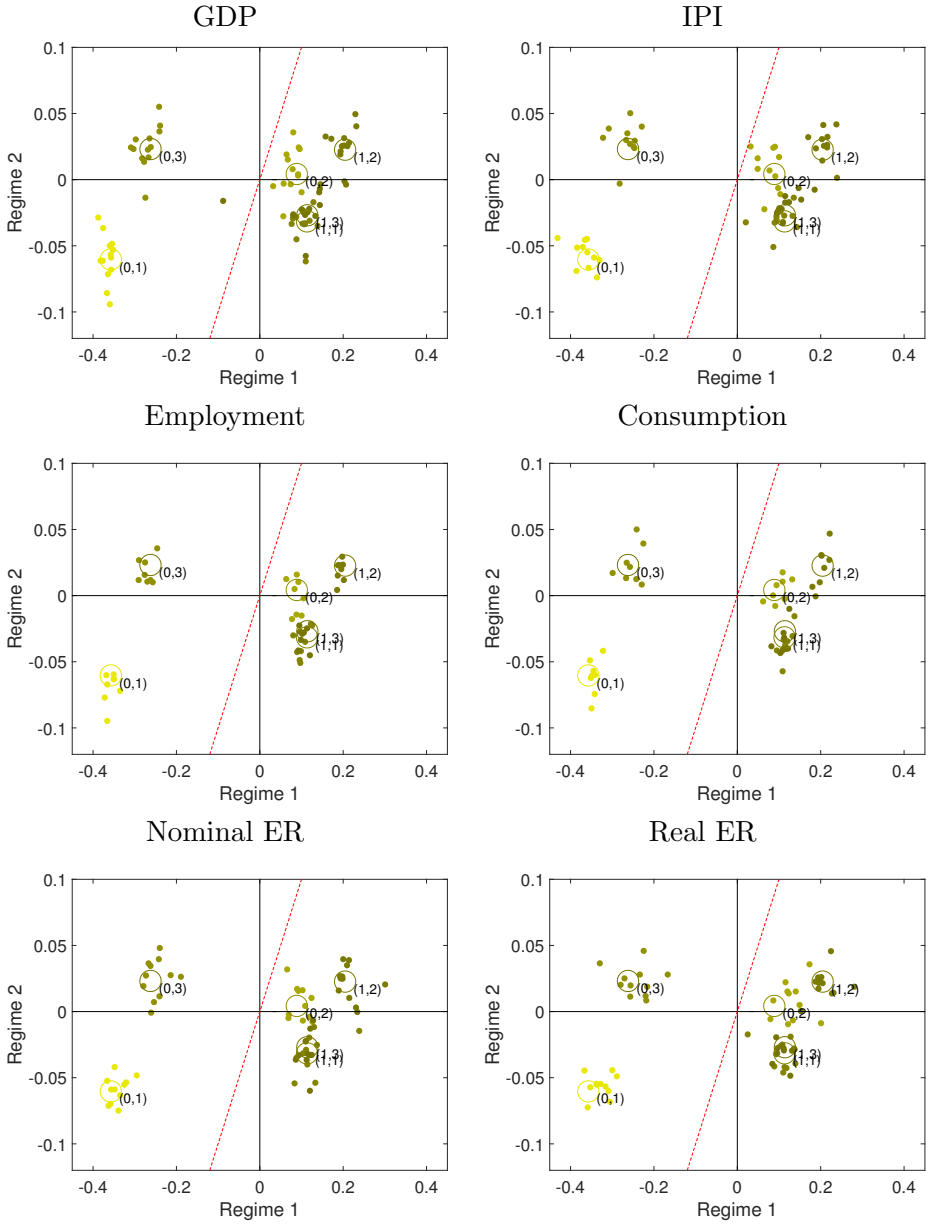

Note: Impact of uncertainty shocks on the different variables ($i = 1, \ldots, n_g$, $g = 1, \ldots, G$), at different months, $j = 1, 2, 3$, lags, $l = 0, 1$ and regimes $k = 1, 2$. Circles: common impact δ_{jlk} in the two regimes, i.e. $(\delta_{jl1}, \delta_{jl2})$, for the pair lag and shock (l, j). Dots: country- and series- specific impact $\delta_{ijlgk} = \delta_{jlk} + \zeta_{\delta,gjlk} + \eta_{\delta,igjlk}$ in the two regimes, i.e. $(\delta_{ijlg1}, \delta_{ijlg2})$ for all countries, $g = 1, \ldots, G$. Dashed line: 45° line.

Figure E.14: Effects of monthly uncertainty, when only macroeconomic uncertainty is considered.

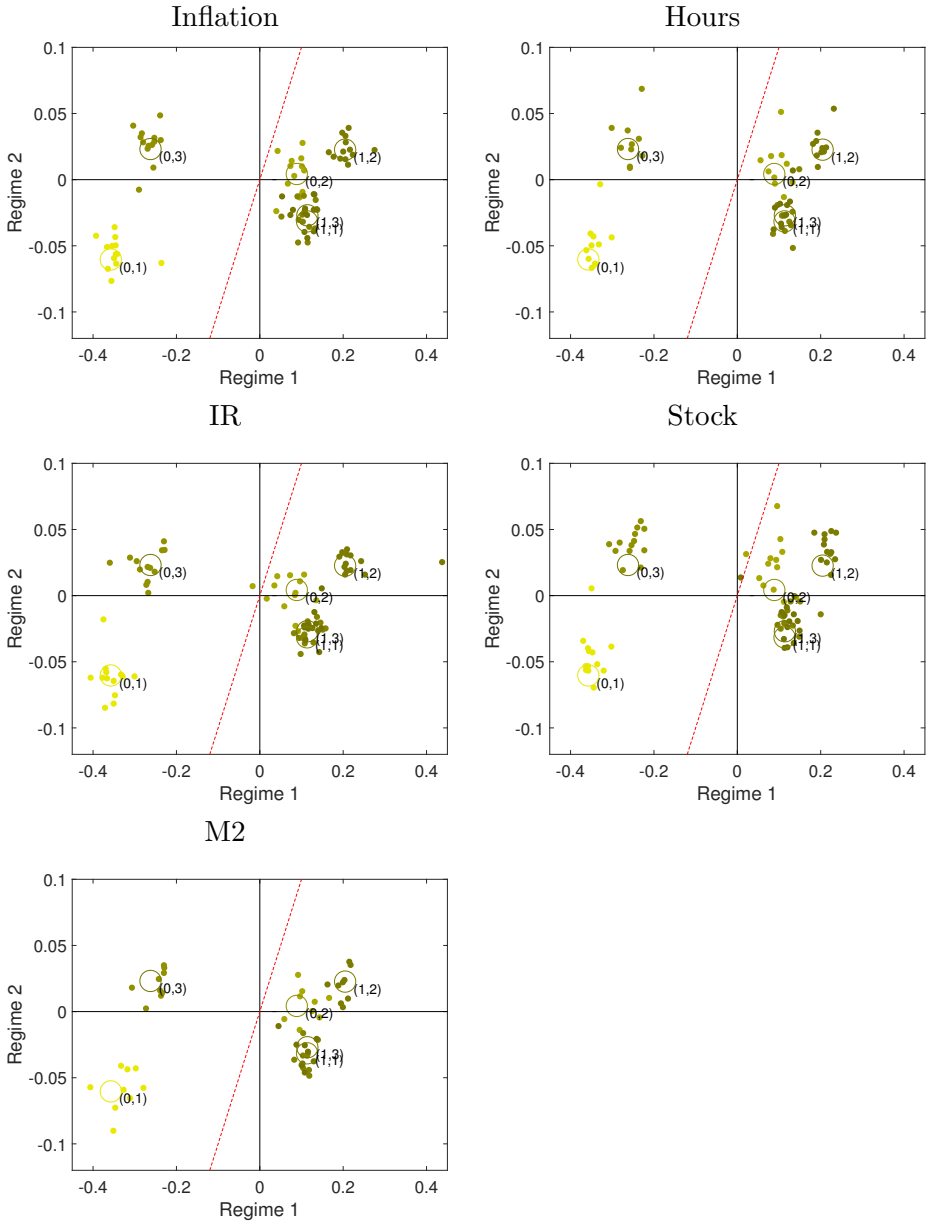

Note: Impact of uncertainty shocks on the different variables ($i = 1, \ldots, n_g$, $g = 1, \ldots, G$), at different months, $j = 1, 2, 3$, lags, $l = 0, 1$ and regimes $k = 1, 2$. Circles: common impact δ_{jlk} in the two regimes, i.e. $(\delta_{jl1}, \delta_{jl2})$, for the pair lag and shock (l, j). Dots: country- and series- specific impact $\delta_{ijlgk} = \delta_{jlk} + \zeta_{\delta,gjlk} + \eta_{\delta,igjlk}$ in the two regimes, i.e. $(\delta_{ijlg1}, \delta_{ijlg2})$ for all countries, $g = 1, \ldots, G$. Dashed line: 45° line.

Figure E.15: Effects of quarterly averaged uncertainty, when only macroeconomic uncertainty is considered.

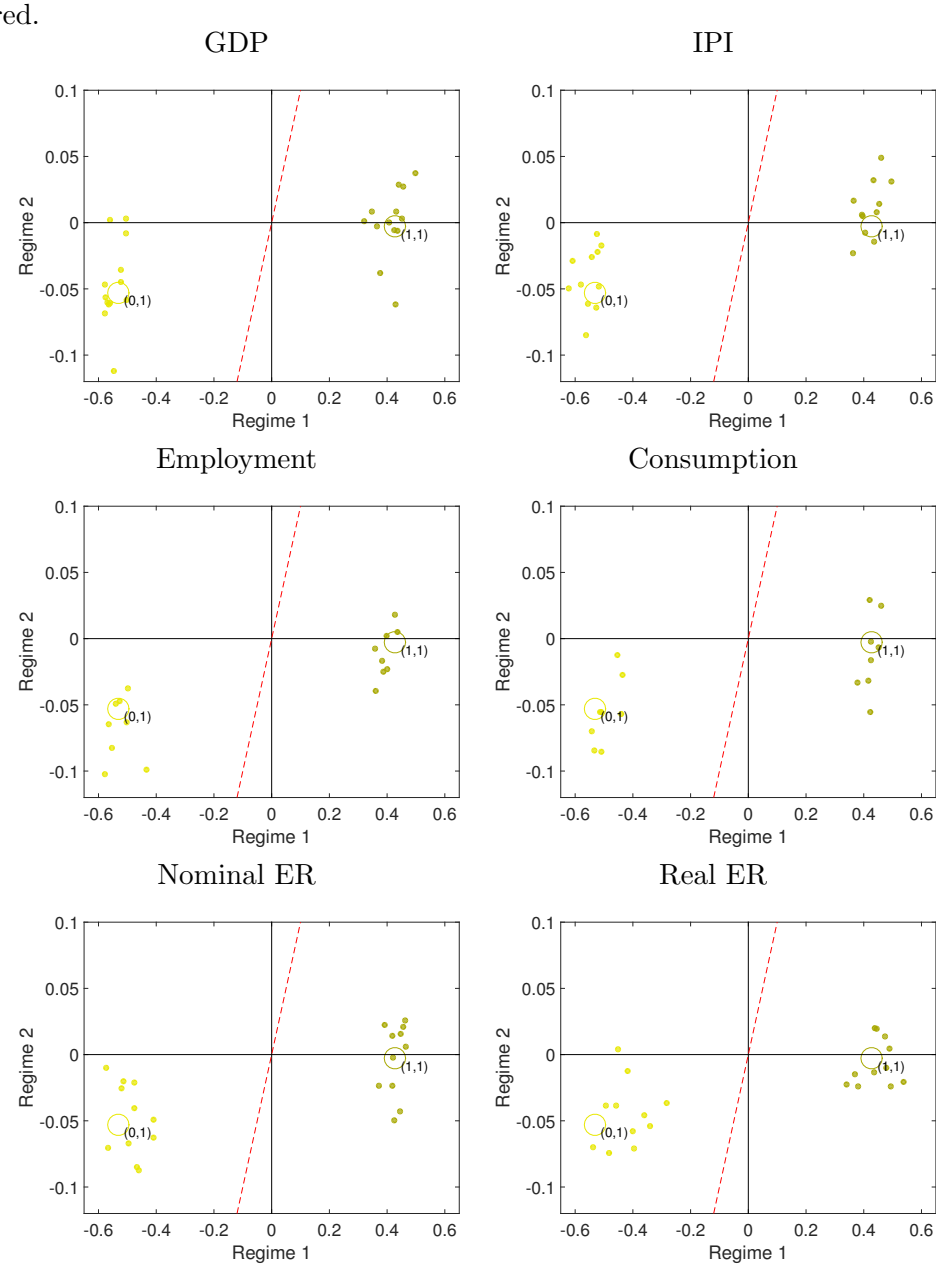

Note: Impact of the average uncertainty shocks ($j = 1$) on the different variables ($i = 1, \ldots, n_g$, $g = 1, \ldots, G$), at different lags, $l = 0, 1$ and regimes $k = 1, 2$. Circles: common impact δ_{jlk} in the two regimes, i.e. $(\delta_{jl1}, \delta_{jl2})$, for the pair lag and shock (l, j). Dots: country- and series- specific impact $\delta_{ijlgk} = \delta_{jlk} + \zeta_{\delta,gjlk} + \eta_{\delta,igjlk}$ in the two regimes, i.e. $(\delta_{ijlg1}, \delta_{ijlg2})$ for all countries, $g = 1, \ldots, G$. Dashed line: 45° line.

Figure E.16: Effects of quarterly averaged uncertainty, when only macroeconomic uncertainty is considered

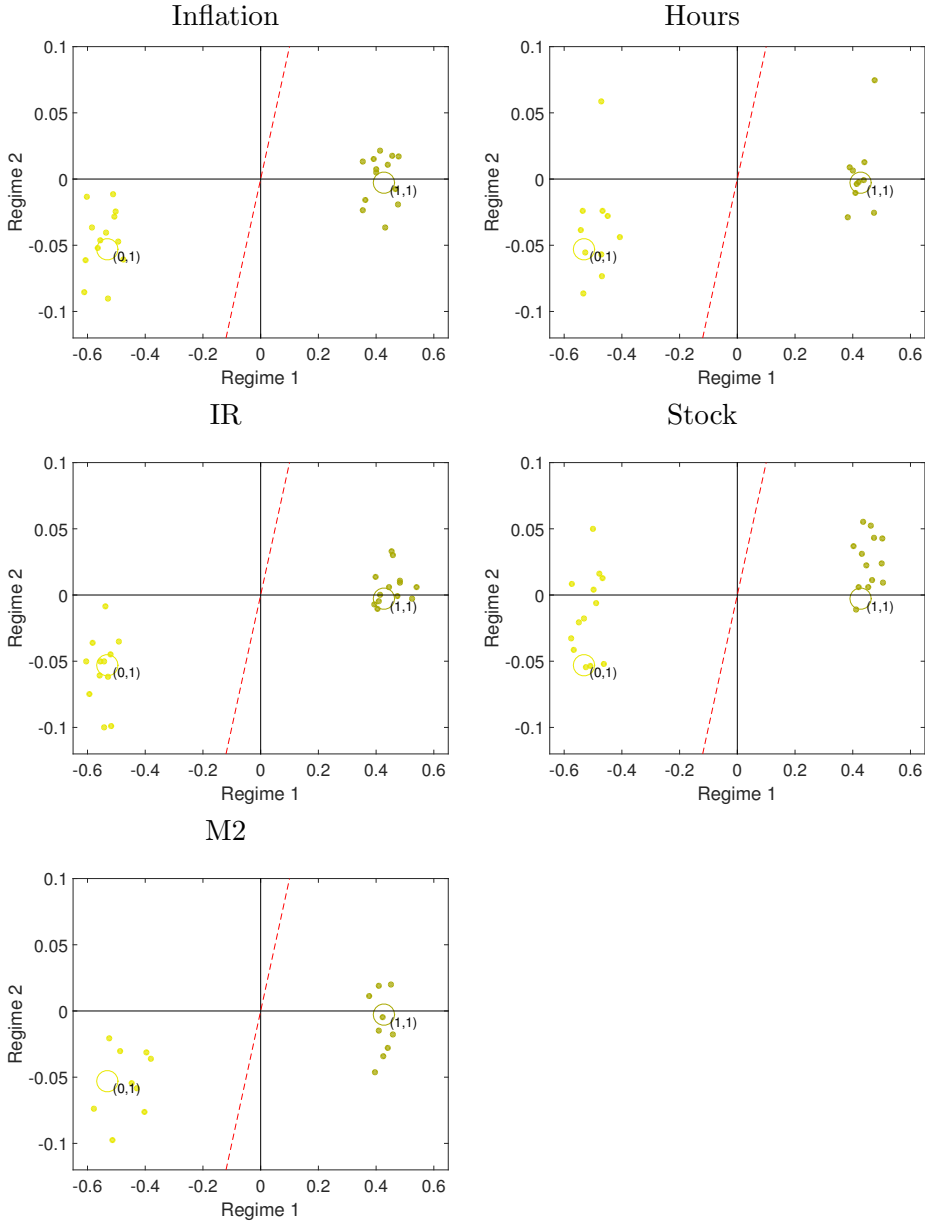

Note: Impact of the average uncertainty shocks ($j = 1$) on the different variables ($i = 1, \ldots, n_g$, $g = 1, \ldots, G$), at different lags, $l = 0, 1$ and regimes $k = 1, 2$. Circles: common impact δ_{jlk} in the two regimes, i.e. $(\delta_{jl1}, \delta_{jl2})$, for the pair lag and shock (l, j). Dots: country- and series- specific impact $\delta_{ijlgk} = \delta_{jlk} + \zeta_{\delta,gjlk} + \eta_{\delta,igjlk}$ in the two regimes, i.e. $(\delta_{ijlg1}, \delta_{ijlg2})$ for all countries, $g = 1, \ldots, G$. Dashed line: 45° line.

Table E.1: Effects of financial uncertainty on macroeconomic variables (when Financial Uncertainty Index is used)

	GDP		IPI		Emp		Con		Inf		Ner		Rer		Hours		IR		Stock		M2	
Regimes	1	2	1	2	1	2	1	2	1	2	1	2	1	2	1	2	1	2	1	2	1	2
US	-4.69		-11.22		-3.56		-3.87		-2.88		-2.12		-3.57		-1.24		-3.48		-62.20		-5.68	
EU	-5.09		-14.29		-2.24		-2.80		-3.79		-	-	-	-	-	-	-3.79		-78.67		-5.51	
JP	-8.03		-33.24		-2.08		-7.14		-2.87		-9.13		-3.57		-2.69		-0.60		-75.75		-2.03	
DE	-6.51		-18.67		-2.22		-4.49		-2.30		-2.38		-3.27		-5.83		-3.78		-86.64		-8.82	
FR	-3.81		-12.97		-2.16		-3.22		-2.71		-1.93		-2.6		-1.95		-3.78		-75.09		-	-
UK	-4.67		-10.81		-2.42		-5.37		-3.78		-4.44		-5.52		-3.81		-3.42		-52.76		-5.32	
IT	-5.39		-18.51		-2.49		-4.24		-2.85		-2.27		-3.57		-		-3.78		-82.11		-17.26	
CA	-4.50		-14.03		-2.56		-3.17		-2.36		-10.15		-10.39		-1.68		-2.92		-65.67		-5.43	
NE	-5.39		-19.73		-	-	-	-	-3.79		-2.48		-4.06		-3.96		-3.78		-89.18		-	-
NW	-7.89		-28.85		-	-	-	-	-5.88		-6.57		-9.52		-	-	-3.79		-93.85		-13.84	0.01
SP	-5.16		-16.34		-	-	-	-	-4.67		-3.74		-5.66		-6.7	0.01	-3.79		-79.46	-	-	-
SW	-7.23		-	-	-	-	-	-	-2.30		-3.65	0.01	-4.24	0.01	-4.71	0.01	-4.24		-87.97		-13.26	0.01
CH	-4.34		-	-	-	-	-	-	-2.03		-	-	-	-	-2.76	0.01	-3.79		-67.96		-	-

Note: Sum of the Financial Uncertainty Index coefficients for the different variables in the 13 countries in regime 1 (recession, first column) and regime 2 (second column). Symbol "-": not available. Empty cell: not significant.

Table E.2: Effects of macroeconomic uncertainty on macroeconomic variables (when Financial Uncertainty Index is used)

	GDP	IPI	Emp	Con	Inf	Ner	Rer	Hours	IR	Stock	M2
US	3.16	7.57	2.40	2.63	1.94		2.44		2.35	41.94	3.87
EU	3.41	9.61		1.88	2.55	- -		- -		53.03	3.7
JP	5.41	22.40	1.40	4.83	1.94	6.16		1.81		51.06	1.39
DE	4.37	12.56	1.48	3.03	1.54		2.23	3.93		58.40	5.95
FR	2.56	8.74		2.18	1.82			1.32	2.55	50.62	
UK		7.27	1.62	3.61		2.99		2.57	2.28	35.57	
IT	3.63	12.47	1.67	2.87	1.91	1.56	2.45	- -	2.55	55.36	11.66
CA	3.02	9.46	1.72	2.13		6.85	7.02	1.12	1.97	44.27	3.68
NE	3.62	13.30	- -	- -	2.56			2.70	2.54	60.13	- -
NW		19.46	- -	- -	3.97			- -	2.55	63.25	9.33
SP	3.47	11.01	- -	- -		2.54	3.86	4.52	2.54	53.58	- -
SW	4.87	- -	- -	- -	1.57	2.47	2.88 0.1	3.19	2.85	59.32	8.96
CH	2.91	- -	- -	- -		- -	- -	1.88		45.82	- -

Note: Sum of the Disagreement coefficients, when the Financial Uncertainty Index is used as proxy for financial uncertainty shocks, for the different variables in the 13 countries in regime 1 (recession, first column) and regime 2 (second column). Symbol "-": not available. Empty cell: not significant.

Table E.3: Effects of financial uncertainty on macroeconomic variables (when Financial Entropy is used)

	GDP		IPI		Emp		Con		Inf		Ner		Rer		Hours		IR		Stock		M2	
US	-1.05	-0.52	-2.53	-1.26	-0.78	-0.22	-0.84	-0.42	-0.66	-0.14	-0.44		-0.78	-0.17	-0.28		-0.80	-0.22	-13.92	-6.99	-1.23	-0.62
EU	-7.78	-4.01	-33.05	-3.40	-1.79	-4.26	-2.23	-5.76	-3.01	-	-	-	-	-	-	-5.80	-2.98	-120.20	-61.79	-8.39	-4.35	
JP	-1.8	-0.90	-7.45	-3.73	-0.47		-1.60	-0.79	-0.64	-0.18	-2.04	-1.02	-0.80	-0.4	-0.61	-0.18	-0.13		-16.96	-8.53	-0.45	
DE	-9.95	-5.11	-43.17	-3.40	-1.72	-6.89	-3.51	-3.50	-1.77	-3.64	-1.84	-5.02	-2.53	-8.94	-4.58	-5.79	-2.96	-132.4	-68.02	-13.5	-6.89	
FR	-5.83	-3.03	-29.97	-3.30	-1.69	-4.93	-2.56	-4.13	-2.12	-2.97	-1.52	-4.02	-2.02	-2.99	-1.52	-5.78	-2.98	-114.73	-58.95		-	-
UK	-7.14	-3.67	-16.5	-8.47	-3.69	-1.88	-8.19	-4.23	-5.8	-2.94	-6.81	-3.46	-8.45	-4.35	-5.82		-5.23	-2.67	-80.64	-41.43	-8.11	-4.15
IT	-8.24	-4.23	-42.8	-3.77	-1.96	-6.49	-3.33	-4.35	-2.22	-3.50	-1.81	-5.51	-2.81	-	-	-5.8	-2.96	-125.47	-64.46	-39.95		
CA	-1.00	-0.50	-3.15	-1.57	-0.58		-0.71	-0.2	-0.53	-0.13	-2.26	-1.13	-2.31	-1.16	-0.37		-0.65	-0.19	-14.69	-7.39	-1.20	-0.63
NE	-8.22	-4.22	-45.62	-	-	-	-	-5.79	-2.95	-3.79	-1.93	-6.25	-3.20	-6.08	-3.12	-5.76	-2.96	-136.27	-70.00		-	-
NW	-12.07	-6.2	-66.73	-	-	-	-	-8.97	-4.60	-10.02	-5.13	-14.57	-7.45	-	-	-5.79	-2.97	-143.39	-73.69	-32.05		
SP	-7.93	-4.05	-37.80	-	-	-	-	-7.13	-3.64	-5.71	-2.93	-8.71	-4.44	-10.24	-5.25	-5.78	-2.97	-121.43	-62.39		-	-
SW	-11.06	-5.69	-	-	-	-	-	-	-3.53	-1.80	-5.63	-2.87	-6.52	-3.33	-7.17	-3.70	-6.44	-3.31	-134.53	-69.08	-30.75	
CH	-6.63	-3.41	-	-	-	-	-	-	-3.11	-1.59	-	-	-	-	-4.21	-2.12	-5.80	-2.98	-103.87	-53.34	-	-

Note: Sum of the Financial Entropy coefficients for the different variables in the 13 countries in regime 1 (recession, first column) and regime 2 (second column). Symbol "-": not available. Empty cell: not significant.

Table E.4: Effects of macroeconomic uncertainty on macroeconomic variables (when Financial Entropy is used)

	GDP	IPI	Emp	Con	Inf	Ner	Rer	Hours	IR	Stock	M2
US	0.93	2.16	0.68	0.77	0.58	0.41	0.74	0.25	0.69	12.15	1.14
EU	7.06	19.82	3.08	3.88	5.27	- -	- -	-	5.28	109.10	7.64
JP	1.59	6.49	0.41	1.40	0.57	1.78	0.72	0.54		14.78	0.41
DE	9.04	25.86	3.08	6.24	3.18	3.32	4.58	8.11	5.24	120.18	12.25
FR	5.27	17.97	2.99	4.46	3.74	2.69	3.64	2.71	5.22	104.13	- -
UK	6.45	14.98	3.34	7.44	5.27	6.15	7.66	5.31	4.70	73.17	7.37
IT	7.46	25.66	3.43	5.9	3.95	3.2	5.00	-	5.25	113.88	23.98
CA	0.88	2.74	0.49	0.63	0.47	1.96	2.02	0.31	0.55	12.8	1.08
NE	7.46	27.36	- -	- -	5.25	3.45	5.7	5.53	5.23	123.71	- -
NW	10.94	40.03	- -	- -	8.16	9.12	13.21	-	5.27	130.18	19.21
SP	7.16	22.64	- -	- -	6.44	5.2	7.89	9.29	5.23	110.22	- -
SW	10.04	- -	- -	- -	3.19	5.07	5.88	6.59	5.88	122.15	18.36
CH	6	- -	- -	- -	2.79	- -	- -	3.84	5.23	94.26	- -

Note: Sum of the Disagreement coefficients, when the Financial Entropy index is used as proxy for financial uncertainty shocks, for the different variables in the 13 countries in regime 1 (recession, first column) and regime 2 (second column). Symbol "-": not available. Empty cell: not significant.